A STUDY OF CERTAIN VARIABLES INFLUENCING LIQUID DIFFUSION RATES

By

ROBERT LOUIS ROBINSON, JR.

Bachelor of Science
Oklahoma State University
Stillwater, Oklahoma
August, 1959

Master of Science
Oklahoma State University
Stillwater, Oklahoma
May, 1962

Submitted to the Faculty of the Graduate School of
the Oklahoma State University
in partial fulfillment of the requirements
for the degree of
DOCTOR OF PHILOSOPHY
May, 1964

A STUDY OF CERTAIN VARIABLES INFLUENCING
LIQUID DIFFUSION RATES

W. C. Edmister
Thesis Adviser

R. N. Maddox

John B. West

George L. Gravin

J. H. Brown
Dean of the Graduate School

PREFACE

The effects of temperature and of molecular interactions on the diffusion rates in binary liquid systems of non-electrolytes were studied. Experimental data were gathered on the four systems n-octane-methylcyclohexane, n-octane-cyclohexanone, n-heptanol-methylcyclohexane, and n-heptanol-cyclohexanone at 25°C. The data include diffusivities, viscosities and densities. For the last-named system, diffusivities were also measured at 10, 55, and 90°C. The data are discussed in view of current diffusion theories. Some additions to the diaphragm-cell diffusion technique are presented.

I am indebted to Dr. F. A. L. Dullien, under whom I began this work, for his patient guidance and continued interest in the project. Professor W. C. Edmister, who became my thesis adviser upon Dr. Dullien's departure, also receives my appreciation for his contributions.

Discussions with my fellow graduate students were of considerable help during this study. Messrs. P. O. Haddad, J. L. Webster, and L. Yarborough deserve a special thanks for their assistance in various phases of this work.

Financial support and equipment funds for the duration of this study were gratefully received from the National Science Foundation and the School of Chemical Engineering.

Phillips Petroleum Company supplied the hydrocarbon chemicals for this work, and Pan American Petroleum Corporation generously donated

time on their IBM 704 computer to the project.

I owe an unspeakable debt of gratitude to my wife, Gayle, and to my parents for their aid and support during my entire graduate studies.

TABLE OF CONTENTS

LIST OF TABLES

LIST OF FIGURES

CHAPTER I

INTRODUCTION

This study encompasses an investigation of certain factors affecting diffusion rates in liquid solutions of non-electrolytes. In particular, the effect on the diffusion coefficient of temperature and of association of the components was studied.

A survey of literature on the subject of liquid diffusion reveals an increasing interest in this field. From an engineering viewpoint, knowledge of diffusion rates is needed for design of such equipment as distillation and extraction units and chemical reactors. On a theoretical basis, a knowledge of the diffusion process goes hand-in-hand with the development of a satisfactory liquid state theory.

At present, there exists no diffusional theory capable of predicting rates of diffusion in non-ideal systems. The failure of existing theories is often ascribed to the presence of association in the solutions (1, 36, 43, 17). In an effort to assess the validity of such reasoning, experimental data were gathered on selected associating systems and on structurally similar (homomorphic) systems which are non-associating. The goal was to compare the diffusion rates in these homomorphic systems and obtain a qualitative insight into the specific effects of association. For this purpose the following systems were chosen:

1) normal octane - methylcyclohexane

2) normal heptanol - methylcyclohexane

3) normal heptanol - cyclohexanone

4) normal octane - cyclohexanone

Note that these four systems are geometrically (structurally) similar. However, the first system should be unassociated, the second system should display association by the alcohol, the third system should display association by the alcohol and also association between constituents, and the fourth should be unassociated, but contains one polar constituent. These systems were each studied over the entire composition range at 25°C.

At the beginning of this study there existed no data over a sufficiently wide range of temperatures and compositions to test adequately existing models (33, 34, 69, 6) for the temperature influence on diffusion. Thus, in the present study, system 3 (see above) was investigated at 10°, 25°, 55° and 90°C over the entire composition range. This 80° temperature range is approximately twice as large as that of any other similar study to date and should allow an exacting test of models for the diffusion coefficient-temperature relation.

A fitting conclusion to this introductory section is the words of Bird, Stewart and Lightfoot (12) from their treatise on transport phenomena. At the close of their review of liquid-diffusional theories, they comment (p. 515)

> If the reader has by now concluded that little is known about prediction of ··· liquid diffusivities, he is correct. There is an urgent

> need for experimental measurements, both for their own value and for development of future theories.

It was with this realization that the present study was initiated.

CHAPTER II

REVIEW AND EXTENSION OF DIAPHRAGM-CELL THEORY

The experimental measurements of liquid diffusion coefficients in this study were made using the diaphragm-cell technique. The diaphragm-cell method was introduced by Northrup and Anson (56) in 1928. Since that time a rather continuous succession of contributions, both theoretical and experimental, has served to improve, define limitations, and confirm the validity of the method.

In the course of the current study, some additions to diaphragm-cell theory were evolved. As a prelude to presenting these new findings, a brief review of the current status of diaphragm-cell theory seems appropriate. This topic is presented in this early section of the thesis since it provides a convenient avenue for introducing definitions and concepts regarding the diffusion coefficient which are important to later developments.

The diaphragm-diffusion cell consists of two compartments or reservoirs, separated by a porous diaphragm (membrane or disc). The compartments are filled with solutions of different, homogeneous concentrations, and mass transfer between the compartments occurs through the diaphragm. Gordon (35) pictured the diaphragm "to be equivalent to a collection of parallel pores of average effective

length L and of total cross-sectional area A."

In the remainder of this chapter the following topics concerning diaphragm-cell theory are considered: first, the basic equation for diffusion; second, the nature of the fluxes inside the diaphragm; third, a general method of determining the binary diffusion coefficient from diaphragm-cell results; fourth, a criterion for determining the duration of a diaphragm-cell experiment.

A. The Diffusion Equation

Fick (31) originally defined the diffusion coefficient as

$$N_A \equiv -D_{Fick} \nabla \rho_A \qquad \text{(II-1)}$$

where N_A = mass flux of component A relative to a fixed coordinate system, gm A/cm^{2}sec.

D_{Fick} = diffusion coefficient as defined by Equation II-1.

ρ_A = mass concentration of A, gm A/cc.

Equation II-1 states that the mass flux of component A, relative to a fixed coordinate system, is directly proportional in magnitude and opposite in direction to the gradient of the concentration of A. To date, Equation II-1 has been utilized almost exclusively in the analysis of diaphragm-cell experiments.

A more satisfactory definition of the diffusion coefficient is given by

$$J_A \equiv - \rho D \nabla \omega_A \qquad \text{(II-2)}$$

where J_A = mass flux of A relative to the mass-average velocity, gm A/cm^{2}sec.

ρ = total mass density, gm solution/cc.

D = diffusion coefficient as defined by Equation II-2, cm^2/sec.

ω_A = mass fraction A, gm A/gm solution.

D is termed the "true" or "differential" coefficient.

Using Equation II-2, the same value of D applies whether the flux and concentration are written in terms of A or B, i.e., D is characteristic of the thermodynamic state of the system. Also, the D of Equation II-2 is not influenced by the geometry or convective flow conditions in the measuring apparatus. All theoretical interpretations of the diffusional process refer to the D of Equation II-2. None of the above statements may be made for D_{Fick}.

An equivalent relation for D, in terms of N_A, may be written for a binary system as

$$N_A = -D \nabla \rho_A + \rho_A \left[N_A V_A + N_B V_B \right] \qquad \text{(II-3)}$$

mass fluxes

where V_A = partial specific volume of A, cc A/gm A in solution.

The development of Equation II-3 from Equation II-2 appears in Appendix A.

Note that the term in brackets in Equation II-3 is the total volume flux relative to a fixed coordinate system. If this volume flux is zero, Equation II-3 reduced to Equation II-1, and Fick's law applies. In diaphragm-cell experiments, one compartment is always closed, so volume flux in the diaphragm will be zero (and Fick's law will be applicable) if the system exhibits no volume changes on mixing.

The assumption of no volume changes on mixing has almost always been employed in diaphragm-cell experiments. Thus Equation II-1 has customarily been applied and integrated as follows.

Let $y = 0$ and $y = L$ correspond to the coordinates of the lower and upper faces of the diaphragm, respectively, with y measured orthogonally to the faces of the diaphragm. Then by material balances on the two compartments,

$$(N_A)_{y=o} = -\frac{V'}{A}\frac{d\rho_A'}{dt}$$
$$(N_A)_{y=L} = \frac{V''}{A}\frac{d\rho_A''}{dt} \qquad \text{(II-4)}$$

where V = volume of solution, cc.

A = effective diaphragm cross-sectional area for mass transfer, cm^2.

t = time, sec.

$'$, $''$ = refer to conditions in the (closed) lower compartment and upper compartment, respectively.

The assumption is made that the flux, N_A, is constant throughout the diaphragm at any given time, θ, i.e.,

$$(N_A)_{y=o} = (N_A)_{o<y<L} = (N_A)_{y=L} \qquad \text{(II-5)}$$

at any instant. This is the so-called "quasi-steady state" assumption and is discussed below.

Since N_A is constant from $y = 0$ to $y = L$, the right side of Equation II-1 may be replaced by an equally constant expression, viz.

$$N_A = - D \frac{d\rho_A}{dy} \equiv - \tilde{D} \frac{\rho_A'' - \rho_A'}{L} \qquad \text{(II-6)}$$

where $\tilde{D}$ = diffusion coefficient defined by Equation II-6.

(Note that D here is identical to D_{Fick}.) Combining equations II-4 with II-6,

$$d \Delta\rho_A \equiv d\rho_A'' - d\rho_A' = - \frac{A}{L} \left[\frac{1}{V''} + \frac{1}{V'} \right] \tilde{D} \, \Delta\rho_A \, dt \qquad \text{(II-7)}$$

or

$$d \ln \Delta\rho_A = - \beta \tilde{D} \, dt \qquad \text{(II-8)}$$

where $\Delta\rho_A \equiv \rho_A'' - \rho_A'$

$\beta \equiv \frac{A}{L} \left[\frac{1}{V''} + \frac{1}{V'} \right]$, the "cell constant", cm^{-2}.

Integrating from t = 0 to t = θ, Equation II-8 becomes

$$\ln \frac{(\Delta\rho_A)_o}{(\Delta\rho_A)_f} = \beta \bar{D} \, \theta \qquad \text{(II-9)}$$

where $\bar{D}$ = the "integral diaphragm diffusion coefficient,"

a time-averaged value of $\tilde{D}$.

In Equation II-9 the subscripts o and f refer to initial and final conditions, respectively. Equation II-9 is used almost exclusively to obtain the diffusion coefficient from diaphragm experiments and is referred to as the "simple logarithmic formula."

The general use of Equation II-9 may be questioned on several points. First, and most obvious, the quasi-steady state assumption must be justified. Second, the derivation applies only to the case of no volume changes on mixing. Third, some means must be known to relate the known values of

$\bar{D}$ to the differential diffusion coefficient, D, since from Equations II-6, II-8, and II-9,

$$\bar{D} = \frac{1}{\theta} \int_0^{\theta} \left[\frac{1}{\Delta \rho_A} \int_{\rho_A'}^{\rho_A''} D \, d\rho_A \right] dt \qquad \text{(II-10)}$$

Each of the three above mentioned points is considered below.

B. The Quasi-Steady State Assumption

The distribution of fluxes in the diaphragm has been studied by Barnes (7) and by Dullien (26).

Using the three assumptions that D is not a function of solution composition, that V' = V", and that no volume changes occur during diffusion, Barnes obtained formal solutions to the diffusion equation for two sets of initial conditions. These initial conditions were a) pure solvent fills one compartment and the diaphragm, and b) pure solvent fills one compartment, and a linear concentration profile exists in the diaphragm. From his formal solutions, Barnes found that for case a) the quasi-steady state assumption may be significantly in error, but in case b) the assumption introduces negligible error when the ratio of diaphragm pore volume to reservoir volume is less than 0.1. (In the present study this ratio was 0.007.)

Dullien, employing the same assumptions as Barnes (except dropping the requirement that one initial solution be pure solvent), integrated the diffusion equation numerically for typical diaphragm-cell conditions. He concluded that even if D varied with concentration, the quasi-steady

state assumption should introduce errors of less than 0.2% (here Dullien misplaced a decimal point and reported 0.02%).

Toor (72) has investigated another point concerning the fluxes in the diaphragm. He points out that although the only net flux is in the y-direction, the tortuous paths of the pores in the diaphragm give rise to local fluxes in the x and z directions. Thus, the intuitive assumption of unidirectional diffusion might not be valid since $d\rho_A/dy$ must be replaced by $\partial\rho_A/\partial y$, which may be a function of the x and z coordinates. However, Toor proceeded to prove mathematically that the solution of the diffusion equation without the unidirectional flow assumption is identical to that when the assumption is employed.

Conclusions from the studies of Barnes, Dullien, and Toor may be summarized as a) the quasi-steady state assumption appears to be applicable in diaphragm-cell experiments, b) a concentration profile should be established through the diaphragm prior to beginning a diffusion run, and c) integration of the diffusion equation does not require the assumption of unidirectional diffusion.

C. Calculation of Diffusion Coefficients from Diaphragm-Cell Experiments

For the case where the system volume is invariant, Equation II-10 gives the relation of the experimental coefficient, $\overline{D}$, to the differential coefficient, D. For this situation Gordon (35) has presented an iterative technique to obtain D from $\overline{D}$. (An interesting special case occurs when D is linear in ρ_A, and $V' = V''$. Then from Equation II-10, $\overline{D} = D$ at the average value of ρ_A, $(\rho_A)_{Avg}$, in the diaphragm.)

When volume changes occur during diffusion Equations II-9 and II-10 are inapplicable. Dullien and Shemilt (24) first attempted to solve the

general diffusion equation (Equation II-2) for the diaphragm cell. Olander (57) subsequently pointed out a tacit assumption in the work of Dullien and Shemilt. Olander then presented a simplified solution of his own. Olander's method of solution employs a series of assumptions which, it appears to this author, would in most cases be more in error than that of Dullien and Shemilt.

To resolve the situation concerning calculation of the diffusion coefficient in the general case, a rigorous set of equations was derived as part of this study. These equations involve an iterative solution to yield the D versus ρ_A relation from measured $\bar{D}$ values. The development of the following equations follows a pattern similar to that of Gordon (35) for the simple case.

Equation II-3 may be written for unidirectional diffusion as

$$N_A = \frac{-D}{1 - \rho_A V_B \left[\frac{V_A}{V_B} + \frac{N_B}{N_A}\right]} \frac{d\rho_A}{dy} \qquad \text{(II-11)}$$

The ratio of fluxes in the denominator of Equation II-11 may be eliminated as follows. Consider the total volume flux through the lower face of the diaphragm,

$$\text{Total vol. flux (at } y = 0) = N_A V'_A + N_B V'_B \qquad \text{(II-12)}$$

The primes on the partial specific volumes are applicable since the compositions at $y = 0$ are identical to those in the lower compartment. The fluxes are unprimed since, under the quasi-steady state assumption, the fluxes are independent of y.

Since the lower compartment is closed, the volume, V', of solution in the compartment is constant during the diffusion process. Using material balances on the lower compartment, the fluxes may be written as

$$N_A = -\frac{V'}{A}\frac{d\rho'_A}{dt} \qquad \text{(II-13)}$$

$$N_B = -\frac{V'}{A}\frac{d\rho'_B}{dt}$$

and Equation II-12 becomes

$$\text{Vol. flux } (y=0) = \frac{-V'}{A\ dt}\left[\bar{V}'_A\ d\rho'_A + \bar{V}'_B\ d\rho'_B\right] \qquad \text{(II-14)}$$

Recall the following relations (which are generally valid for partial properties) from thermodynamics,

$$V_T = \omega_A \bar{V}_A + \omega_B \bar{V}_B \qquad \text{(II-15)}$$

$$0 = \omega_A d\bar{V}_A + \omega_B d\bar{V}_B \qquad \text{(II-16)}$$

where V_T = specific volume of solution, cc solution/gm solution. Multiplying Equation II-15 by $\rho = 1/V_T$, recalling $\rho_A = \rho\omega_A$, yields

$$1 = \rho_A \bar{V}_A + \rho_B \bar{V}_B \qquad \text{(II-17)}$$

Forming the differential of Equation II-17,

$$0 = \rho_A d\bar{V}_A + \rho_B d\bar{V}_B + \bar{V}_A d\rho_A + \bar{V}_B d\rho_B \qquad \text{(II-18)}$$

however, multiplying Equation II-16 by ρ yields

$$0 = \rho_A \, dV_A + \rho_B \, dV_B \tag{II-19}$$

Combining Equations II-18 and II-19,

$$V_A \, d\rho_A + V_B \, d\rho_B = 0 \tag{II-20}$$

Applying Equation II-20 to the solution in the lower compartment and combining with Equations II-14 and II-12,

$$N_A V_A' + N_B V_B' = 0$$

or

$$\frac{N_B}{N_A} = \frac{-V_A'}{V_B'} \tag{II-21}$$

which is the desired relation for the flux ratio, N_A/N_B.

Using Equation II-21, Equation II-11 may be written for the diaphragm cell as

$$N_A = \frac{D}{1 - \rho_A V_B \left[\frac{V_A}{V_B} - \left(\frac{V_A}{V_B} \right)' \right]} \frac{d\rho_A}{dy} \tag{II-22}$$

Since N_A is constant throughout the diaphragm at any instant, the right side of Equation II-22 may be replaced by an equally constant function,

$$\frac{D_* \, (\rho_A'' - \rho_A')}{L} \equiv \frac{D}{1 - \rho_A V_B \left[\frac{V_A}{V_B} - \left(\frac{V_A}{V_B} \right)' \right]} \frac{d\rho_A}{dy} \tag{II-23}$$

where D_* is defined by Equation II-23. In addition, denote

$$\begin{aligned} D/D_o &\equiv 1 + f(\rho_A) \quad , \quad D_o = D \text{ at } \rho_A = 0 \\ G(\rho_A, \rho_A') &\equiv \rho_A V_B \left[\frac{V_A}{V_B} - \left(\frac{V_A}{V_B} \right)' \right] \end{aligned} \tag{II-24}$$

Thus

$$\frac{D_* (\rho_A'' - \rho_A') \, dy}{L} = \frac{D_o \left[1 + f(\rho_A)\right]}{1 - G(\rho_A, \rho_A')} d\rho_A \qquad \text{(II-25)}$$

Integrating from y = 0 to y = L,

$$\frac{D_*}{D_o} = \frac{1}{\Delta \rho_A} \int_{\rho_A'}^{\rho_A''} \frac{1 + f(\rho_A)}{1 - G(\rho_A, \rho_A')} d\rho_A \qquad \text{(II-26)}$$

Now, writing material balances around the individual compartments, allowing for possible changes in V",

$$V' \, d\rho_A' = - N_A A \, dt = \frac{A D_* \Delta \rho_A}{L} dt$$

$$d(V'' \rho_A'') = N_A A \, dt = - \frac{A D_* \Delta \rho_A}{L} dt \qquad \text{(II-27)}$$

Rearranging Equations II-27 and combining them,

$$d\rho_A'' - d\rho_A' = d\Delta \rho_A = - D_* \Delta \rho_A \frac{A}{L}\left[\frac{1}{V'} + \frac{1}{V''}\right] dt - \frac{\rho_A''}{V''} dV''$$

or

$$d\ln \Delta \rho_A = - D_* \beta \, dt - \frac{\rho_A''}{\Delta \rho_A V''} dV'' \qquad \text{(II-28)}$$

Define

$$\frac{D_o}{D_*} = 1 + F(\rho_A', \rho_A'') \qquad \text{(II-29)}$$

Equation II-28 may be written

$$\frac{1 + F(\rho_A', \rho_A'')}{\beta} d\ln \Delta \rho_A = - D_o \, dt - \frac{\left[1 + F(\rho_A', \rho_A'')\right] \rho_A''}{\beta \Delta \rho_A V''} dV'' \qquad \text{(II-30)}$$

Integrating,

$$-\frac{1}{\bar{\beta}} \ln \frac{(\Delta \rho_A)_o}{(\Delta \rho_A)_f} + \int_{(\Delta \rho_A)_o}^{(\Delta \rho_A)_f} \frac{F(\rho_A', \rho_A'')}{\beta \Delta \rho_A} d \Delta \rho_A =$$

$$- D_o \theta - \int_{V_o''}^{V_f''} \frac{[1 + F(\rho_A', \rho_A'')] \rho_A''}{\beta \Delta \rho_A V''} dV'' \qquad \text{(II-31)}$$

where

$$\bar{\beta} = - \ln \frac{(\Delta \rho_A)_o}{(\Delta \rho_A)_f} \Bigg/ \int_{(\Delta \rho_A)_o}^{(\Delta \rho_A)_f} \frac{d\Delta \rho_A}{\beta \Delta \rho_A} \qquad \text{(II-32)}$$

Define

$$\bar{D} \beta_o \theta \equiv \ln \frac{(\Delta \rho_A)_o}{(\Delta \rho_A)_f} \quad , \quad \beta_o = \beta \text{ at } t = 0 \qquad \text{(II-33)}$$

The $\bar{D}$ thus defined reduces to the integral diffusion coefficient of Equation II-9 when no volume changes occur on mixing. Equation II-31 may be written

$$-\frac{\bar{D} \beta_o \theta}{\bar{\beta}} + \int_{(\Delta \rho_A)_o}^{(\Delta \rho_A)_f} \frac{F(\rho_A', \rho_A'')}{\beta \Delta \rho_A} d\Delta \rho_A = - D_o \theta - \int_{V_o''}^{V_f''} \frac{[1 + F(\rho_A', \rho_A'')] \rho_A''}{\beta \Delta \rho_A V''} dV''$$

(II-34)

Thus

$$\frac{\bar{D}}{D_o} = \frac{\bar{\beta}}{\beta_o}\left[1 + \frac{1}{D_o\,\theta}\int_{(\Delta\rho_A)}^{(\Delta\rho_A)_f} \frac{F(\rho_A', \rho_A'')}{\beta\,\Delta\rho_A}\, d\Delta\rho_A + \frac{1}{D_o\,\theta}\int_{V_o''}^{V_f''} \frac{\left[1 + F(\rho_A', \rho_A'')\right]\,\rho_A''}{\beta\,\Delta\rho_A\,V''}\, dV''\right] \qquad \text{(II-35)}$$

The above set of equations contains no assumptions other than that of the quasi-steady state. Calculation of the D versus ρ_A relation from experimental results may be done via the iterative process described in the following steps:

1. Assume a D vs ρ_A relation. $\bar{D}$ vs $(\rho_A)_{Avg}$ is a logical first approximation.
2. Determine $f(\rho_A)$ via Equation II-24.
3. Determine $F(\rho_A', \rho_A'')$ via Equations II-26 and II-29.
4. Evaluate Equation II-35.
5. Define ρ_A^* as the concentration at which $\bar{D}$ is equal to D. By comparison of Equations II-24 and II-35, it follows that ρ_A^* may be found by equating $1 + f(\rho_A)$ to the right-hand side of Equation II-35 and solving for ρ_A^*.
6. For a second iteration, assume the D vs ρ_A relation equals the $\bar{D}$ vs ρ_A^* relation. Repeat steps 2-6 until the ρ_A^* values from two successive iterations vary insignificantly.

Application of the above method requires a knowledge of the volumetric properties of the system, i.e., a knowledge of the ρ vs ρ_A relation. Application of the equations may be done graphically. However, if analytical expressions for $\bar{D}$, ρ, V_B, and V_A/V_B as functions of ρ_A can be obtained, the solution is simplified since high-speed digital computers may be used to solve the equations. The use of this method is discussed and illustrated in Chapter VII.

Before leaving this section, note that if no volume changes occur during diffusion, $dV'' = 0$, $\bar{\beta} = \beta_o = \beta$, and Equation II-35 becomes

$$\frac{\bar{D}}{D_o} = 1 + \frac{1}{D_o \beta \theta} \int_{(\Delta \rho_A)_o}^{(\Delta \rho_A)_f} \frac{F(\rho_A', \rho_A'')}{\Delta \rho_A} d\Delta \rho_A \qquad \text{(II-36)}$$

Equation II-36 is precisely Gordon's (35) Equation 17 for the case of no volume changes on mixing.

D. Optimum Duration of Diaphragm-Cell Experiments

The question of the effect of analytical errors on the accuracy of the diaphragm-cell diffusion coefficient has not received the attention it deserves in the literature. Stokes (68) has presented an approximate analysis for the maximum percent error $\Delta D/D$, in the diffusion coefficient resulting from analytical errors. He presented a tabulation of minimum values of $\Delta D/D$ as a function of initial concentration ratio $(\rho_A''/\rho_A')_o$. However, Stokes gave no indication as to the point on the diffusion path at which this minimum occurs. Dullien (8) also studied the effects of analytical errors but did not attempt to optimize the duration

of his experiments.

The general procedure in conducting diffusion experiments has been to allow the concentration difference to decrease by 40 to 50% during the course of diffusion; no logical justification for this procedure is known to this author.

As a part of this study, a logical criterion for determining the "optimum" time of diffusion was established, and the method is presented below.

A reasonable criterion for the optimum duration of a diaphragm-cell experiment is that the fractional standard deviation, (s_D/D), in the diffusion coefficient be a minimum. The simple Equation II-9 will be employed in the subsequent treatment; also, the cell compartments will be assumed to be of equal volume, $V' = V''$.

Using Equation II-9, s_D, the standard deviation of the diffusion coefficient, may be estimated using statistical theory of error propagation (11). In general, for a variable y which may be expressed as a function of n variables $x_1, \cdots, x_n$,

$$s_y^2 = \sum_{i=1}^{n} \left(\frac{\partial y}{\partial x_i}\right)^2 s_{x_i}^2 + 2 \sum_{\substack{i=1 \\ i>j}}^{n} \sum_{j=1}^{n-1} \tilde{\rho}_{x_i x_j} \left(\frac{\partial y}{\partial x_i}\right)\left(\frac{\partial y}{\partial x_j}\right) s_{x_i} s_{x_j} \qquad \text{(II-37)}$$

where

$$s_{x_i}^2 = \frac{1}{k-1} \sum_{m=1}^{k} (\delta x)_m^2 \qquad \text{(II-38)}$$

$$\tilde{\rho}_{x_i x_j} = \frac{1}{(k-1)\, s_{x_i} s_{x_j}} \sum_{m=1}^{k} (\delta x_i \delta x_j)_m \qquad \text{(II-39)}$$

s_y = standard deviation from the mean for the sample of items, y

k = total number of observations in the sample

$\tilde{\rho}_{x_i x_j}$ = correlation coefficient for the x_i-x_j pair, defined by Equation II-39

In particular, from Equation II-9, we may write for the diffusion coefficient,

$$\bar{D} = \bar{D}\left(\beta, \theta, \rho'_{Ao}, \rho''_{Ao}, \rho'_{Af}, \rho''_{Af}\right) \qquad \text{(II-40)}$$

Two cases will be considered,

a) All four concentrations are measured experimentally, as in cells using conductivity probes for analysis (64).

b) Three concentrations are measured, and the fourth, ρ'_{Ao}, is determined by material balance, as in the present study.

We shall assume that errors in measurement of β and θ are negligible. In most measurements of concentration, errors are essentially independent of concentration, so we shall assume for the two cases,

a) $s_{\rho'_{Ao}} = s_{\rho''_{Ao}} = s_{\rho'_{Af}} = s_{\rho''_{Af}} \equiv s$ (II-41)

b) $s_{\rho''_{Ao}} = s_{\rho'_{Af}} = s_{\rho''_{Af}} = s$

For case b), recalling V' = V", a material balance yields

$$\rho'_{Ao} = \rho'_{Af} + \rho''_{Af} - \rho''_{Ao} \qquad \text{(II-42)}$$

The value of $s_{\rho'_{Ao}}$ for case b) may be determined from Equations II-37, II-41, and II-42. (The errors in measured concentrations are assumed to be uncorrelated, so the second term in Equation II-37 vanishes.) The result is

$$s_{\rho'_{Ao}} = \sqrt{3}\, s \qquad \text{(II-43)}$$

Equation II-37 will now be used to estimate s_D; the following correlation coefficients apply (from Equation II-39),

a) All $\tilde{\rho}$'s = 0

b) $-\tilde{\rho}_{\rho'_{Ao}\rho''_{Ao}} = \tilde{\rho}_{\rho'_{Ao}\rho'_{Af}} = \tilde{\rho}_{\rho'_{Ao}\rho''_{Af}} = \frac{1}{\sqrt{3}}$ (II-44)

The partial derivatives required for Equation II-37 are

$$\frac{\partial D}{\partial \rho'_{Ao}} = -\frac{\partial D}{\partial \rho''_{Ao}} = \frac{1}{R}\frac{\partial D}{\partial \rho'_{Af}} = -\frac{1}{R}\frac{\partial D}{\partial \rho''_{Af}} = -\frac{1}{\beta\,\theta\,R\,(\rho''_A-\rho'_A)_f} \qquad \text{(II-45)}$$

where $R = (\Delta\rho_A)_o/(\Delta\rho_A)_f$

Substituting the above into Equation II-37 yields

a) $$s_D^2 = \frac{2\,s^2\,(R^2+2)}{\left[\beta\,\theta\,(\rho''_A-\rho'_A)_o\right]^2} \quad \text{or} \quad \frac{s_D}{D} = \frac{\sqrt{2}\,s}{(\rho''_A-\rho'_A)_o\,\ln R}\sqrt{R^2+2} \qquad \text{(II-46)}$$

b) $$s_D^2 = \frac{2\,s^2\,(R^2+3)}{\left[\beta\,\theta\,(\rho''_A-\rho'_A)_o\right]^2} \quad \text{or} \quad \frac{s_D}{D} = \frac{\sqrt{2}\,s}{(\rho''_A-\rho'_A)_o\,\ln R}\sqrt{R+3} \qquad \text{(II-47)}$$

For a given set of initial conditions, ρ'_{Ao} and ρ''_{Ao}, the value of ρ'_A may be found such that s_D/D is a minimum. (Recall that ρ''_A is related to ρ'_A via Equation II-42.) This condition may be stated as

$$\frac{\partial(s_D/D)}{\partial \rho'_{Af}} = 0 \qquad \text{(II-48)}$$

The results of applying this operation to Equation II-46 for case a) is

$$0 = \frac{\sqrt{2}\,s}{(\rho''_A-\rho'_A)_o^2}\,\frac{R}{\ln R}\left[\frac{R^2}{\sqrt{R^2+2}} - \frac{\sqrt{R^2+2}}{\ln R}\right]$$

which leads to

$$R^2 (\ln R - 1) = 2$$

or

$$R = 3.27 \qquad \text{(II-49)}$$

From the definition of R and Equation II-49,

$$\rho'_{Af} = \rho'_{Ao} + 0.347 (\rho''_A - \rho'_A)_o \qquad \text{(II-50)}$$

A similar treatment for case b) yields

$$\rho'_{Af} = \rho'_{Ao} + 0.356 (\rho''_A - \rho'_A)_o \qquad \text{(II-51)}$$

The results for the two cases are so similar that an average relation should suffice for both cases, i.e.,

$$\rho'_{Af} = \rho'_{Ao} + 0.35 (\rho''_A - \rho'_A)_o \qquad \text{(II-52)}$$

Equation II-52 indicates that diffusion should be allowed to proceed until the concentration in the lower cell has changed by an amount equal to 35% of the original concentration difference. This is equivalent to a 70% decrease in the concentration difference, as compared to the 40-50% decrease usually employed.

Equation II-52 corresponds to a value of R = 3.33. Combining this with Equation II-9,

$$\theta_{opt.} = 1.2/\beta\bar{D} \qquad \text{(II-53)}$$

where $\theta_{opt.}$ = optimum diffusion time, sec.

Equation II-53 may be used to predict the optimum diffusion time for a given experiment if some estimate of the magnitude of the diffusion coefficient is available. Although Equation II-53 is based on the simple logarithmic formula, it should prove a useful estimator in all cases when

$V' = V''$. (Similar derivations could be easily made for other volume ratios.)

The effect of diffusion time on the error in D is illustrated for case a) in Figure 1. Figure 1 was constructed by use of Equations II-9, II-46, and II-49. Note that the minimum in the curve of Figure 1 is fairly broad; deviations of 40% from $\theta_{opt.}$ cause increases of less than 20% in the error in D.

Another interesting consequence of Equation II-53 is that the optimum diffusion time is not dependent on the initial conditions of the experiment. However, the percentage standard deviation is directly affected by the initial conditions, as shown in Equations II-46 and II-47. The percentage standard deviation for any given diffusion duration is inversely proportional to the initial concentration difference, i.e., a two-fold increase in initial concentration difference results in a corresponding two-fold decrease in the percentage standard deviation.

In past experiments very small initial concentration differences have often been employed to minimize the magnitude of volume changes on mixing (and render Equation II-9 applicable). The effects of such procedures on the accuracy of the resulting D values is apparent from the discussion in the previous paragraph. This point serves to indicate the value of the general procedure, presented in section C of this chapter, for calculating D. The general procedure is applicable regardless of the magnitude of volume changes; subsequently, large concentration differences may be employed with attendant increases in the precision of results.

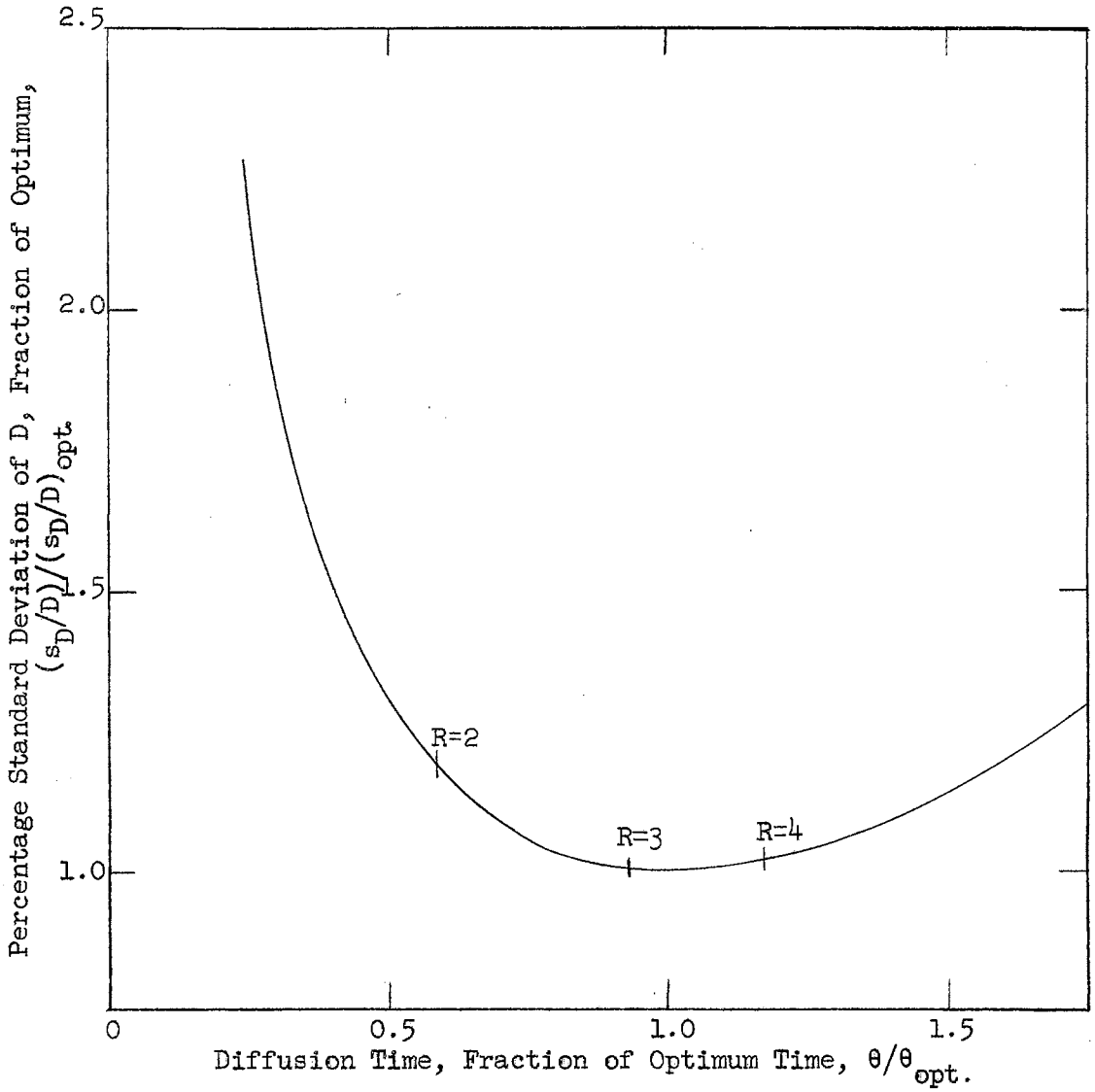

Figure 1

The Relation of Standard Deviation of the Diffusion Coefficient to the Diffusion Time

CHAPTER III

REVIEW OF PERTINENT LITERATURE CONCERNING THEORIES OF LIQUID DIFFUSION

Experimental and theoretical investigations of diffusion have been of interest since before the dawn of the twentieth century. As a result, there exists a considerable literature on the subject (e.g., see reference 44). This chapter makes no pretense of encompassing all previous contributions. However, a selected fraction of these contributions are presented to illustrate the present status of diffusional theory as it applies to this study. The order of discussion is a) general diffusional theories, b) temperature effects on diffusion rates, and c) some studies of specific effects of association on diffusion rates.

A. Diffusional Theories

The establishment of models to represent the diffusional process in liquids has proceeded along four main lines, notably the hydrodynamic, rate-theory, thermodynamic, and statistical mechanical approaches.

From a hydrodynamic viewpoint, the motion of a particle, i, in a continuous medium may be represented via the relation

$$F_{ri} = f_i v_i \qquad \text{(III-1)}$$

where F_{ri} = the force on the particle opposing the motion

f_i = a proportionality factor of "friction coefficient"

v_i = the velocity of the particle relative to the medium

If F_{ri} is taken as the resistive force on a diffusing particle, and equated to the diffusive driving force, written in terms of the osmotic pressure gradient, the following relation results for an ideal solution (21),

$$D_i = \frac{RT}{\tilde{N} f_i} \qquad \text{(III-2)}$$

where R = universal gas constant

T = absolute temperature

$\tilde{N}$ = Avagadro's number

Equation III-2 was first derived by Einstein who utilized Stokes' law to represent f_i, the result being

$$D_i = \frac{RT}{6 \pi \tilde{N} \mu r_i} \qquad \text{(III-3)}$$

where μ = viscosity of the medium

r_i = radius of diffusing particle

Equation III-3 is the Stokes-Einstein equation, perhaps the most famous of all diffusion relations. Since Stokes' law assumes the particle is diffusing in a continuous medium, Equation III-3 should be most applicable when the solute molecules are much larger than those of the solvent. Such has been found to be the case (44).

The best-known relation for the diffusion coefficient in binary mixtures of non-electrolytes is the Hartley-Crank equation (38). This equation is based on reasoning analogous to that used in developing Equation III-2 for ideal mixtures. Extending this reasoning to non-ideal

mixtures, Hartley and Crank derived the following expression

$$D = \frac{RT}{\tilde{N}} \frac{d\ln a_A}{d\ln x_A} \left[\frac{x_A}{\sigma_A \mu} + \frac{x_A}{\sigma_B \mu} \right] \qquad \text{(III-4)}$$

where a = activity

x = mole fraction

σ = parameter with dimensions of length

Here Hartley and Crank use $\sigma_i \mu$ to represent the friction coefficient f_i; they make no specific assumptions regarding the dependence of σ on temperature or composition. In Equation III-4, the practice has been to assume the σ's independent of concentration and determine the values of the σ's from the diffusivities at the two limits of concentration. The behavior of D at intermediate concentrations may then be predicted. Equation III-4 has been shown to fail in predicting the behavior of non-ideal systems (16, 36). Reasons for this failure will become evident later.

An important part of the theory of Hartley and Crank is their definition of a new set of diffusion coefficients, their "intrinsic diffusion coefficients." These coefficients have received considerable notice, and are discussed in Appendix D, where they are shown to be trivial.

Carman and Stein (17) extended the Hartley-Crank theory by identifying these intrinsic coefficients with the respective self-diffusion coefficents to obtain the relation

$$D = N_B D_A^* + N_A D_B^* \qquad \text{(III-5)}$$

where D_A^* = self-diffusion coefficient of component A.

This relation is also unsatisfactory for explaining results in the few non-ideal systems where it has been tested (53).

The "absolute rate theory" of Eyring (34) and his co-workers has also been applied to diffusion. This theory envisions the liquid as a lattice-type structure in which the molecules move about in "jumps" of finite length, λ. The assumption is made that the molecules exist in normal and activated states, with only those in the latter state capable of jumping from one site to another. In addition, the postulate is made that the frequency of the jumps is given in terms of a rate constant, k.

Regarding the diffusional flux of a component as proportional to the jump length, λ, and assuming the rate constant to be identical for forward and reverse jumps, the following equation results (34, p. 519) for an ideal solution,

$$D = \lambda^2 k \qquad \text{(III-6)}$$

A similar treatment of viscous flow results in

$$\mu = \frac{\lambda_1}{\lambda_2 \lambda_3} \frac{\tilde{k} T}{\lambda^2 k} \qquad \text{(III-7)}$$

where $\tilde{k}$ = Boltzmann's constant

λ_1 = distance between successive layers of molecules sliding past each other

λ_2 = distance between molecules in same layer perpendicular to direction of flow

λ_3 = distance between molecules in direction of flow

Equating λ, k for viscous flow to the corresponding parameters in diffusion yields

$$D = \frac{\lambda_1}{\lambda_2 \lambda_3} \frac{\tilde{k}T}{\mu} \qquad \text{(III-8)}$$

Alternatively, if the complete rate-theory expression of k is introduced into Equation III-6,

$$D = \lambda^2 \frac{\tilde{k}T}{h} \frac{F^*}{F} e^{-\epsilon_o/kT} \qquad \text{(III-9)}$$

where h = Planck's constant

F^* = partition function for the activated molecule

F = partition function for the normal molecule

ϵ_o = activation energy per molecule at 0^oK.

If the activated complex is characterized by the loss of one degree of translational freedom, and the liquid is taken as having a cubic packing, the best-known form of Eyring's equation results, i.e.,

$$D = \frac{\lambda^2}{v_f^{1/3}} \left[\frac{\tilde{k}T}{2\pi m}\right]^{1/2} e^{-\Delta E_{vap}/nRT} \qquad \text{(III-10)}$$

where v_f = "free volume" of the liquid, the effective volume for movement of a molecule in the liquid lattice.

ΔE_{vap} = energy of vaporization per mole

$n = E_{vap}/\epsilon_o$

m = reduced mass of A and B

In considering non-ideal mixtures, Eyring develops the equations

$$D = \frac{\lambda_1}{\lambda_2 \lambda_3} \frac{\tilde{k}T}{\mu} \frac{d\ln a_A}{d\ln x_A} \qquad \text{(III-11)}$$

or

$$D = D^o \frac{d\ln a_A}{d\ln x_A} \qquad \text{(III-12)}$$

where $D^{\circ} = D$ for the ideal system, Equation III-8

The above equations III-6 through III-12 have been found to give only order of magnitude agreement with experimental results (15, 33). The various forms of the equations are included here since they will be required in the discussion of results in this study.

The thermodynamic approach to diffusion is exemplified by the works of Prigogine (60), de Groot (53), Laity (52), and Dunlop (27). Employing methods of irreversible thermodynamics, relations for the diffusion coefficient in terms of the phenomenological coefficients are deduced. This approach gives an interesting and valuable macroscopic view of the diffusion process without regard to mechanisms of transport. However, no prediction of D (or the phenomenological coefficients) is possible without recourse to molecular hypotheses.

Attempts to predict the diffusion rate from models for molecular behavior using methods of statistical mechanics is currently receiving much attention. From consideration of interactions between molecular pairs, equations for the diffusion coefficient may be formulated, but rigorous solution of the equations has not been accomplished (51).

Bearman and Kirkwood (10) have circumvented the problems presented in rigorous solution of the statistical mechanical equations by adopting a semiphenomenological approach (i.e., by assuming linear relations between certain variables). Even with such simplification, results are too complex to be applied to prediction of rates of diffusion. The form of their results is

$$D = \frac{V_A \breve{k}T}{\zeta_{AB}} \frac{d\ln a_B}{d\ln c_B} = \frac{V_B \breve{k}T}{\zeta_{AB}} \frac{d\ln a_A}{d\ln c_A} \qquad \text{(III-13)}$$

where V_A = partial volume of component A

ζ_{AB} = coefficient of friction between A and B

c_A = concentration of A in units consistent with V_A

The friction coefficient ζ_{AB} enters into Equation III-13 by way of the definition, based on the phenomenological theory of transport,

$$\frac{d\mu_A}{dy} = - c_B \zeta_{AB} (v_A - v_B) \qquad \text{(III-14)}$$

where μ_A = the chemical potential of component A

y = distance along the transport path

The tracer-diffusion coefficient is given in terms of the same theory by the relation

$$D_A^* = \tilde{k}T / (c_A \zeta_{AA} + c_B \zeta_{AB}) \qquad \text{(III-15)}$$

Bearman (9) simplified his equations by restricting his consideration to a class of solutions essentially equivalent to the "regular" solutions of Hildebrand and Scott (40).

In a very enlightening discussion (9), Bearman has demonstrated that the results of Hartley and Crank, Carman and Stein, and Eyring may be obtained from the statistical mechanical approach under the assumption of regular solutions. This offers a logical explanation for the failure of the above theories to predict the behavior of strongly non-ideal or associating systems.

Mention should be made at this point of the works of Lamm (47) who derived equations of the form of Equations III-13 and III-15 from a hydrodynamic viewpoint. Lamm's work has fallen into some disfavor since, to be tested, it must be put in some approximate form, i.e., some relation assumed between the friction coefficients. Failure of the approximate

equation (53) to predict behavior in very non-ideal systems should not be construed as failure of Lamm's general theory. In fact, Dullien (23) recently used Lamm's complete theory to relate D and μ with amazingly good results for even very polar compounds.

B. Temperature Dependence of Diffusion Coefficients

The effect of changes in temperature on the diffusion coefficient may be inferred from certain of the above-mentioned models as well as from other (largely empirical) sources.

The earliest investigators assumed a linear temperature-diffusion coefficient relation (69). This model was used mainly due to a lack of sufficient data to justify any other relation.

Eyring's theory is often used as a basis for assuming an exponential variation of D with T (assuming the pre-exponential term in Equation III-9 to be temperature independent). However, Meyer and Nachtrieb (52) have suggested that D/T rather than D should follow the exponential rule.

The Stokes-Einstein relation, Equation III-3, predicts that $D\mu/T$ is constant if the molecular radius, r_i, is temperature insensitive. Note from Equation III-4 that the Hartley-Crank model gives the same result, subject to constancy of the thermodynamic factor. This relation has also been employed by Wilke and Chang (76) in their semi-empirical correlation of diffusion coefficients, while Sitaraman, et al (63) incorporated $(\mu/T)^{0.93}$ in a similar correlation.

Garner and Marchant (33) found the ln D versus ln μ relation to be linear for several associated compounds in water. Othmer and Thakar (58) utilized the relation

$$D \propto \left[\mu_w^{1.1} L_s/L_w V^{0.6} \mu_s \right]^{-1} \qquad \text{(III-16)}$$

where μ_w = viscosity of water, cp

L_s = molal latent heat of vaporization of solvent

L_w = molal latent heat of vaporization of water

V = molal volume of solute, cc/gmole

μ_s = viscosity of solvent, cp

in their empirical data correlation.

Finally, Arnold (6) has suggested the following models,

$$D \propto \mu^{-a} \qquad \text{(III-17)}$$

where a = constant

and

$$D \propto (\mu V^{2/3})^{1/2} T \qquad \text{(III-18)}$$

Equation III-17 agrees with the above-mentioned model of Garner and Marchant.

The success of these various models in fitting experimental data will be discussed in Chapter VII.

C. Some Specific Effects of Association in Diffusion

Only two studies of the type indicated in the above heading are known to the author, those of Anderson and Babb (1) and Irani and Adamson (43).

Anderson and Babb studied the behavior of non-ideal mixtures in which association should be prevalent. These authors acknowledged the failure of the Hartley-Crank theory in regard to such systems and proceeded to modify it as follows. They applied Dolezalek's theory (see reference 40) that an associating mixture obeys the ideal solution

laws if the concentrations of the "true" species in solution are employed. (Dolezalek's theory has successfully predicted the equilibrium properties in many associating systems.)

For a solution forming a 1:1 complex, an equilibrium of the form

$$K = \frac{x_{12}}{x_1 \, x_2} \qquad \text{(III-19)}$$

is assumed, where K is the equilibrium constant for the equilibrium between the dimer and monomers. Using Equation III-19 and stoichiometric relations, Equation III-14 becomes

$$D = \frac{R \, T}{\tilde{N} \, \mu} \left[\frac{x_B \, x_1^o}{x_A \, \sigma_1} + \frac{x_A \, x_2^o}{x_B \, \sigma_2} + \frac{(x_B - x_A)^2 \, x_{12}^o}{x_A \, x_B \, \sigma_{12}} \right] \frac{d\ln a_A}{d\ln x_A} \qquad \text{(III-20)}$$

where $x_1^o = x_1/(1 + x_{12})$

$x_2^o = x_2/(1 + x_{12})$

$x_{12}^o = x_{12}/(1 + x_{12})$

σ_{12} = parameter analogous to σ_1 and σ_2 but for the 1:1 complex

The subscripts A and B refer to the stoichiometric quantities and 1, 2, and 12 refer to "true" quantities in solution. Similar treatments were made (2) for association of one component. To apply the equation σ_1 and σ_2 were found as in the case of the usual Hartley-Crank equation, and using σ_1 and σ_2, and D at $x = 0.5$, σ_{12} was evaluated. The equilibrium constant, K, was evaluated from spectroscopic studies or back-calculated from data on equilibrium properties (i.e., vapor pressures).

Results from the modified equation were improvements on those from Equation III-4 in most cases. However, the method is open to criticism on the points that a) Dolezalek's theory has required absurd association

mechanisms to explain equilibrium properties in some systems, and b) the theory introduces an additional (empirical) parameter, σ_{12}, which should result in a better fit to data.

Adamson and Irani (43) used a somewhat different approach to the problem. They postulated that in a mixture of Y and Z, the following species may exist: Y_β, $(ZY_\alpha)_\gamma$, and Z_λ. They then derived expressions for the thermodynamic factor, dlna/dlnx, in terms of the hypothesized constituents in solution. Some existing theories were then applied to data, utilizing the modified thermodynamic factor.

Results of Adamson and Irani's treatment were none too favorable, since β, α, γ, and λ vary with concentration, and unreasonable association numbers were required to fit much of the data tested.

The preceding review of contributions to the literature on diffusion serves to indicate the current state of progress in the field. The lack of agreement of experiment and theory reflects the absence of a satisfactory theory of the liquid state. Particular note should be taken of the inability of any available theory to predict the diffusional behavior of non-ideal systems of the type investigated in the present study.

CHAPTER IV

EXPERIMENTAL APPARATUS

During the course of this study, experimental measurements were made on diffusion rates, viscosities, and densities of several binary liquid systems. A description of the experimental apparatus employed, with reasons for its selection and design, follows.

A. Diffusion Apparatus

1. The Diffusion Cells

The diffusion measurements were made using the diaphragm-cell technique. This technique was chosen for this study since a) Babb and Johnson (44) recommended the technique as "promising for work at higher temperatures, where difficulties with optical techniques increase significantly," b) the author's initial adviser (Dullien) had recently completed a study (26) which confirmed the applicability of this type apparatus, and c) the equipment is relatively rugged and economical.

The type of cell designed for this study is illustrated in Figure 2 and Plate I. The design is a modification of that used by Dullien (25) and is similar to one used by Burchard and Toor (14). The cell is a cylindrical vessel divided into two compartments, A and B (letters refer to Figure 2), separated by a porous diaphragm, C. The upper and lower

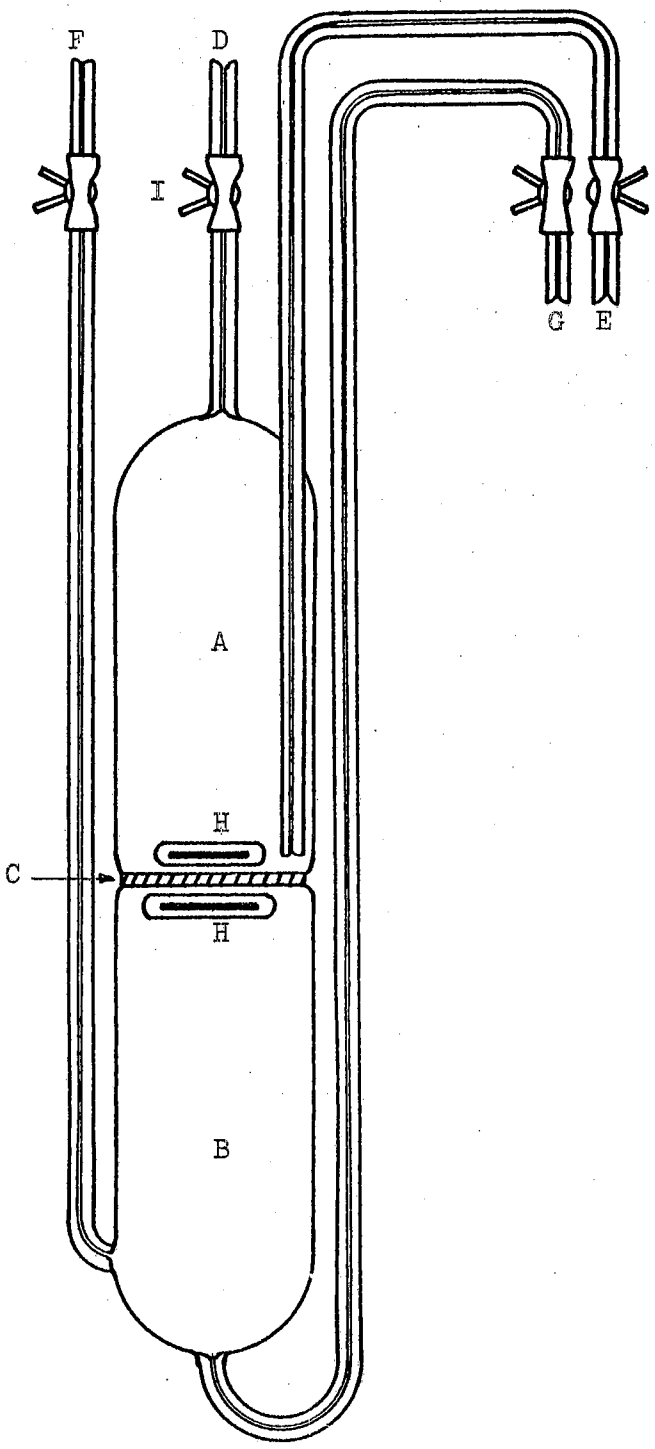

Figure 2

Modified Diaphragm Diffusion Cell

Plate I

Modified Diaphram Diffusion Cell

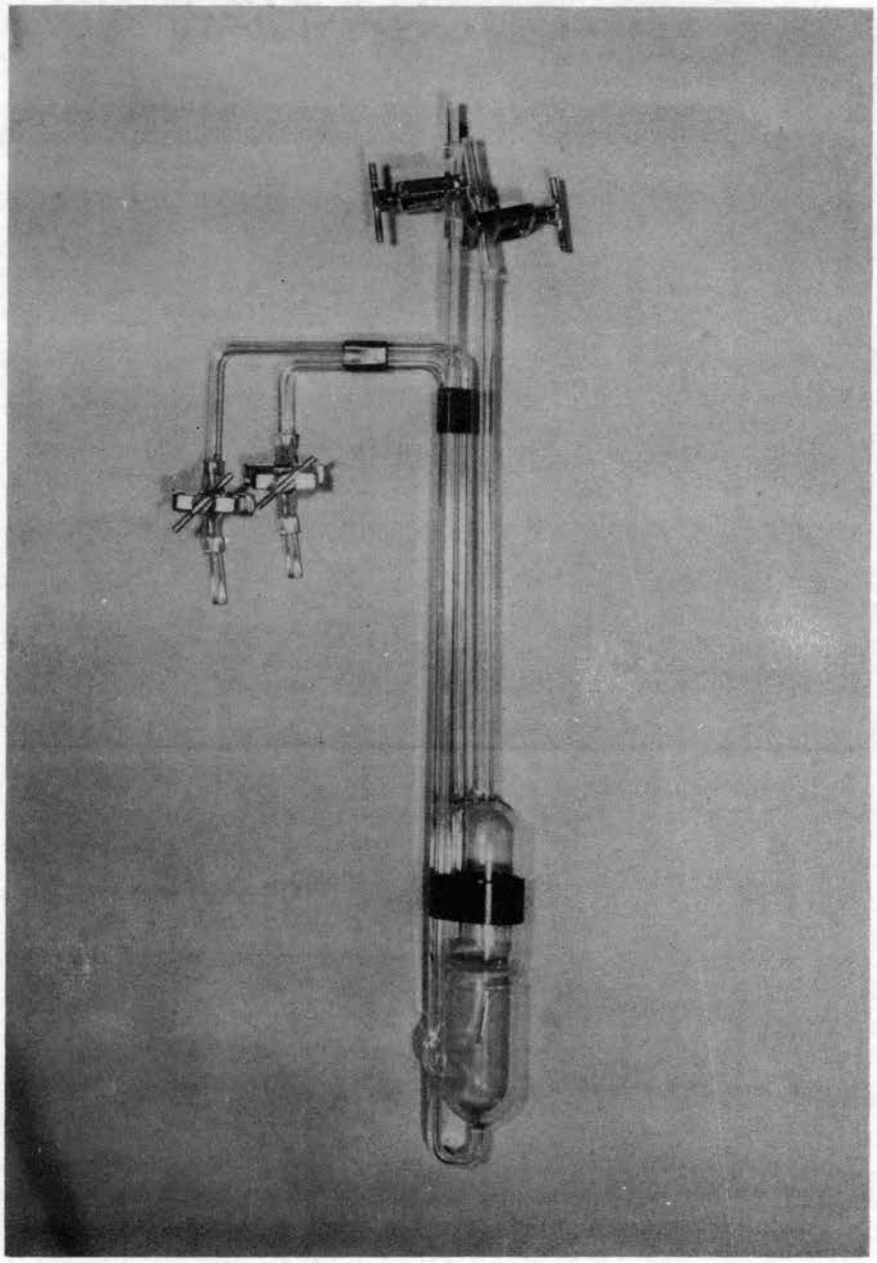

compartments are each connected to the surroundings by capillary legs, D and E, and F and G, respectively. The legs are fitted with valves, I, of a type discussed below. Each compartment contains a stirrer, H. The body of the cell, diaphragm, and legs are constructed of pyrex glass, the stirrers are iron wire sealed in soft glass.

The dimensions of the apparatus are as follows: cylinder diameter, 35 mm; diaphragm diameter, 30 mm; diaphragm thickness, 2.5 mm; height of each compartment, 7 cm; capillary tube size, 3/4 mm. i.d.; overall height of cell and legs, 48 cm. The compartment volumes are approximately 50 cc.

The diaphragms used in this study are F (fine) grade (Fisher Catalog, Item 11-136). This corresponds to pore sizes in the range 2-5 microns, which has been recommended (35) since more porous diaphragms have been reported to allow bulk streaming between compartments. The use of lower porosities (49) or different materials (50) for the diaphragm has been shown to have no effect on experimental results.

The stirrer in each compartment is cylindrical, and its length only slightly less than the diaphragm diameter. Densities of the stirrers were adjusted by inclusion of air to cause them to rest against the faces of the diaphragm (density of upper stirrer > 1.0 gm/cc; lower stirrer ≈ 0.6 gm/cc). The stirrers were driven by externally mounted magnets discussed below.

The valves, I, were constructed from polyethylene tubing fitted with commercial screw clips. These "polyethylene screw clips" were patterned after those used by Dullien (26) and were used in an effort to avoid the conventional use of stoppers (26, 67), stopcocks (48, 50), or ground glass joints (26, 64). Stoppers may be attacked by the solutions, stop-

cock lubricants adversely affect the diaphragm (67, 65) and distillation of solute through ground-glass joints has been shown to be a potential source of error (26). Teflon stopcocks were first envisioned for this work; however, the valves must not leak under aspirator vacuum, and the teflon stopcocks had to be tightened to a point where turning them was entirely too difficult.

The polyethylene screw clips were sealed to the glass capillary by application of heat from a bunsen burner at the ends of the polyethylene. Subsequently, the body of the polyethylene tubing was heated and carefully flattened with pliars. The screw clips were then seated on this flattened portion. Screw clips were reinforced with solder at their joints, and heavy wire handles were attached to facilitate tightening.

In Figure 2, the capillary legs are shown on opposite sides of the cell for clarity; reference to Plate I shows the legs are actually side-by-side and are in contact with the side of the cell. The legs were fastened to each other and to the cell by use of electrical tape (see Plate I). This reinforcement gave a surprisingly sturdy apparatus. During the entire course of the study only two breakages occurred, one by dropping a cell, the other while attempting to attach a polyethylene screw clip to an untaped cell.

Since diaphragm-cell experiments required 4 to 21 days to obtain a single data point, six experiments were run simultaneously, requiring six cells of the type described above.

2. Cell Support and Stirring

The apparatus to support the six cells and provide magnetic stirring

was essentially the same as used by Dullien (26), with minor modifications. Figure 3 and Plate II illustrate the apparatus, with the cells in place. As shown in Figure 3, six brass sleeves, D, were arranged in a hexagonal pattern. Each sleeve was designed to enclose and hold a diffusion cell. The sleeve contained three cut-out sections, or windows, L, to allow free circulation of the temperature bath fluid around the cell. The sleeve had two brass dowells protruding from its base; the dowells fit into holes drilled in a solid brass supporting column, C. These six columns were brazed to a common base plate, B. The above arrangement gave sturdy support for the cells, while allowing any cell and surrounding sleeve to be easily removed from the supporting structure.

To facilitate stirring in the cells, each cell was surrounded by a pair of bar magnets, M, whose poles were at the level of the diaphragm. Some care in aligning the diaphragm and poles was required to assure that the stirrers were not drawn away from the diaphragm faces. The two magnets were seated with epoxy resin into the face of a gear, E. The bottom face of the gear, in turn, was attached to a cylindrical shell of mild steel, J, which rested in a closely-machined hole in a large plate, G, made of "Garlite" (a linen-laminated phenol-formaldehyde resin).

The six gears, so arranged in a hexagonal pattern, were driven by a central gear, F. This central gear was mounted on a drive shaft, H, and driven by a variable-speed motor (Gerald K. Heller, Co., Model 6T60-20). Motor speed was regulated by a Model C25 Motor Controller (Gerald K. Heller, Co.). The central gear was securely positioned by means of a foot bearing, K, attached to the base of the drive shaft. The foot bearing rested in a receptacle in the brass central supporting structure, A.

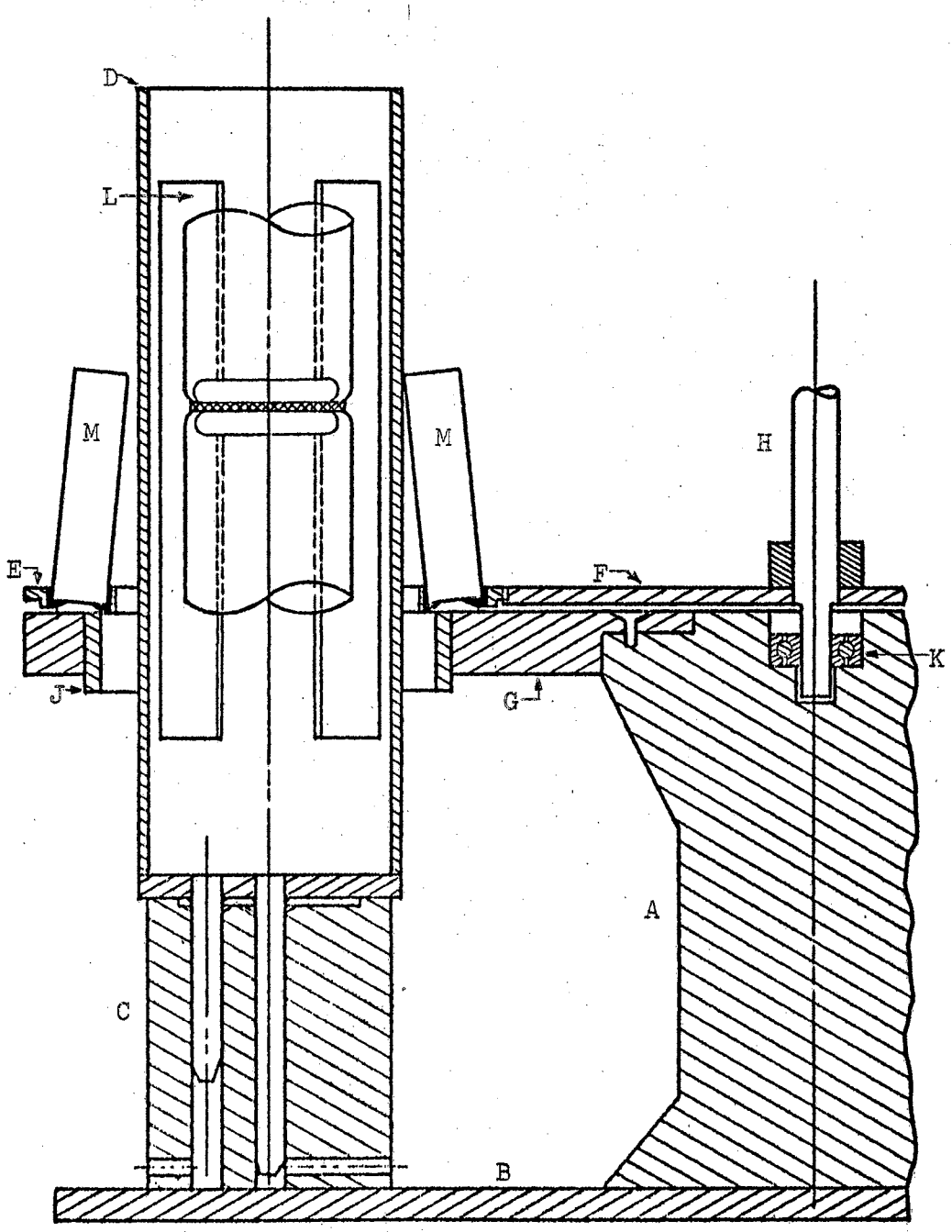

Figure 3

Cell Support and Stirring Device in Section

Plate II

Cell Support and Stirring Device

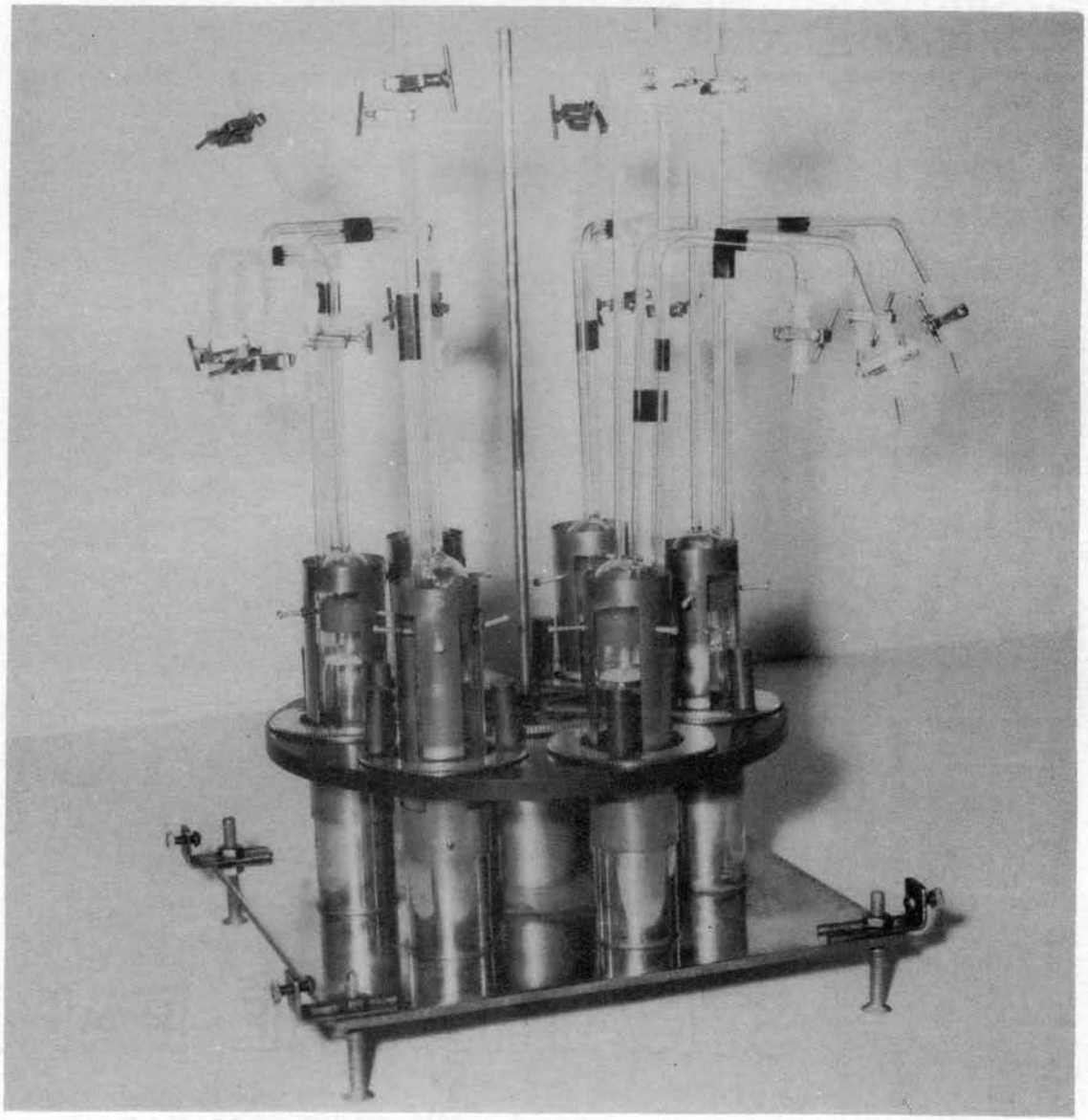

The cells were supported within the brass sleeves as follows. A cylindrical polyethylene block was machined to fit into the bottom of each sleeve. The upper face of the block was concave to seat the hemispherical base of the cell. The blocks were also slotted to allow clearance for the capillary leg which protruded from the base of the cell. These slots were sufficiently narrow to allow minimum margin for rotation of the cell within the sleeve.

Near the top of each sleeve, between the windows, three small bolts were threaded through the sleeve (not shown in Figure 3, but easily seen in Plate II). These bolts were used to position the cell and insure a level diaphragm, i.e., a horizontal diaphragm.

3. The Constant Temperature Bath

The constant temperature bath was of standard design. It was a rectangular vessel of galvanized sheet metal, lapped with two inches of corkboard, supported in a wooden housing. The bath fluid was an absorber oil petroleum fraction.

Heat was supplied to the oil via two ring heaters rated at 300 and 500 watts. The 300 watt heater was connected through a Powerstat Variable Transformer and was used as required as a constant heat supply. The 500 watt heater was connected directly to line voltage through a relay (Fisher Catalog, Item 13-99-75V2). The relay was activated by a mercury-in-glass thermoregulator (Fisher Catalog, Item 15-180-5) in the bath.

Cooling was achieved by pumping water through a cooling coil in the bath. Temperature of the cooling water was maintained at 15°C below the bath temperature by a Blue M Cooling Unit, Model PCC-1A.

The bath fluid was stirred with a variable speed mixer (Lightning Mixer, Model F); rotation of the bar magnets and gears of the cell support and stirring apparatus aided in stirring the bath fluid.

Temperatures were measured with a NBS calibrated thermometer (Princo, No. 580362). The temperature control varied from $\pm$ 0.03 to $\pm$ 0.07°C, depending on the temperature of the bath.

B. Viscosity Apparatus

Viscosities were measured using two standard Ostwald viscometers (Aloe Scientific Catalog, Item V82000). The viscometers were suspended in a 10 gallon glass bath filled with water. Temperature control and heating were furnished by a "Tecam" (Arthur S. Lapine Co.) temperature controller. The Tecam unit also pumped the bath water externally through a coil in a refrigeration unit, which served as a cold sink. Temperature control was $\pm$ 0.03°C.

Flow times were measured with a stop watch.

C. Density Apparatus

Densities were determined using 6 modified Sprengel pycnometers (Fisher Catalog, Item 3-290). The pycnometers were supplied with ground glass caps for each leg to prevent evaporation losses. The pycnometers were modified to obtain increased accuracy (26). One of the capillary legs was heated at the tip to almost close the opening. Care was taken to leave a portion of the ground glass fitting undamaged so the cap could still be seated. A portion of the other leg was drawn out to form a very narrow constriction in the leg. At this point, a hash mark was made with

a scribe.

In operation, the pycnometer was filled to the hash mark on one leg, the other leg being completely filled to the tip. The very small opening at the tip of the filled leg resulted in capillary forces which easily held the leg full of liquid.

The reasons for the above modifications were as follows. The constricted opening of the tip of one leg resulted in great reduction of fluctuations in the position of the liquid meniscus in the opposite leg due to tilting of the pycnometer. The constriction in the hash-marked leg allowed more accurate adjustment of the liquid meniscus.

The constant temperature bath for pycnometry was the same one described for viscometry.

D. Materials

The organic chemicals used in this study were from the following sources, listed with the manufacturer's minimum purity values:

Normal octane	Phillips Petroleum, Co.	99 mol %
Methylcyclohexane	"	99 mol %
Cyclohexanone	Eastman Organic Chemicals	Eastman Grade*
Normal heptanol	"	Eastman Grade

*"Highest purity chemicals...suitable for reagent use" is Eastman's purity statement.

All chemicals except n-heptanol were used as received. The heptanol was distilled on a one-inch diameter, 30 plate Oldershaw distillation column at a 10/1 reflux ratio. The first 25 volume percent of the overhead product was discarded and the remainder retained (except for the final reboiler contents).

The chemicals were analyzed on a gas chromatograph at 100°C using two different columns: six feet of tricresylphosphate (20 weight percent) on 35-80 mesh Chromosorb Red, and six feet of dinonyl phthalate on the same packing. The alcohol was also run on two feet of silicone gum rubber at 150°C. In all cases the chemicals analyzed to be in excess of 99.5 mol % pure.

Refractive indices were determined at 20°C using sodium light on a Bausch and Lomb Precision Refractometer, and densities were determined at 25°C by procedures described in Chapter V. The results, with corresponding literature values, are given below.

Chemical	Refractive Index, 20°C		Density, gm/cc, 25°C	
	Exptl.	Lit.	Exptl.	Lit.
n-Octane	1.3975_5	1.39743(5)	0.70050	0.69849(5)
Methylcyclohexane	1.4231^5	1.4232 (5)	0.76524	0.76506(5)
Cyclohexanone	1.4505_5	1.4505(37)	0.94240	0.94207*(71)
n-Heptanol, #1	1.4242_5	[1.42351(74)]	0.81874	0.8188(70)
#2	1.4242_5	[1.4249(29)]	0.81866	

*Interpolated value by author.

The two values, #1 and #2, listed for n-heptanol correspond to two separate batch purifications.

The potassium chloride used was 'Baker Analyzed' Reagent, J. T. Baker Chemical Company and had a stated purity of 99.9 wt. %. No purification was attempted.

The water used was deionized and distilled. Evaporation of water samples to dryness produced no detectible residues.

CHAPTER V

EXPERIMENTAL PROCEDURE

The experimental techniques used in obtaining the data of this study are detailed below. Many of the techniques employed were devised by Dullien (26).

A. Volumetric Data on the Diaphragm Cells

The volumes for the two compartments and the diaphragm had to be known for each cell. Volumes were determined from the weights of pure water required to fill them.

The compartment volumes were determined as follows. The cell and capillary legs were completely filled with water, and the valves, F and G (see Figure 2), on the bottom compartment were closed. Valve E was also closed and the cell was inverted. Valve E was then opened, and water began to drain from the upper compartment through leg D while air invaded leg E. As soon as leg E was completely empty, collection of the water from leg D began. A tared 100 cc weighing bottle was used to collect the water. As soon as the water level reached the entrance to leg D collection was ceased, and the contents of leg D were discarded. This sample represented the volume of the upper compartment. No water from the diaphragm or lower compartment entered the upper compartment during the above process since the lower cell was completely closed. The capillary

forces at the face of the diaphragm also served as flow barriers.

The cell was then placed in an upright position, the upper compartment and legs refilled, and valves D and E closed. Valves F and G were then opened and compressed air applied at F. As soon as leg F emptied, collection of the effluent water began. Collection ceased just as the air-water interface started into leg G. This sample represented the volume of the lower compartment.

Volumes of each compartment were determined in duplicate with an average deviation from the mean of 0.04 cc.

The diaphragm volume was determined by measuring the volume of water that was imbibed from the diaphragm surface. Using a hypodermic syringe, water was placed, drop-by-drop, on the diaphragm surface. Addition was ceased when a drop failed to be imbibed by the diaphragm. This simple procedure gave diaphragm volumes reproducible to 0.01 cc.

Complete volumetric data for the cells is listed in Table I.

B. Leveling the Diaphragm

Prior to beginning the diffusion experiments, each cell was assigned to a particular position in the supporting apparatus. The cells were placed in their specified sleeves and positioned to assure that the diaphragm was level.

Leveling of the diaphragms was begun by first carefully leveling the Garlite table of the supporting apparatus; this served as a reference point for future checks on leveling. A cell was then placed in its sleeve in the leveled supporting apparatus. The three leveling bolts were tightened to contact the cell and adjusted until the cell walls, as checked through the

three windows in the sleeve, were vertical. (Tests made by placing a glass bead on the diaphragm showed that the diaphragm was horizontal when the cylindrical body of the cell was vertical.) Two of the three leveling bolts were then fixed in position by tightening them to the sleeve with nuts. The third bolt was adjustable to allow entering and removing the cell from the sleeve.

Using the above method, the cells had to be leveled only once. Each time a cell was returned to its sleeve and the adjustable screw tightened, the cell returned to its pre-determined level position.

This care in leveling was exercised since only when the diaphragm is level and the less dense solution is above the diaphragm is the system stable with respect to gravity. Stokes (67) experimentally demonstrated that the mass-transfer rate increases as an approximately quadratic function of the angle of departure from the horizontal of the diaphragm.

C. Stirring Rate

The need for mechanical stirring in the cells has been amply demonstrated (26, 48, 67). Stirring insures homogeneity in the individual compartments and, more important, eliminates any possible stagnant layers at the diaphragm faces (which can increase the effective path length for diffusion).

Diaphragm cell results have been shown to vary with the speed of stirring when this speed is below some "critical stirring rate." Above the critical rate, results are independent of stirrer speed. Unfortunately, the values reported for the critical stirring rate vary widely. Critical stirring rates from one to 100 rpm have been reported (48, 64, 67).

To insure adequate stirring, rates of 80 rpm were used throughout this study. This is well above the critical rates reported for cells in which the stirrers rest against the diaphragm face.

Before leaving this point, brief mention should be made of a very recent work by Holmes, Wilke, and Olander (42). These authors studied the effect of properties of the solution (i.e., viscosity, diffusion rate) on the critical stirring rate. This author believes that their results may not be representative of actual diaphragm-cell performance since a) the diaphragm was in a vertical position, increasing the possibility of bulk streaming, and b) stirrers were mounted perpendicular to and away from the diaphragm, which in no way represents the situation in typical diaphragm cells.

D. Preparation of Solutions

Prior to each diffusion run, solutions of known composition were prepared. The solutions for the upper compartment had to be prepared very accurately. However, since the initial concentration in the lower compartment was always calculated via material balance, solutions for the lower compartment did not require great accuracy of preparation.

Solutions for the upper compartment were prepared gravimetrically, by mixing weighed portions of the two components forming the mixture. Solutions for the lower compartment were made by mixing predetermined volumes of the two components. The volumes were delivered from a 10 cc hypodermic syringe. One of the two compartments always contained a pure component, and the composition in the other compartment was formulated to give the desired average concentration for the run.

In the KCl-water runs, water was always in the upper compartment and approximately 0.1N KCl in the lower compartment.

E. Filling the Cells

To begin an experiment, the lower cell was filled as follows. With valves E and F closed, a shallow beaker of solution was placed at the mouth of leg G and aspirator vacuum was applied at D. Solution was drawn into the cell until the lower compartment was filled and 2 to 3 cm. of solution covered the diaphragm. Suction was removed from D, valve F opened, and suction applied to F until that leg filled above the valve. Valve F was then closed and suction discontinued. Valve G was then closed.

After filling the lower compartment, the cell was immersed to a point just below the diaphragm in a 1-liter beaker of Dow-Corning silicone oil. The beaker was situated on a hot plate, and the oil was heated until the contents of the cell boiled under a mild aspirator vacuum applied at D.

During heating, the solution first expanded to increase the liquid level above the diaphragm, then a vapor space formed beneath the diaphragm, and finally boiling began in the lower compartment. The rapid boiling forced vapors through the diaphragm at a high rate; the vapors subsequently condensed in the upper compartment.

Boiling the solution served two purposes. First, it degassed the solution in the lower compartment. Second, the flow of vapors through the diaphragm served to flush out any entrapped air from the diaphragm pores. The effectiveness of the air displacement was evidenced by the fact that a pea-sized air bubble always remained in the lower compartment after filling; after boiling the bubble was always gone.

With the lower cell thus filled and degassed, it was placed in its sleeve and seated in the supporting apparatus in the bath. The bath fluid covered the top compartment by about one inch. The cell was allowed to remain in the bath for 30 minutes to establish thermal equilibrium. No stirring was employed during this time to lessen the uptake of air by the degassed solution.

After the cell had attained the bath temperature, the solution in the upper cell was removed by opening valve E and applying compressed air at D. Since leg E terminates a few millimeters above the diaphragm, a small amount of liquid remained above the diaphragm. This liquid was removed by inserting a very fine metal capillary tube through leg D and attaching the metal capillary to aspirator vacuum. The tip of the metal tube was brought very near the diaphragm to withdraw the last few drops of solution from the upper compartment.

The upper compartment was then rinsed with a portion of solution of the composition to be used in the upper cell. This solution was drawn in through E using suction at D. The rinse solution was emptied as above, the compartment refilled with solution of desired composition, and valve E was closed. Valve D was left open so any volume changes during diffusion could occur at constant pressure.

All solutions introduced into the upper compartment were pre-adjusted to the bath temperature.

F. Degassing Solutions

All solutions were degassed to avoid possible bubble formation in the diaphragm. The lower solutions were always degassed by boiling, as described

above. Different procedures were used for degassing the aqueous and organic solutions for the upper compartment.

Pure water was always used in the upper compartment for the KCl-water runs. The water was degassed by boiling and cooling rapidly to the bath temperature. The degassed water was used immediately.

The organic solutions were degassed by freezing and melting under slight aspirator vacuum. Freezing was accomplished in dry ice-acetone or liquid nitrogen baths, depending on the melting temperature of the mixture.

G. Preliminary Diffusion

The diffusion coefficient calculated from the experimental results is based on the "quasi-steady state" assumption. In Chapter II, the point was made that this assumption is much less in error if a concentration gradient exists across the diaphragm at the start of an experiment. For this reason a short period of diffusion was always employed prior to the actual run to establish such a concentration gradient.

The preliminary diffusion was conducted using approximately 20 cc of solution in the upper cell. The solution was identical to that used in the actual run. Low stirring rates were used during preliminary diffusion to minimize air absorption by the upper solution. Duration of the preliminary diffusion was estimated from the relation $Dt/L^2 = 1.2$, as suggested by Gordon (35).

At the end of the preliminary diffusion run, the upper compartment was emptied, refilled with fresh solution, the higher stirring rate employed, and timing of the actual run begun.

During preliminary diffusion a small, but significant, change in

concentration occurred in the lower solution. However, since the initial concentration of the lower solution was not measured, but determined by material balance, the effect of this concentration change was accounted for.

H. Sampling

Sampling from the upper compartment was done by applying compressed air at D then opening valve E. The first few drops from E, the contents of leg E, were discarded; the remainder was collected in a 2 oz. sample bottle fitted with a screw-on plastic cap. This point marked the end of the diffusion time.

The lower compartment was then sampled by opening valve F (any solution above the valve was withdrawn via a hypodermic syringe and discarded) and applying compressed air at F. Several bubbles of air were allowed to enter the lower compartment prior to opening valve G. This air forced some of the lower solution and/or air into the diaphragm. Valve G was then opened, the first few drops from G discarded, and the rest collected as above.

Note that during sampling the lower cell, about 0.2 cc of solution below the valve in leg F was collected with the sample. This 0.2 cc was essentially at the initial concentration of the lower solution, and account for it may be easily made. The liquid, rather than air, was used to fill F since fluctuations in room temperature would cause more pulsing in the leg if air were used.

Total sampling time varied with the viscosity of the solution and, consequently, with bath temperature. The sampling time, from a few seconds to several minutes, was always entirely insignificant when compared to the total time of the experiment.

I. Calibration of the Cells

In order to use a diaphragm cell, the "effective" length and total cross-sectional area for diffusion must be known for that cell. These quantities are always "back-calculated" by performing an experiment with a system whose diffusion coefficient is accurately known.

In this work, all cells were calibrated using the system potassium chloride-water as the standard. The integral diaphragm-cell diffusion coefficient was taken from Stokes (66). This standard, with a few exceptions (14), is used exclusively in diaphragm-cell experiments.

These diffusion runs required four days for the 0.1 N KCl solution to decrease to 0.075 N, as Stokes (66) recommends. The results, expressed in terms of the cell constant, β (see Equations II-8 and II-9), are given for each cell in Table II.

The cell constant was determined for each cell at the start of this study and again after approximately 2,400 hours of diffusion. The recalibration was necessary since attrition of the stirrers causes some wear on the diaphragm.

J. Analysis of Samples

1. The KCl-Water Runs

The aqueous KCl samples were analyzed by evaporating known aliquots of sample to dryness and determining the residue weight. Each sample concentration was determined in triplicate.

To exploit the potential accuracy of this analytical method, considerable care was exercised in the experimental technique. The 100 cc weighing

bottles (Kimax Catalog, Item 1514 6) used in the analysis were first carefully washed and rinsed in distilled water. The bottles were then placed in a clean enameled pan and put in an oven (Fisher Catalog, Item 696) at 100°C to dry; the temperature was finally raised to 280°C. After cooling, the bottles were covered by a plastic sheet to shield them from dust.

The empty bottles were weighed on a Mettler Gram-atic Semi-Micro Balance with a stated precision of 0.00002 grams. The bottles were wiped with a moist chamois and placed, four at a time, inside the balance case. Approximately 30 minutes was allowed for the bottles to reach the temperature of the balance case. The caps were placed on the bottles "upside-down" to prevent contact of the ground-glass surfaces, since minor chippage frequently occurred during opening and closing of the lids.

In all cases, one of the four bottles in the balance case was a "standard bottle" or "blank", identical to the others, but one which would not receive a sample. The standard bottle was used to facilitate bouyancy corrections to the weighings. Bouyancy corrections are discussed in Appendix C.

The four empty bottles were each weighed on the balance. The procedure was to zero the balance, place the first bottle on the pan, then move the second, third, and fourth bottles, in turn, into the positions vacated by their predecessor. The first bottle was then weighed, removed from the pan, and placed in the position vacated by the fourth bottle. The balance was re-zeroed, and the second bottle was weighed by the above procedure. In this rotating manner, weighings were continued until each bottle had been weighed three times. The average weight of each bottle was recorded. Three new bottles were then placed in the case with the standard bottle and the above procedure repeated.

The rotating procedure described above was used to reduce the effect of radiated body heat on the bottle weights. Without rotation, variation in weight of the bottles nearest the operator were much greater than when rotation was used.

The tared bottles were filled with 10 cc aliquots of samples delivered from a calibrated pipet. A three-way pipet bulb (Fisher Catalog, Item 13-681-50) was used for very precise positioning of the meniscus at the hash mark on the pipet stem. Precision of pipeting was estimated as $\pm$ 0.002 cc. The pipet was calibrated with water and results appear in Table E-III.

A porcelaintray, containing the filled sample bottles and standard bottle, was placed in the oven at 60°C. The samples were left in the oven overnight to evaporate to dryness. The next day the temperature was gradually raised to 280°C to expell the last traces of moisture. (This drying procedure was recommended by McBain (49).

On removal from the oven, the bottles were capped and re-covered with the plastic sheet. The gross weights were determined in exactly the same manner as the tare weights, except the bottle lids were left in place.

The weight of KCl residue was calculated from the equation

$$W_r = W' - \frac{W}{W_s}(W'_s - W_s) - W \qquad \text{(V-1)}$$

where W_r = weight of the KCl residue, gms

W, W' = weight of sample bottle, tare and gross, respectively, gms

W_s, W'_s = weight of standard bottle at the time weights W and W', respectively, were measured, gms

Equation V-1 is derived in Appendix C.

2. The Organic Runs

The organic samples were analyzed by pycnometry, i.e., by determining their densities. Six 20 cc pycnometers of the type described in Chapter IV were calibrated with distilled water using procedures identical to those described below. The precision of the volumes was estimated as $\pm$ 0.0003 cc. Results of the calibrations are given in Table E-III.

Pycnometers were cleaned in chromic-acid solution, rinsed in water, then acetone, and dried by the flow of dried compressed air. Tare weights were then determined as follows.

The pycnometers and caps were wiped with a moist chamois, and the caps were placed on the pycnometer legs. The caps were secured to the pycnometers by looping each cap with a fine wire and joining the opposite ends of the two wires. Without this precaution, frequent cap breakage occurred. The pycnometers were then placed, three each, on two wire supporting frames beside the balance. A standard bottle, kept inside the balance case, was also wiped with the chamois.

The standard bottle used in the pycnometry was a 125 cc erlenmeyer flask, sealed at the top by a glass blower. The bottle was calibrated such that the air density was known as a function of the bottle weight. (See Appendix C for details.)

After a 30 minute period of temperature equilibration, the standard bottle was weighed. The six pycnometers were then weighed, using a rotating scheme on the wire supporting frames. A wire hook was used to suspend the pycnometer above the pan during weighing. After each pycnometer had

been weighed, in turn, three times, the hook was weighed. Weights of the pycnometers, standard bottle, and hook were recorded.

The pycnometers were then filled with samples. Each sample was run in duplicate. The pycnometers were filled through the leg with the constricted tip by applying very slight aspirator vacuum to the opposite leg. Special tubes with ground glass fitting were supplied with the pycnometers to aid in filling. Each pycnometer was filled to a point just past the mark on the hash-marked leg, then suspended in the water bath.

After a 20 minute period, the meniscus was carefully adjusted to the hash mark by touching the tip of the opposite (filled) leg with a piece of absorbent paper. A very thin roll of the paper was then inserted into the unfilled portion of the leg with the hash mark to remove traces of solution clinging to the tube wall. The pycnometer was removed from the bath, the ground-glass joints wiped thoroughly dry, and the caps immediately replaced, starting with the completely-filled leg.

Gross weights were determined by exactly the same procedure as the tare weights. The sample bottle was also reweighed. The weight of the pycnometer, corrected to vacuo, was determined from the relation

$$W^{o} = W \left[1 + \rho_{air} \left(\frac{1}{\rho} - \frac{1}{\rho_{w}} \right) \right] \qquad \text{(V-2)}$$

where W^{o} = weight, in vacuo, of the pycnometer and contents (if any), gms

ρ_{air} = air density (found from standard bottle weight), gm/cc

ρ = density of pycnometer plus contents (if any), gm/cc

W = weight, in air, of the pycnometer and contents (if any), gms

ρ_W = density of weights used in the balance, gm/cc

The difference in the values for W^o for the filled and empty pycnometer gave the sample weight, in vacuo; the ratio of sample weight to pycnometer volume gave the sample density. Appendix C contains a derivation of Equation V-2 and a description of how it was applied.

The densities, ρ, determined above were converted to concentrations, ρ_A, from experimentally determined ρ-ρ_A relations. Solutions of known compositions were prepared gravimetrically and their densities determined. These gave the desired relation of density to composition.

K. Viscosity Measurements

The viscosity measurements were made using standard techniques for Ostwald viscometers. The viscometers were cleaned in a manner identical to that used for the pycnometers. Each viscometer was then filled with sample and placed in the water bath for 15 minutes. A 5 cc pipet was used to accurately deliver samples to the viscometers.

The viscometers were calibrated with water via the standard technique. Samples of known composition, prepared gravimetrically, were then investigated. Flow times were measured a minimum of two times for each sample. The viscosities were calculated by methods illustrated in Appendix F.

CHAPTER VI

EXPERIMENTAL RESULTS

During this study, diffusion data were obtained over the complete concentration range for each of the following systems at the specified temperatures at ambient pressure:

I. normal octane - methylcyclohexane, 25°C

II. normal octane - cyclohexanone, 25°C

III. normal heptanol - methylcyclohexane, 25°C

IV. normal heptanol - cyclohexanone, 10, 25, 55, 90°C

Viscosity and density measurements were also made on each of the above systems with the exception of system IV at 10°C. These 10°C data were not taken due to limitations of existing equipment.

In the remainder of this chapter, the experimental results are tabulated along with some pertinent comments regarding the data. Appendix E contains much of the measured data from which the tabulated results were obtained. Accuracy of the data is discussed in Chapter VII.

A. Volumetric Data

Table I presents the data on the volumes of the upper and lower compartments and the diaphragm for each of the six diffusion cells. Cell volumes are the average of two measurements, and diaphragm volumes represent

three measurements.

Volumetric data on the pipet and pycnometers used in sample analyses are listed in Appendix E.

B. Diffusion Cell Calibration Data

Cell constants, β, were determined for each cell at the beginning of this study and again after about 2,400 hours of total diffusion time. Initial calibrations were replicated two to four times to establish the accuracy of the techniques employed. Recalibration was not done in replicate. The data appear in Table II.

C. Diffusion Data for Organic Systems

The diffusion data for the seven binary systems studied are listed in Tables III through IX. Each value of the integral diffusion coefficient, $\bar{D}$, represents a single experimental determination. The column headed $(\rho_A)_{Avg}$ contains the average of the two initial and two final concentrations in the cell. The column headed ρ_A presents the value of the concentration at which $\bar{D}$ is numerically equal to the differential diffusion coefficient, D. (Values of D at the two ends of the concentration range are also listed.) These ρ_A values were determined from the set of $\bar{D}$ versus $(\rho_A)_{Avg}$ values by methods discussed in Chapter VII. For certain of the systems, the integral and differential coefficients are identical within the experimental accuracy, and the $(\rho_A)_{Avg}$ and ρ_A columns are combined in these cases. Smoothed diffusion coefficients appear in Table X.

The column headed "Run" in each of the above tables contains numbers

of the form M.N/P. The value of M denotes the chronological order of the system in the experimental study, i.e., the system in Table III was the second system studied. The value of N refers to the order of experimental runs within a system, and P refers to the number of the cell used for that particular data point.

The data of Tables III through IX are illustrated in Figures 4 through 10. Each organic diffusion run was made using the maximum possible initial concentration difference compatible with the desired average concentration.

D. Viscosity Data

The viscosity data from this study are listed in Tables XII through XV. The data are illustrated in Figures 11 through 16.

E. Density Data

The density-composition data are listed in Tables XVI through XX. Each listed density is the mean of two determinations. For completeness, the concentrations (mass fraction times density) are tabulated in addition to the mass fractions and densities.

TABLE I

VOLUMETRIC DATA FOR DIAPHRAGM CELLS

Cell	Upper Volume, cc	Lower Volume, cc	Diaphragm Volume, cc
1 (50)	48.20	49.76	0.37
2 (30)	48.62	47.10	0.31
3 (0)	50.12	47.96	0.33
4 (60)	49.52	49.08	0.27
5 (10)	47.62	50.38	0.34
6 (40)	51.14	49.50	0.29

TABLE II

CELL CONSTANTS FOR DIAPHRAGM CELLS

Cell Constant, β, cm^{-2}

	Cell 1	Cell 2	Cell 3	Cell 4	Cell 5	Cell 6
			Initial Calibration			
	0.1309	0.0922	0.1168	0.0894	0.1247	0.0952
	0.1309	0.0918	0.1166	0.0895	0.1248	0.0959
		0.0922	0.1166		0.1250	0.0954
						0.0952
Avg.	0.1309	0.0921	0.1167	0.0895	0.1248	0.0954
			Recalibration, After 2,400 Hours			
	0.1299	0.0911	0.1155	0.0915	0.1246	0.0949

TABLE III

DIFFUSION COEFFICIENTS AT 25°C FOR THE

N-OCTANE-METHYLCYCLOHEXANE SYSTEM

Run	Integral Diffusion Coefficient, $\bar{D}$, $cm^2/sec \times 10^5$	ρ_{Avg} (n-Octane), gm/cc	ρ (n-Octane), gm/cc
-	1.611*	-	0.0
2.2/1	1.738	0.0588	0.059
2.2/3	1.853	0.1160	0.115
2.1/2	1.976	0.2006	0.190
2.2/5	2.041	0.2728	0.246
2.1/4	1.118	0.3590	0.325
2.2/2	2.190	0.4543	0.430
2.4/6	2.231	0.5428	0.513
2.1/3	2.255	0.5567	0.564
2.2/4	2.290	0.6070	0.661
2.4/4	2.249	0.6088	0.550
2.4/5	2.278	0.6557	0.635
-	2.301*	-	0.70050

*Extrapolated value

TABLE IV

DIFFUSION COEFFICIENTS AT 25°C FOR THE

N-OCTANE-CYCLOHEXANONE SYSTEM

Run	Integral Diffusion Coefficient, $\bar{D}$, $cm^2/sec \times 10^5$	ρ_{Avg} (n-Octane), gm/cc	ρ(n-Octane), gm/cc
-	0.741*	-	0.0
3.2/1	0.708	0.0548	0.055
3.1/3	0.706	0.0552	0.055
3.2/4	0.674	0.1672	0.122
3.3/3	0.661	0.2202	0.168
3.2/2	0.681	0.2683	0.346
3.1/5	0.739	0.3508	0.421
3.1/1	0.759	0.3528	0.441
3.3/5	0.795	0.4341	0.466
3.3/6	0.929	0.5131	0.529
3.3/1	1.139	0.5832	0.590
3.2/5	1.129	0.5845	0.588
3.3/2	1.376	0.6279	0.630
3.1/4	1.686	0.6644	0.664
3.3/4	1.711	0.6691	0.665
3.2/3	1.843	0.6703	0.676
-	2.20*	-	0.70050

*Extrapolated value

TABLE V

DIFFUSION COEFFICIENTS AT 25°C FOR THE

METHYLCYCLOHEXANE(MCH)-N-HEPTANOL SYSTEM

Run	Integral Diffusion Coefficient, $\bar{D}$, $cm^2/sec \times 10^5$	ρ_{Avg} (MCH) gm/cc	ρ(MCH) gm/cc
-	0.470*	-	0.0
4.1/1	0.505	0.0699	0.069
4.2/5	0.528	0.1373	0.140
4.2/2	0.560	0.2550	0.231
4.1/2	0.581	0.3837	0.327
4.2/4	0.601	0.4968	0.491
4.2/3	0.609	0.5931	0.601
4.2/1	0.610	0.6581	0.619
4.2/6	0.616	0.7128	0.730
-	0.618*	-	0.76524

*Extrapolated value

TABLE VI

DIFFUSION COEFFICIENTS AT 25°C FOR THE

N-HEPTANOL-CYCLOHEXANONE SYSTEM

Run	Integral Diffusion Coefficient, $\bar{D}$, $cm^2/sec \times 10^5$	ρ_{Avg} (n-Heptanol), gm/cc	ρ (n-Heptanol), gm/cc
-	0.576*	-	0.0
1.3/1	0.542	0.0564	0.062
1.3/3	0.515	0.1064	0.117
1.4/6	0.526	0.1082	0.096
1.3/4	0.491	0.1981	0.171
1.3/5	0.458	0.2762	0.250
1.3/6	0.432	0.3507	0.315
1.4/1	0.423	0.3779	0.351
1.1/5	0.416	0.4085	0.378
1.3/2	0.406	0.4143	0.417
1.1/1	0.406	0.4635	0.417
1.1/6	0.377	0.5735	0.561
1.1/2	0.368	0.6494	0.610
1.1/3	0.347	0.7227	0.741
1.4/5	0.350	0.7227	0.720
-	0.335*	-	0.81874

*Extrapolated value

TABLE VII

DIFFUSION COEFFICIENTS AT 10°C FOR THE

N-HEPTANOL-CYCLOHEXANONE SYSTEM**

Run	Integral Diffusion Coefficient, $\bar{D}$, $cm^2/sec \times 10^5$	ρ_{Avg} (n-Heptanol), gm/cc, 25°C	ρ(n-Heptanol), gm/cc, 25°C
-	0.394*	-	0.0
7.1/3	0.352	0.1025	0.098
7.1/2	0.321	0.1803	0.175
7.1/4	0.255	0.4077	0.380
7.1/6	0.233	0.5431	0.479
7.1/5	0.195	0.7226	0.771
7.1/1	0.202	0.7306	0.689
-	0.194*	-	0.81874

*Extrapolated value
**Only data taken using batch #2 of n-heptanol (See Chapter IV, D)

TABLE VIII

DIFFUSION COEFFICIENTS AT 55°C FOR THE

N-HEPTANOL-CYCLOHEXANONE SYSTEM

Run	Integral Diffusion Coefficient, $\bar{D}$, $cm^2/sec \times 10^5$	ρ_{Avg} (n-Heptanol),** gm/cc
-	1.051*	0.0
5.1/5	1.020	0.0702
5.1/1	0.961	0.2145
5.1/3	0.926	0.3129
5.1/6	0.838	0.5130
5.1/4	0.812	0.6141
-	0.744*	0.79752

*Extrapolated value
**ρ_{Avg} and ρ are identical for this system.

TABLE IX

DIFFUSION COEFFICIENTS AT 90°C FOR THE

N-HEPTANOL-CYCLOHEXANONE SYSTEM

Run	Integral Diffusion Coefficient, $\bar{D}$, $cm^2/sec \times 10^5$	ρ_{Avg} (n-Heptanol),** gm/cc
-	1.919*	0.0
6.1/5	1.906	0.0611
6.2/1	1.840	0.0817
6.1/2	1.825	0.2098
6.2/6	1.740	0.3226
6.1/3	1.695	0.4979
6.2/2	1.698	0.5566
6.1/4	1.676	0.5951
6.1/1	1.664	0.6675
6.2/3	1.648	0.6687
-	1.647*	0.77044

*Extrapolated value

**ρ_{Avg} and ρ are identical for this system.

TABLE X

SMOOTHED DIFFUSION COEFFICIENTS

Mole Fraction Straight-Chain Component	Smoothed Differential Diffusion Coefficient, $cm^2/sec \times 10^5$						
	I*	II	III	IVa	IVb	IVc	IVd
0.0	1.611	0.741	0.618	0.576	0.394	1.051	1.918
0.1	1.800	0.680	0.613	0.519	0.351	1.007	1.859
0.2	1.940	0.655	0.609	0.475	0.310	0.964	1.812
0.3	2.042	0.659	0.604	0.438	0.281	0.929	1.772
0.4	2.113	0.686	0.598	0.413	0.255	0.893	1.740
0.5	2.166	0.745	0.588	0.395	0.237	0.864	1.714
0.6	2.202	0.841	0.575	0.380	0.220	0.837	1.693
0.7	2.233	0.980	0.557	0.366	0.209	0.812	1.676
0.8	2.258	1.190	0.534	0.355	0.202	0.787	1.663
0.9	2.280	1.590	0.505	0.345	0.197	0.765	1.653
1.0	2.302	2.200	0.470	0.335	0.194	0.744	1.646

* I n-Octane - MCH, 25°C
II n-Octane - Cyclohexanone, 25°C
III n-Heptanol - MCH, 25°C
IV n-Heptanol - MCH, a-25°, b-10°, c-55°, d-90°C

TABLE XI

VISCOSITY DATA AT 25°C FOR THE

N-OCTANE-METHYLCYCLOHEXANE

SYSTEM

Mass Fraction n-Octane	Mole Fraction n-Octane	Viscosity, cp
0.0	0.0	0.680
0.0988	0.0861	0.655
0.1986	0.1756	0.633
0.3586	0.3246	0.602
0.5052	0.4674	0.577
0.6505	0.6153	0.559
0.8046	0.7797	0.535
0.9035	0.8894	0.526
1.0	1.0	0.517

TABLE XII

VISCOSITY DATA AT 25°C FOR THE

N-OCTANE-CYCLOHEXANONE

SYSTEM

Mass Fraction n-Octane	Mole Fraction n-Octane	Viscosity, cp
0.0	0.0	2.000
0.0956	0.0833	1.590
0.1955	0.1727	1.310
0.3515	0.3177	1.023
0.5061	0.4682	0.829
0.6593	0.6244	0.693
0.8072	0.7825	0.602
0.9071	0.8935	0.550
1.0	1.0	0.517

TABLE XIII

VISCOSITY DATA AT 25°C FOR THE

METHYLCYCLOHEXANE-N-HEPTANOL

SYSTEM

Mass Fraction MCH	Mole Fraction MCH	Viscosity cp
0.0	0.0	5.868
0.0955	0.1111	4.608
0.1958	0.2237	3.546
0.3498	0.3890	2.371
0.4962	0.5382	1.643
0.6505	0.6878	1.192
0.8028	0.8282	0.890
0.9045	0.9180	0.757
1.0	1.0	0.680

TABLE XIV

VISCOSITY DATA AT 25°C FOR THE

N-HEPTANOL-CYCLOHEXANONE

SYSTEM

Mass Fraction n-Heptanol	Mole Fraction n-Heptanol	Viscosity, cp
0.0	0.0	2.000
0.1178	0.1014	1.965
0.2282	0.1998	2.034
0.3397	0.3029	2.160
0.4441	0.4029	2.351
0.5415	0.4994	2.584
0.6376	0.5978	2.914
0.7315	0.6971	3.335
0.8264	0.8008	3.921
0.9098	0.8949	4.663
1.0	1.0	5.868

TABLE XV

VISCOSITY DATA AT 55 AND 90°C FOR THE

N-HEPTANOL-CYCLOHEXANONE SYSTEM

Mass Fraction n-Heptanol	Mole Fraction n-Heptanol	Viscosity, cp	
		55°	90°
0.0	0.0	1.149	0.670
0.1122	0.0965	1.119	0.658
0.3013	0.2669	1.164	0.659
0.4993	0.4572	1.280	0.689
0.6991	0.6624	1.533	0.770
0.9011	0.8850	1.982	0.891
1.0	1.0	2.350	0.982

TABLE XVI

DENSITY DATA AT 25°C FOR THE

N-OCTANE-METHYLCYCLOHEXANE

SYSTEM

Mass Fraction n-Octane	Density, ρ, gm/cc	Concentration of n-Octane, ρ_A, gm/cc
0.0	0.76524	0.0
0.11358	0.75716	0.08600
0.22473	0.74940	0.16841
0.43611	0.73528	0.32066
0.63572	0.72246	0.45928
0.91621	0.70534	0.64624
1.0	0.70050	0.70050

TABLE XVII

DENSITY DATA AT 25°C FOR THE

N-OCTANE-CYCLOHEXANONE

SYSTEM

Mass Fraction n-Octane	Density, ρ, gm/cc	Concentration of n-Octane, ρ_A, gm/cc
0.0	0.94240	0.0
0.15174	0.89498	0.13580
0.30124	0.85296	0.25695
0.50153	0.80242	0.40244
0.69907	0.75824	0.53006
0.84582	0.72868	0.61633
1.0	0.70050	0.70050

TABLE XVIII

DENSITY DATA AT 25°C FOR THE

METHYLCYCLOHEXANE-N-HEPTANOL

SYSTEM

Mass Fraction MCH	Density, ρ, gm/cc	Concentration of MCH, ρ_A, gm/cc
0.0	0.81874	0.0
0.09910	0.81303	0.08057
0.29960	0.80150	0.24013
0.50023	0.79026	0.39531
0.62419	0.78353	0.48907
0.69939	0.77964	0.54527
1.0	0.76524	0.76524

TABLE XIX

DENSITY DATA AT 25°C FOR THE

N-HEPTANOL-CYCLOHEXANONE

SYSTEM

Mass Fraction n-Heptanol	Density, ρ, gm/cc	Concentration of n-Heptanol, ρ_A, gm/cc
0.0	0.94240	0.0
0.22821	0.91028	0.20773
0.33966	0.89554	0.30418
0.44411	0.88226	0.39182
0.54153	0.87038	0.47134
0.63764	0.85895	0.54770
0.73154	0.84814	0.62045
0.82637	0.83756	0.69213
0.90976	0.82846	0.75370
1.0	0.81874	0.81874

TABLE XX

DENSITY DATA AT 55° AND 90°C FOR THE

N-HEPTANOL-CYCLOHEXANONE SYSTEM

Mass Fraction n-Heptanol	Density, , gm/cc, 55°C	Concentration of n-Heptanol, ρ_A, gm/cc, 55°	Density, , gm/cc, 90°	Concentration of n-Heptanol ρ_A, gm/cc, 90°
0.0	0.91594	0.0	0.88390	0.0
0.11223	0.90050	0.10101	0.86839	0.09746
0.30127	0.87510	0.26364	0.84440	0.25439
0.50138	0.85079	0.42657	0.82107	0.41167
0.69907	0.82854	0.57921	0.79990	0.55919
0.90112	0.80736	0.72834	0.77978	0.70268
1.0	0.79752	0.79752	0.77044	0.77044

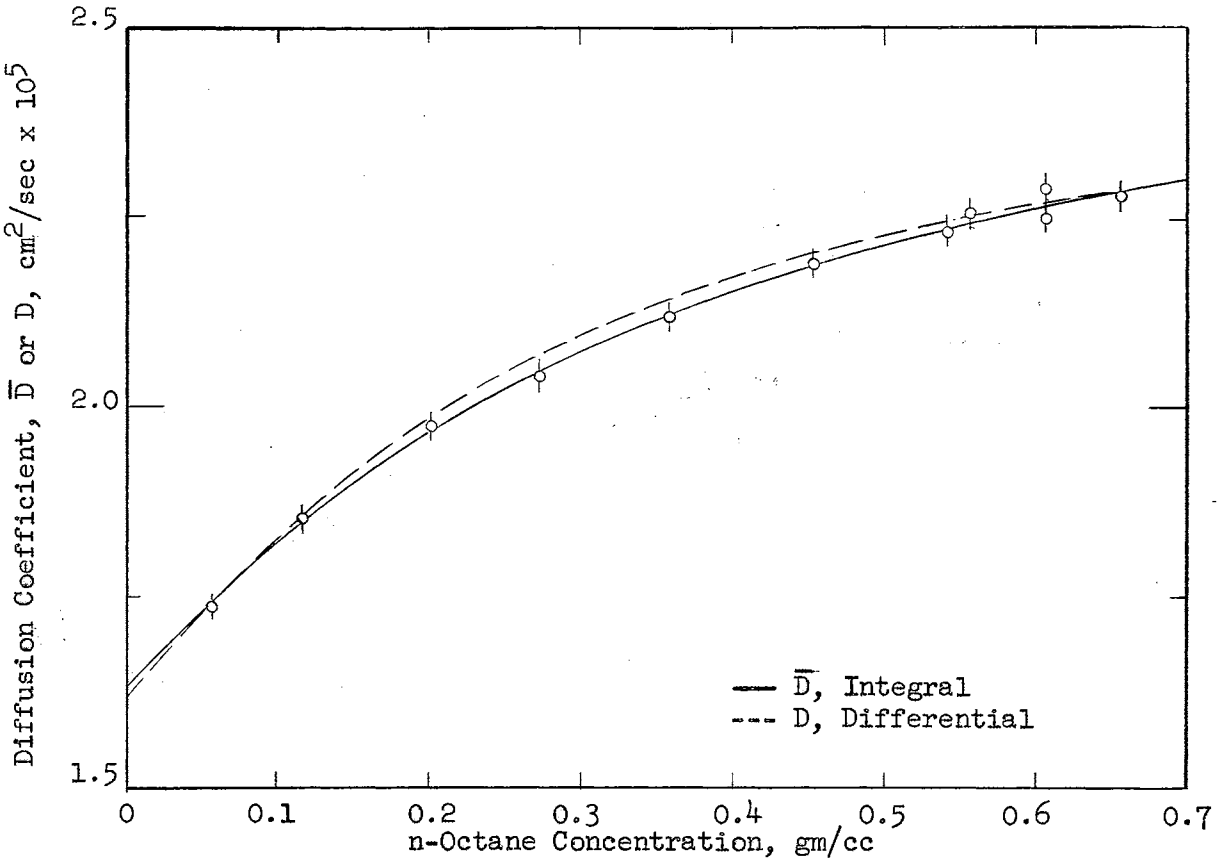

Figure 4

Diffusion Coefficients for the n-Octane-MCH System, 25°C

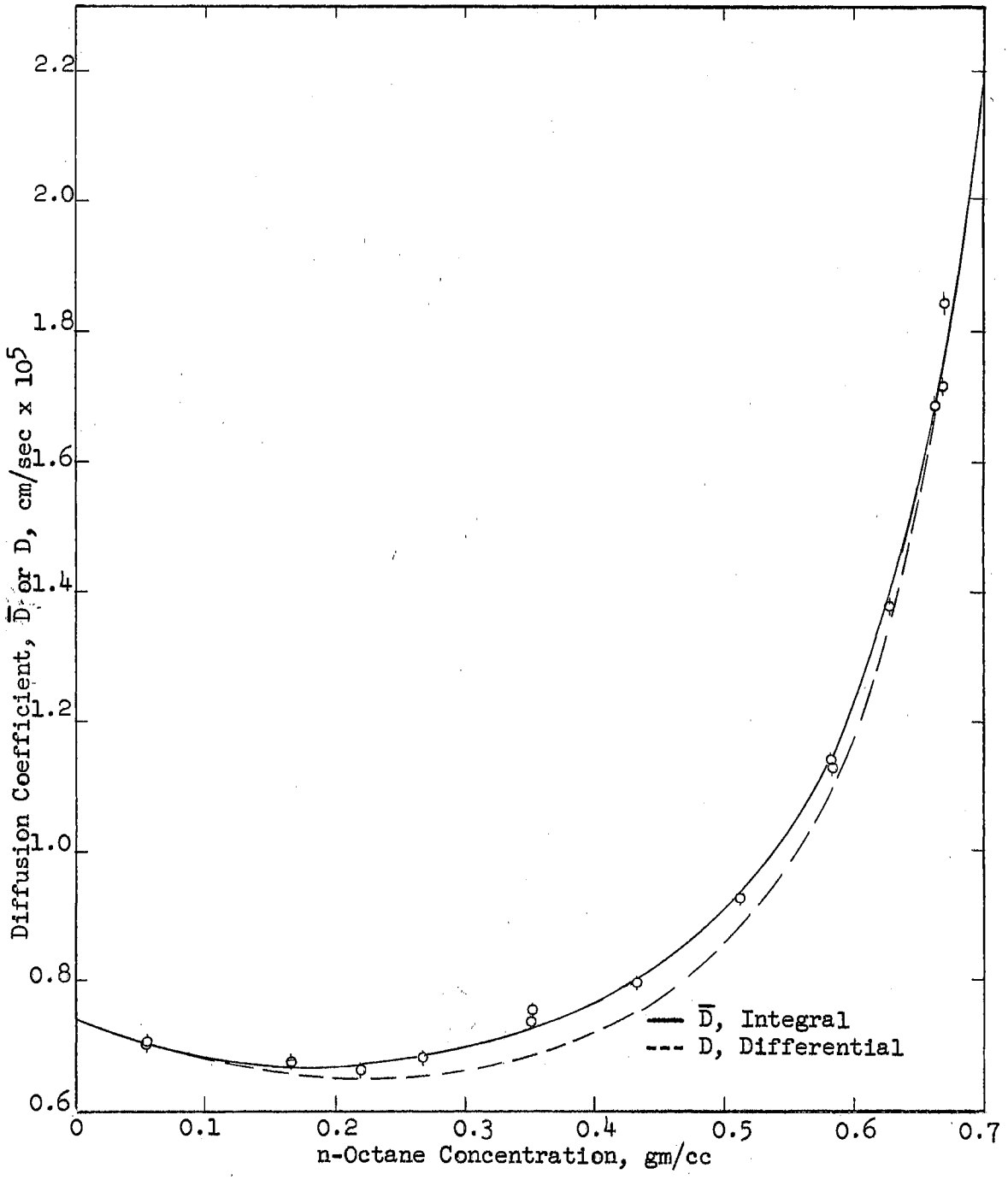

Figure 5

Diffusion Coefficients for the n-Octane-Cyclohexanone System, 25°C

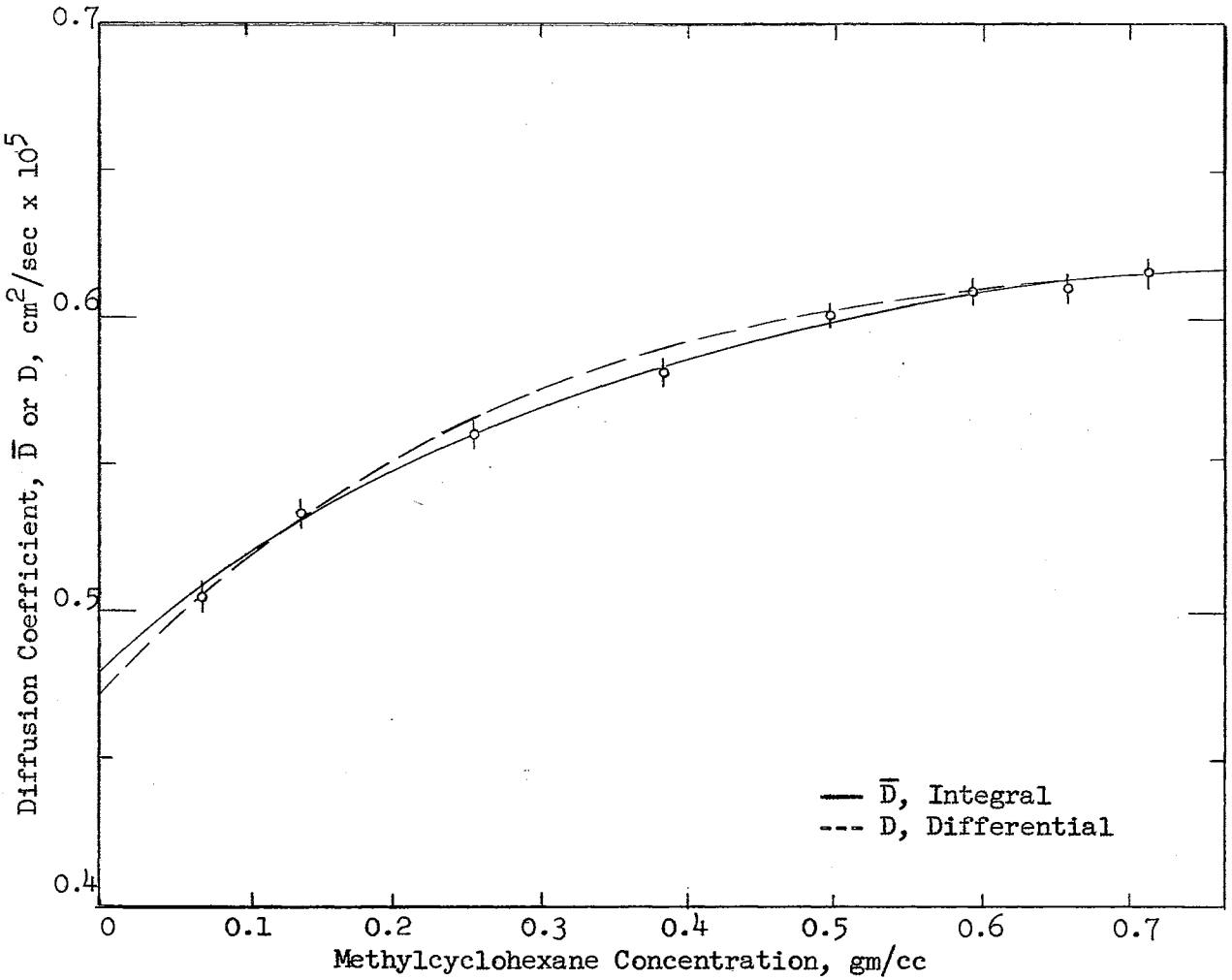

Figure 6

Diffusion Coefficients for the MCH-n-Heptanol System, 25°C

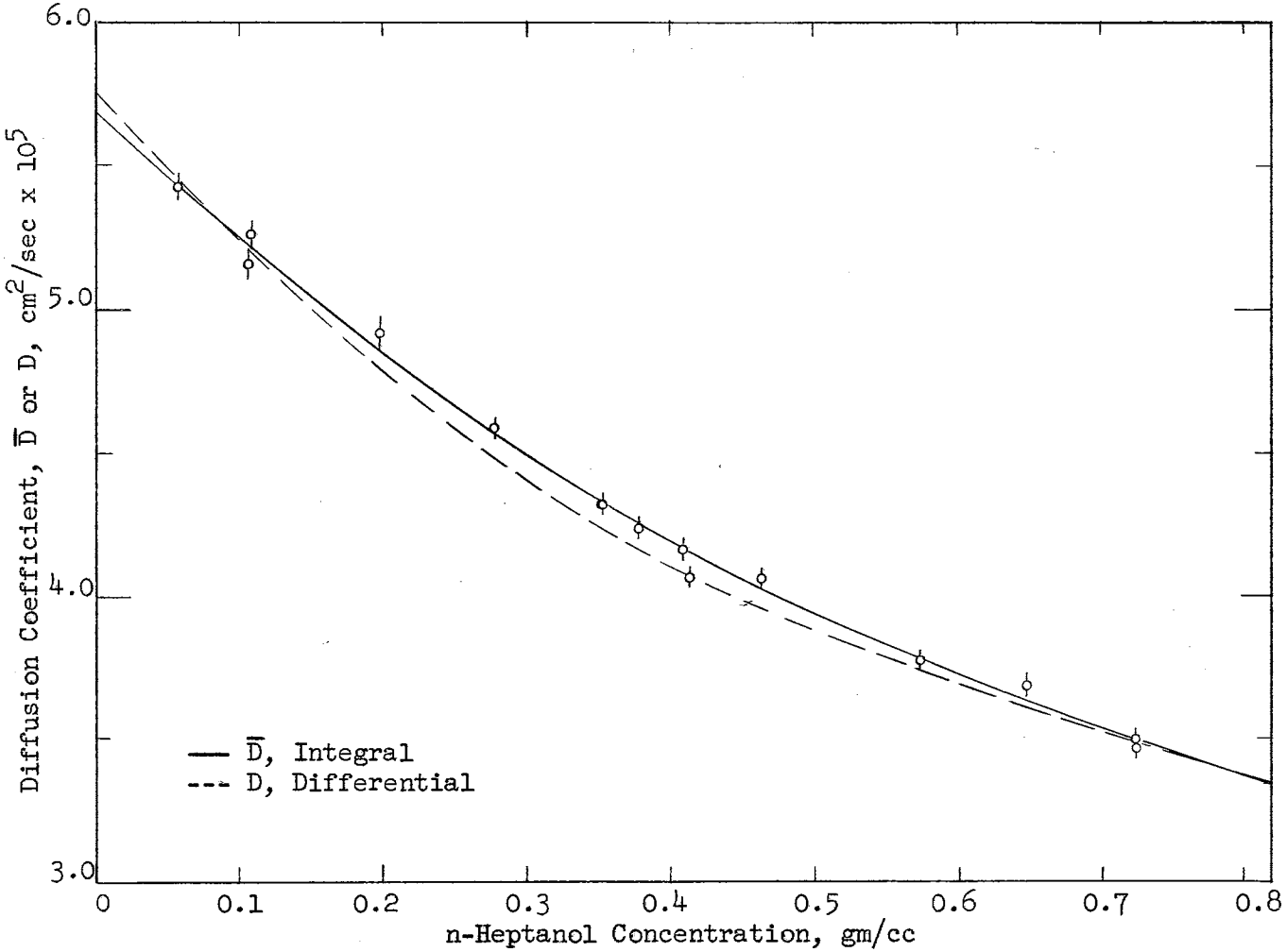

Figure 7

Diffusion Coefficients for the n-Heptanol-Cyclohexanone System, 25°C

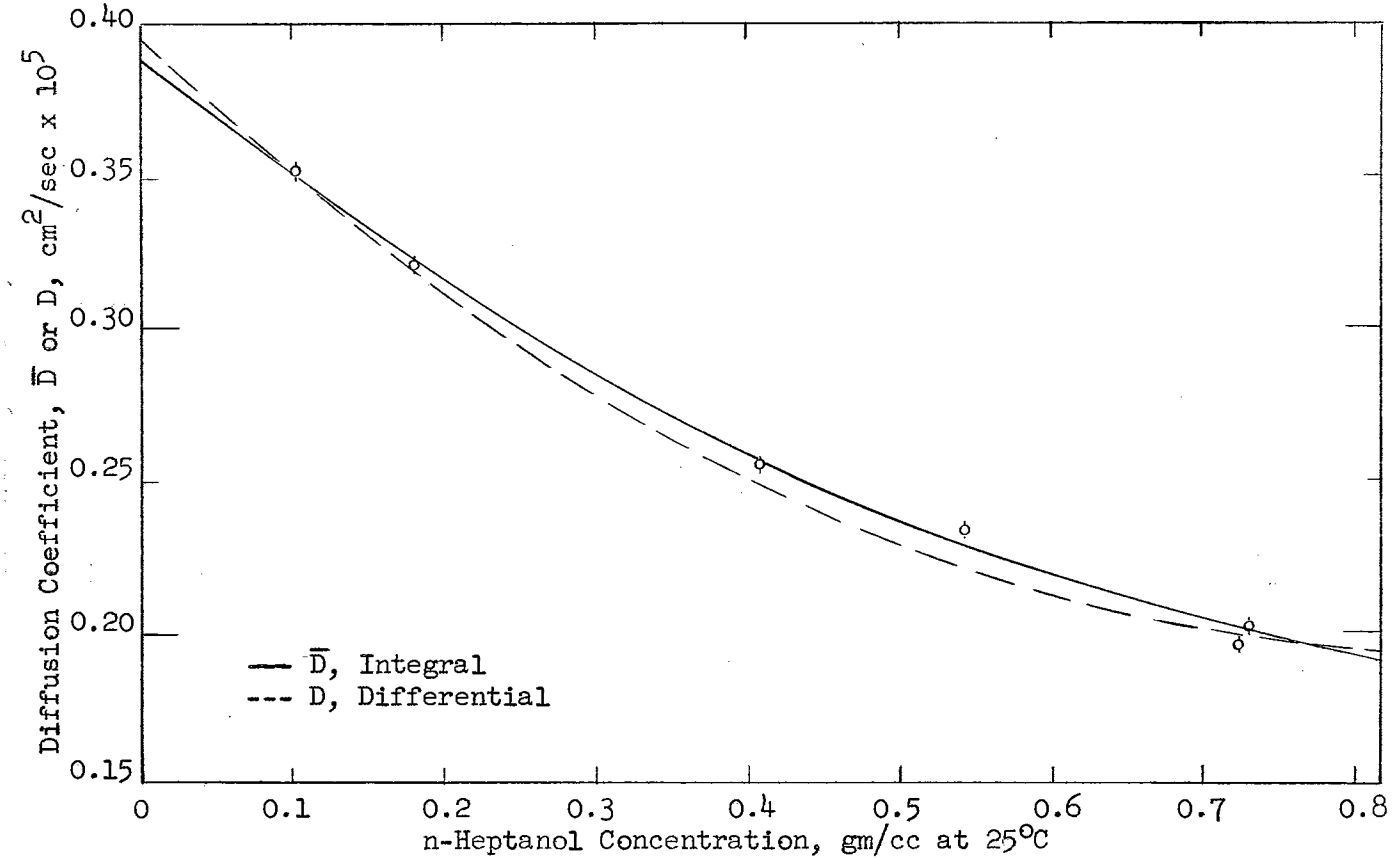

Figure 8

Diffusion Coefficients for the n-Heptanol-Cyclohexanone System, 10°C

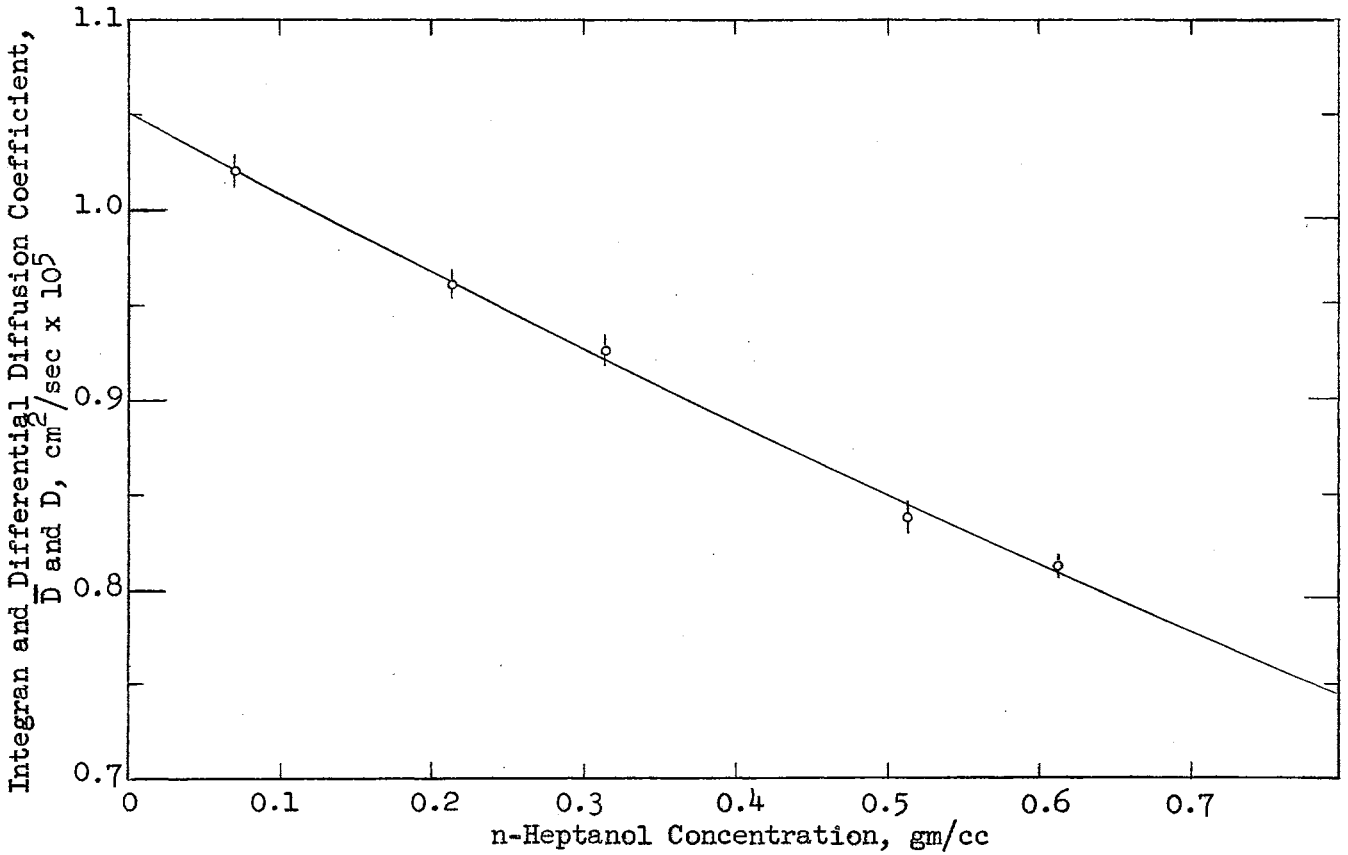

Figure 9

Diffusion Coefficients for the n-Heptanol-Cyclohexanone System, 55°C

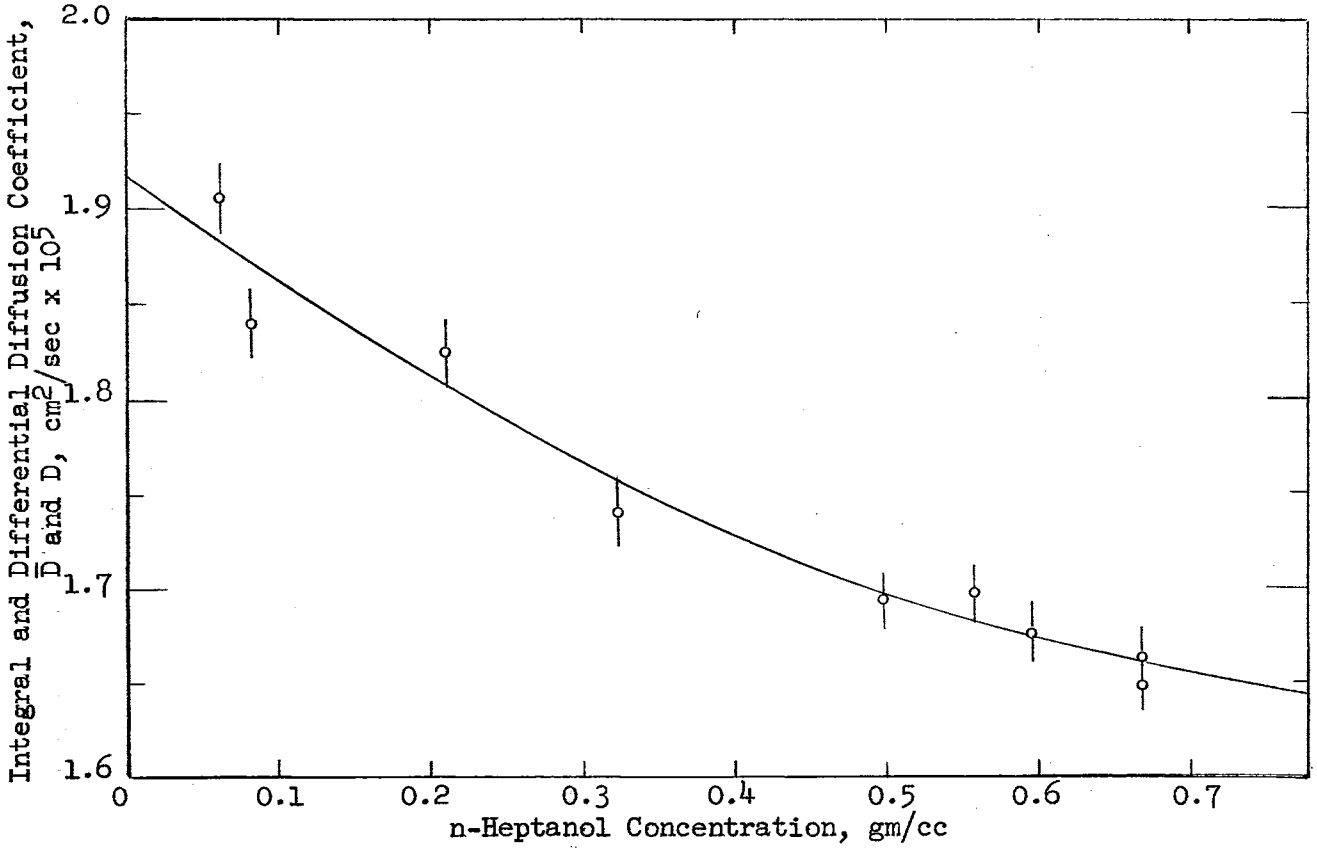

Figure 10

Diffusion Coefficients for the n-Heptanol-Cyclohexanone System, 90°C

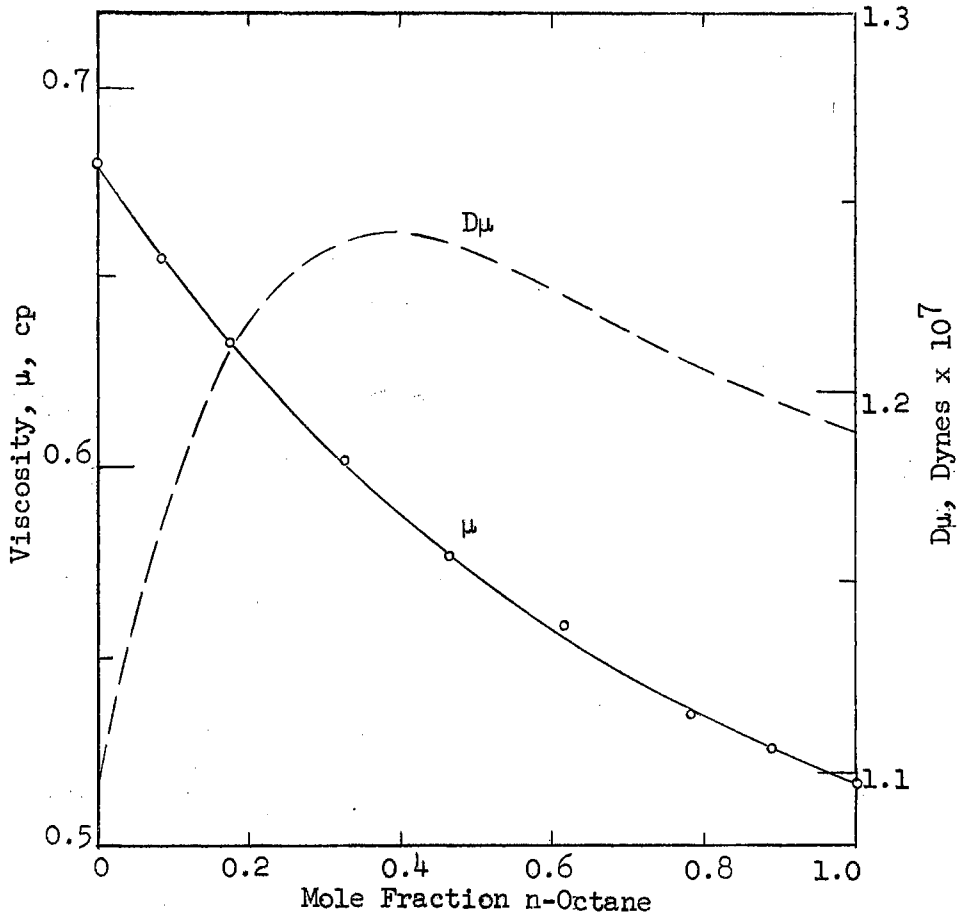

Figure 11

Viscosity of n-Octane-MCH System, 25°C

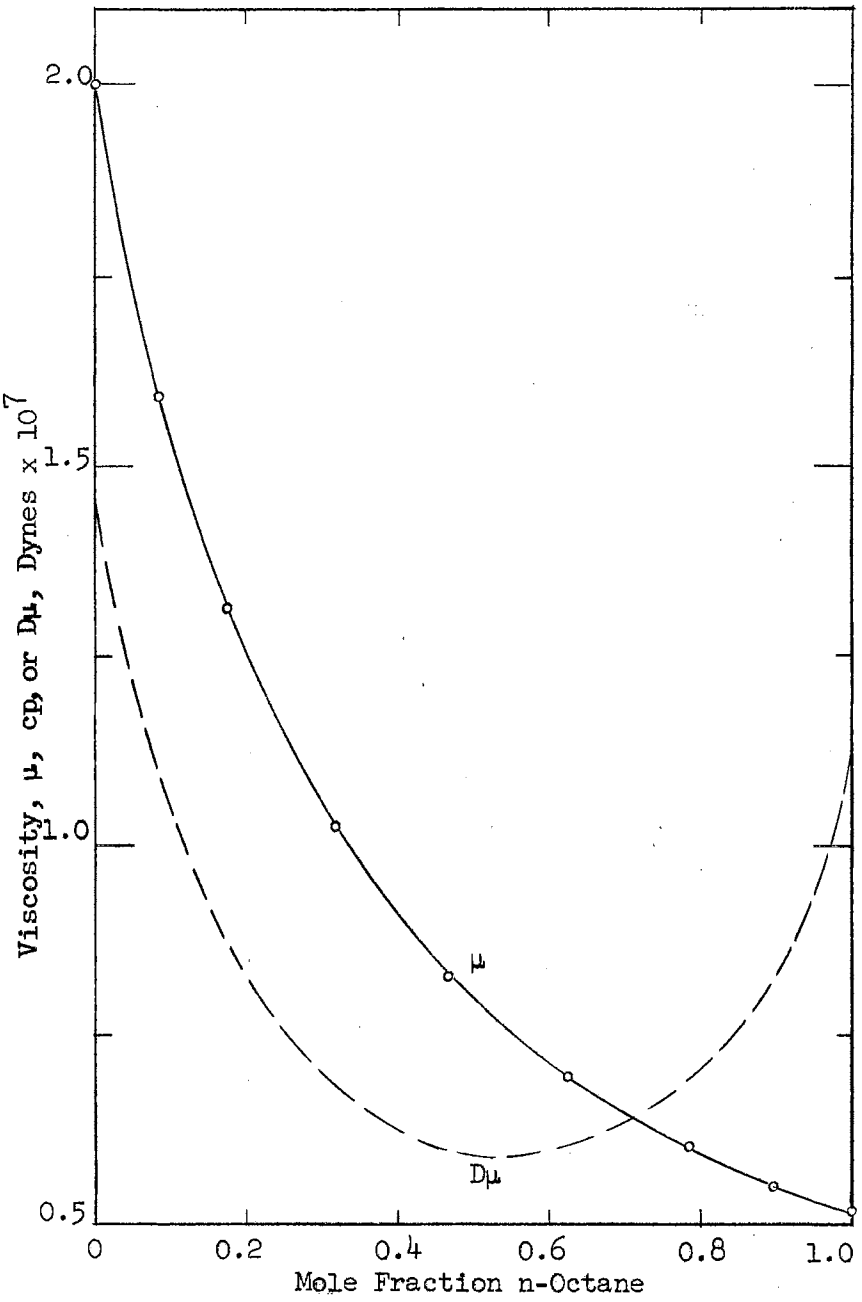

Figure 12

Viscosity of n-Octane-Cyclohexanone System, 25°C

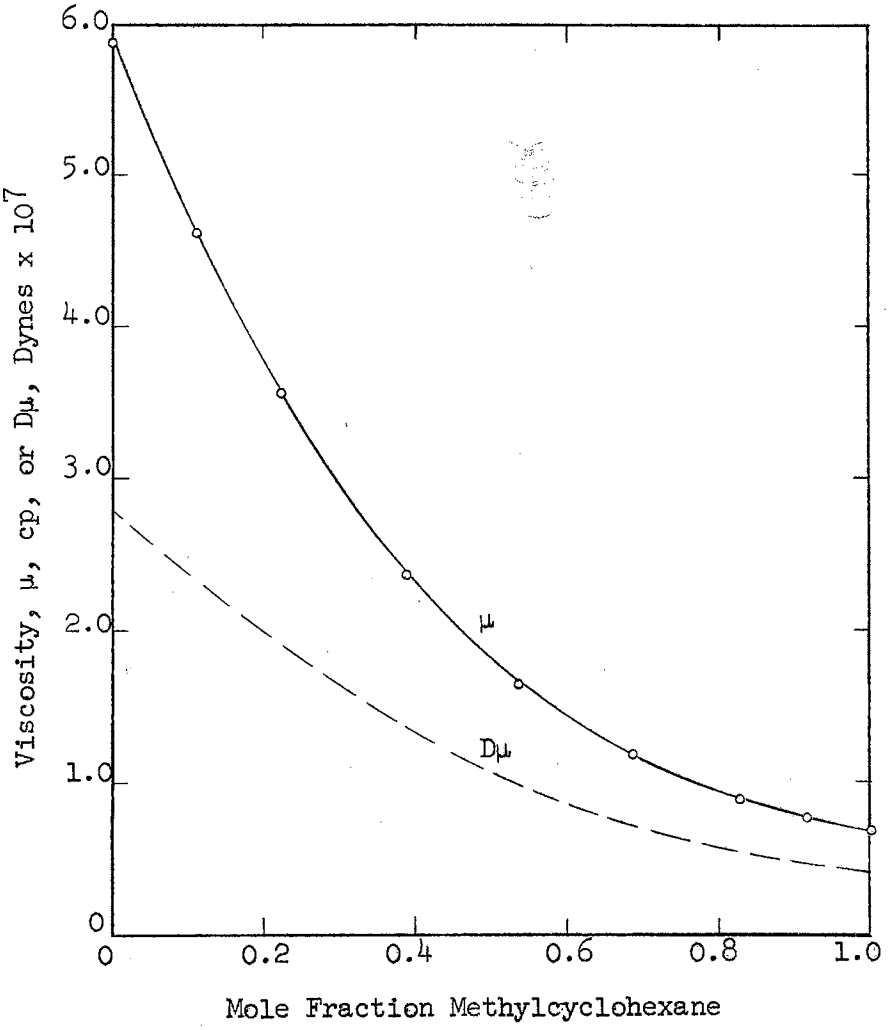

Figure 13

Viscosity of MCH-n-Heptanol System, 25°C

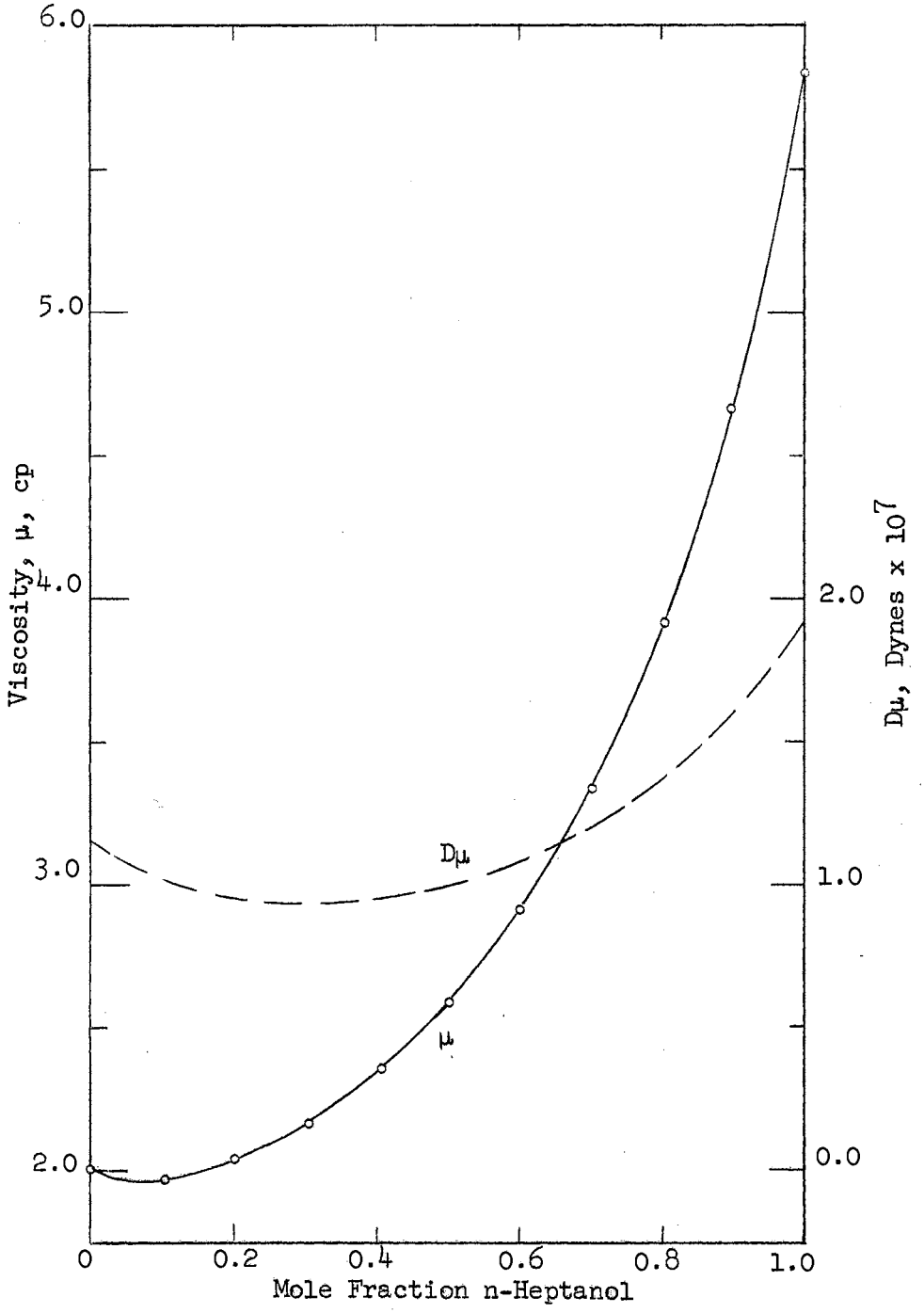

Figure 14

Viscosity of n-Heptanol-Cyclohexanone System, 25°C

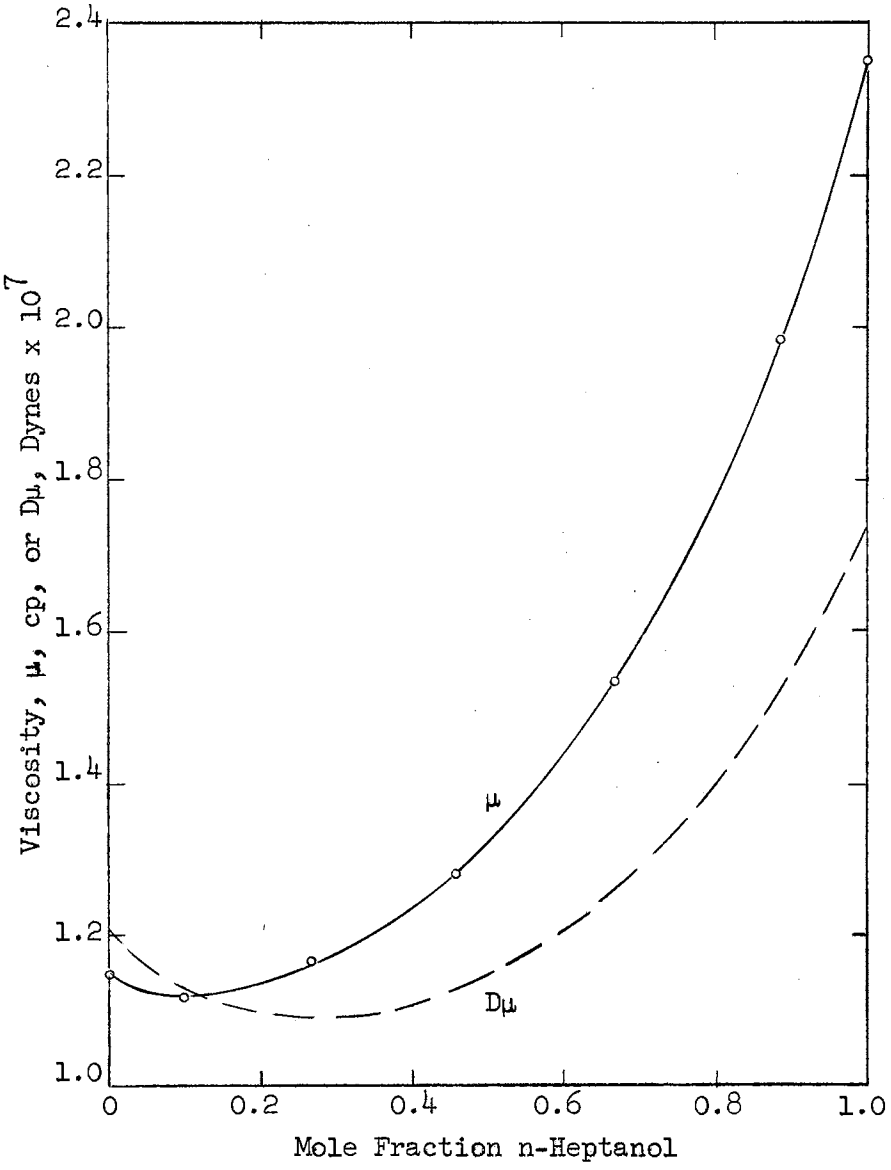

Figure 15

Viscosity of n-Heptanol-Cyclohexanone System, 55°C

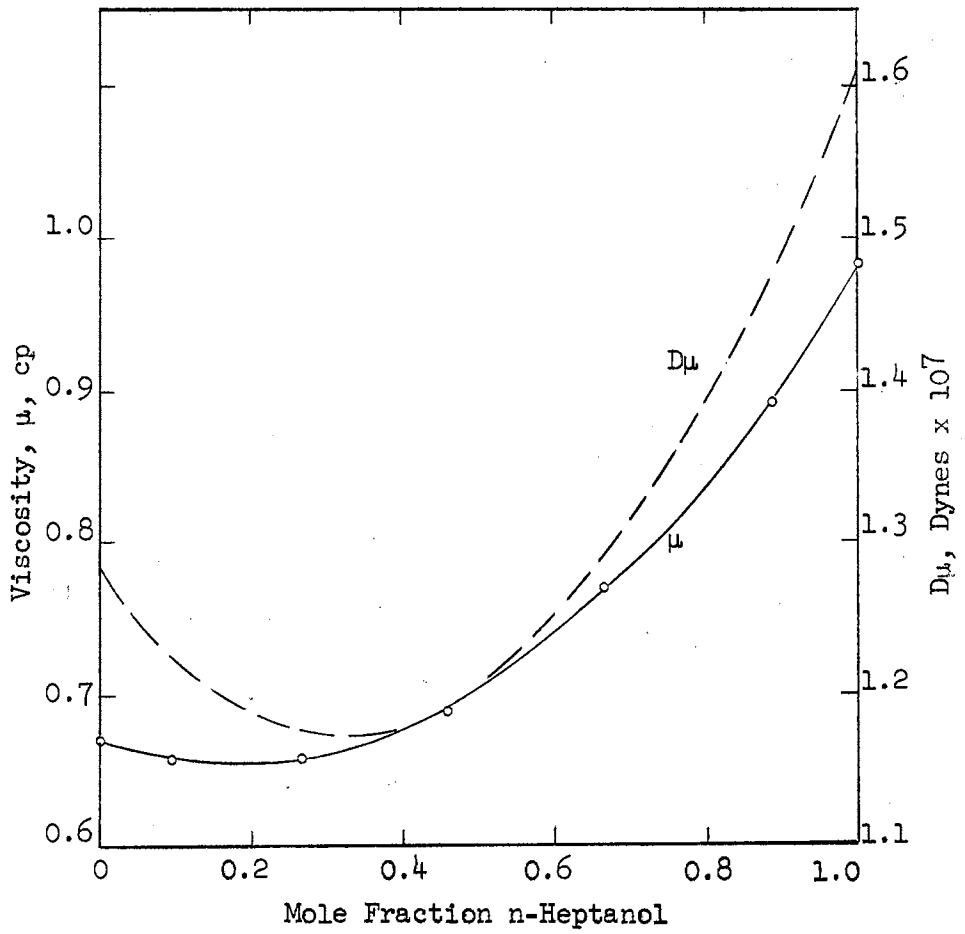

Figure 16

Viscosity of n-Heptanol-Cyclohexanone System, 90°C

CHAPTER VII

DISCUSSION OF RESULTS

The experimental data from this study are catalogued in the preceding chapter. In this chapter an analysis of the significance of the data is presented.

First, the precision of the experimental data is assessed. Next, the method used in determining the differential diffusion coefficients from the data is outlined. Then the effects of temperature on the diffusion rates and viscosities in the n-heptanol-cyclohexanone system are evaluated. A comparison of the diffusion rates and viscosities at 25°C for the four homomorphic systems of varying degrees of non-ideality follows. Two widely-used empirical diffusivity correlations are then tested against the data. Finally, the general equations for determining differential diffusivities in systems where volume changes occur (see Chapter II) are applied to the ethanol-water system to illustrate their use.

A. Precision of the Data

A detailed analysis of the effects of analytical errors on the precision of the data is presented in Appendix B. The results are briefly summarized here.

In the KCl-water calibration runs, the limiting factor in the analytical accuracy appears to be the determination of the KCl residue weights from the 10 cc samples. From an analysis of analytical errors, the predicted standard deviation of the cell constant β is 0.4%. This value is larger than the data of Table II indicate. Thus, the excellent agreement (±0.1%) of the cell constant data may be in part fortuitous. The error analysis does, however, offer proof that no unsuspected error-causing factors are present. Such factors, if present, would make the actual errors larger than those predicted from an analysis of analytical errors.

The changes in the cell constant with time differed in magnitude and even in direction among the cells. This is not unreasonable since plugging of pores (reduction of transfer area) and wearing of diaphragm (decrease of transfer length) have opposite effects on β. Stokes, (68) using similar cells, reported drifts of about 0.5 to 1.0% per 1,000 hours in the cell constant, which agrees well with our results. The cell constant at the time of a given experiment was established by linear interpolation or extrapolation of a β versus time plot based on the measured values at two times.

For the organic systems, the average absolute deviations of the data points from the curves of Figures 4 through 10 are as follows:

System		Average Absolute Deviation, %
n-octane - MCH,	25°C	0.5
n-octane - cyclohexanone,	25	1.2
n-heptanol - MCH,	25	0.5
n-heptanol - cyclohexanone,	10	1.4
	25	0.8
	55	0.5
	90	0.8

Although the curves in Figures 4 through 10 were simply drawn by inspection, the above numbers offer a reasonable measure of prediction.

Analysis of analytical errors predicts a standard deviation of about

0.2% for the organic runs. The limiting factor in the accuracy of the organic analyses is the precision of the pycnometer volumes.

The organic data show greater scatter than that predicted from error analysis. This points to the presence of some unknown factor(s) contributing to the errors. The temperature fluctuations and mechanical vibrations in the bath could contribute to errors. Also, evaporation of samples at high temperature or condensation of moisture at low temperatures could enhance errors.

The density determinations of this study showed an average absolute deviation from the mean of 1.6×10^{-5} gm/cc for 134 data pairs. The viscosities showed approximately 0.3% average absolute deviation from the curves of Figures 11 through 16.

B. Calculation of the Differential Diffusivities

Methods for determining the differential diffusivity-composition relation from diaphragm-cell data are discussed in Chapter II. For the systems investigated in this study, volume changes on mixing were less than 0.2% in all cases. Thus, the general equations derived in Chapter II were not required, and Gordon's complete equation, Equation II-36, was employed.

The application of Gordon's equation followed the pattern described for the general equations. The integral diffusion coefficients were fitted in sections, as required, to polynomial series in the mean concentrations. The relation for $f(\rho_A)$ was then found from Equation II-24. Equation II-26 ($G\left[\rho_A', \rho_A''\right] = 0$) was then integrated for each data point at 10 equally-spaced values of $\Delta \rho_A$ from $(\Delta \rho_A)_o$ to $(\Delta \rho_A)_f$. These

integrations were performed analytically since $f(\rho_A)$ was known as a polynomial function of ρ_A.

Using the 10 values of D_*/D from Equation II-26, corresponding values of F (ρ_A', ρ_A'') were found from Equation II-29. Then Equation II-36 was integrated numerically to give $\bar{D}/D_o$ for each data point. Setting $\bar{D}/D_o$ equal to $1+f(\rho_A)$, the polynomial expression for $f(\rho_A)$ was solved for ρ_A^*. The six step procedure outlined in Chapter II was then followed until successive values of ρ_A^* differed by less than 0.003 gm/cc for all data points.

The method described has one disadvantage relative to a graphical solution of the equations. The disadvantage is that the diffusion curves are represented by an arbitrary analytical function or set of functions. The results, particularly the extrapolation of the curves to the pure-component axes, may depend on the particular functional relation selected.

The procedure adopted in selecting the degree and number of polynomial relations for a given data set was to use the minimum number of low-power curves which adequately represented the $\bar{D}$ versus $(\rho_A)_{Avg}$ data. Adequate representation was judged from the standard error of estimate for the curve fits and by agreement of the extrapolated end points with those from curves drawn by hand.

Using the above criteria, six of the seven systems were represented by single curves of second or third order in the concentration. The n-octane-cyclohexanone system was fitted with three second order curves. Since the integral and differential diffusivity curves are quite similar for the systems of this study, the above procedures should yield satisfactory values of D. The values of the differential diffusivities in

Tables III through X correspond to those obtained from the above mentioned calculations.

The above calculations were performed on the IBM 1410 digital computer at Oklahoma State University. Since the program of Gordon's equation is merely a simplification of one written for the general equations for the IBM 704, the IBM 1410 program is not listed in this thesis. The IBM 704 program is discussed below and listed in Appendix G.

C. The Temperature Dependence of Diffusivities

Various models for the effect of temperature on the diffusion coefficient are presented in Chapter III. At the beginning of this study, data satisfactory for testing these models were very scare. Only the data of Cohen and Bruins (19) on acetylene tetrabromide-acetylene tetrachloride from 0 to 50°C and Scheffer and Scheffer (62) on mannitol-water, 0 to 70°C, covered a sufficient temperature range to permit strict test of the models. Both of these sets of data are at only single dilute concentrations, and both were measured prior to 1925.

Only one set of mutual diffusion data on non-electrolytes which cover the complete concentration range and span more than a 40°C temperature range are known to the author. They are the data of Smith and Storrow (64) on the ethanol-water system from 25 to 75°C. Unfortunately, these data were discredited by Hammond and Stokes (36) and Dullien (25). These authors studied the same ethanol-water system at 25°C; their results agreed well while differing from those of Smith and Starrow by 100% in some areas.

This lack of data over a range of temperature and compositions

prompted the investigation of the n-heptanol-cyclohexanone system from 10° to 90°C over the entire composition range. This doubles the temperature range of any comparable data presently available.

The n-heptanol-cyclohexanone system was chosen for study for several reasons. The system fitted into the scheme for study of several homomorphic systems, as mentioned previously. This system had the highest pure-component boiling points of the four systems studied, thus evaporation problems at high temperatures should be less than for the other systems. Also, the expected non-ideality of the system would present a rigorous test of the models.

The diffusion data at the four temperatures are listed in Chapter VI. These results were used to test the models described in Chapter III as follows. Diffusion data at a fixed composition were fitted to an equation of the form

$$f(D) = A + B\, g(T) \qquad \text{(VII-1)}$$

where f(D) and g(T) are the functions of D and T, respectively, which are postulated to vary linearly. Thus from the data at four temperatures, four values of the functions f(D) and g(T) existed at each fixed composition.

Table XXI presents the results of the linear regression via Equation VII-1 for several models. The complete data from which the variables entering Table XXI were taken are listed in Table E-IV. Results in Table XXI are read as follows. For Model 1, at 0.0 mole fraction n-heptanol, the average deviation of the four data points (one at each temperature) from the least-mean-square linear regression is 0.8%. The maximum deviation is 1.2%. Considering all three compositions (0.0, 0.5, and 1.0), the average

TABLE XXI

COMPARISON OF VARIOUS MODELS FOR

TEMPERATURE DEPENDENCE OF

DIFFUSION COEFFICIENTS

Mole Fraction n-Heptanol		Percentage Absolute Deviation from Model*						
		Model 1	Model 2	Model 3	Model 4	Model 5	Model 6	Model 7
0.0	Avg.	0.8	0.8	1.5	0.7	0.6	0.9	1.0
	Max.	1.2	2.4	3.3	1.2	1.0	1.4	2.0
0.5	Avg.	3.2	3.5	3.5	3.4	3.1	1.3	-
	Max.	3.8	4.3	8.9	3.8	3.4	3.4	-
1.0	Avg.	1.7	1.9	7.5	7.9	2.0	6.2	17.4
	Max.	2.6	3.6	20.1	10.6	3.9	16.5	69.5
	--	--	--	--	--	--	--	--
Overall	Avg.	1.9	2.1	4.1	4.0	1.9	2.8	9.2
	Max.	3.8	4.3	20.1	10.6	3.9	16.5	69.5

*Model	Dependent Variable	Independent Variable	Reference
1	lnD	1/T	34
2	ln(D/T)	1/T	52
3	D	T/μ	76
4	lnD	$\ln(T/\mu)$	63
5	lnD	$\ln\mu$	33
6	D	$1/v^{0.6}\mu^{1.1}$	58
7	D	$1/v^{0.6}\mu(1.1L/L_s)$	58

deviation for Model 1 is 1.9%; the maximum deviation is 3.8%. From the lower portion of the table, Model 1 is seen to be the exponential model, i.e., lnD versus 1/T, and reference 34 is given as an example of a source suggesting this model.

From Table XXI, Models 1, 2, and 5 appear to be of comparable applicability and superior to the other models.

Model 1 confirms the inverse exponential variation of D with temperature. This exponential variation for both D and μ is illustrated in Figures 17 and 18. Note in Figure 18 the extremely linear variation of $\ln\mu$ with 1/T, within the accuracy of the data. From this linearity follows the fact that lnD is equally well represented by 1/T or $\ln\mu$, as demonstrated by the equivalent accuracy of Models 1 and 5. The poorer accuracy of Model 1 at intermediate compositions may be due to the influence of the thermodynamic factor.

Models 1 and 5 are insignificantly better than Model 2, suggested by Meyer and Nachtrieb (52). From the Eyring theory, the difference in Models 1 and 2 is seen in Equation III-9. This difference consists of simply assuming different pre-exponential factors to be temperature invariant. The present data offer no basis for selection of one assumption over the other.

Model III represents the dependence generally attributed to the Stokes-Einstein equation, and Wilke (76) used this model in his empirical correlation of diffusion rates. The factor $D\mu/T$ is sometimes assumed constant to extrapolate data over a temperature range (75). Certain studies have indicated the factor to be constant over substantial temperature intervals (6, 33, 39). However, for the data of this study the following

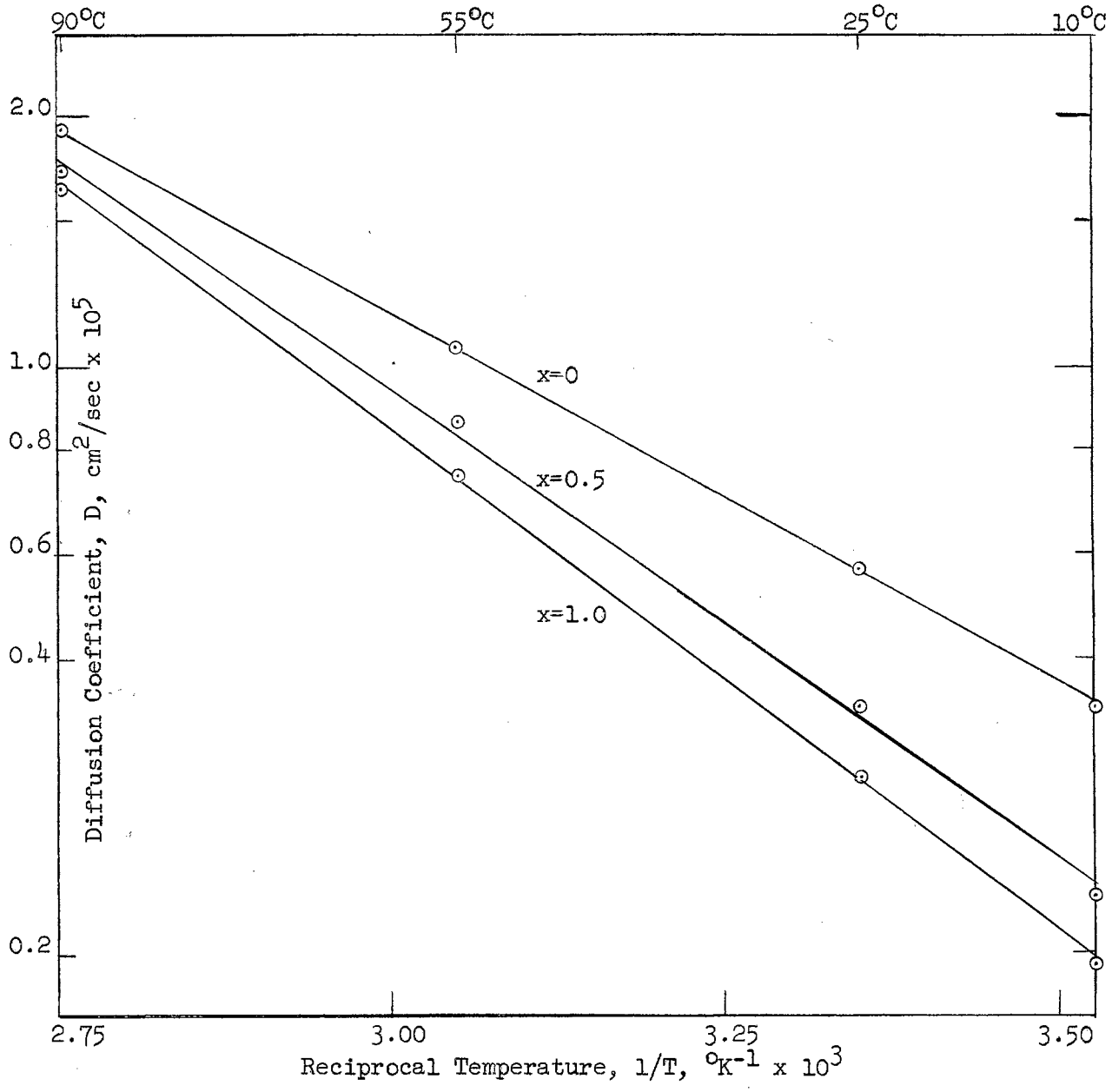

Figure 17

Diffusivity-Temperature Relation for n-Heptanol-Cyclohexanone System

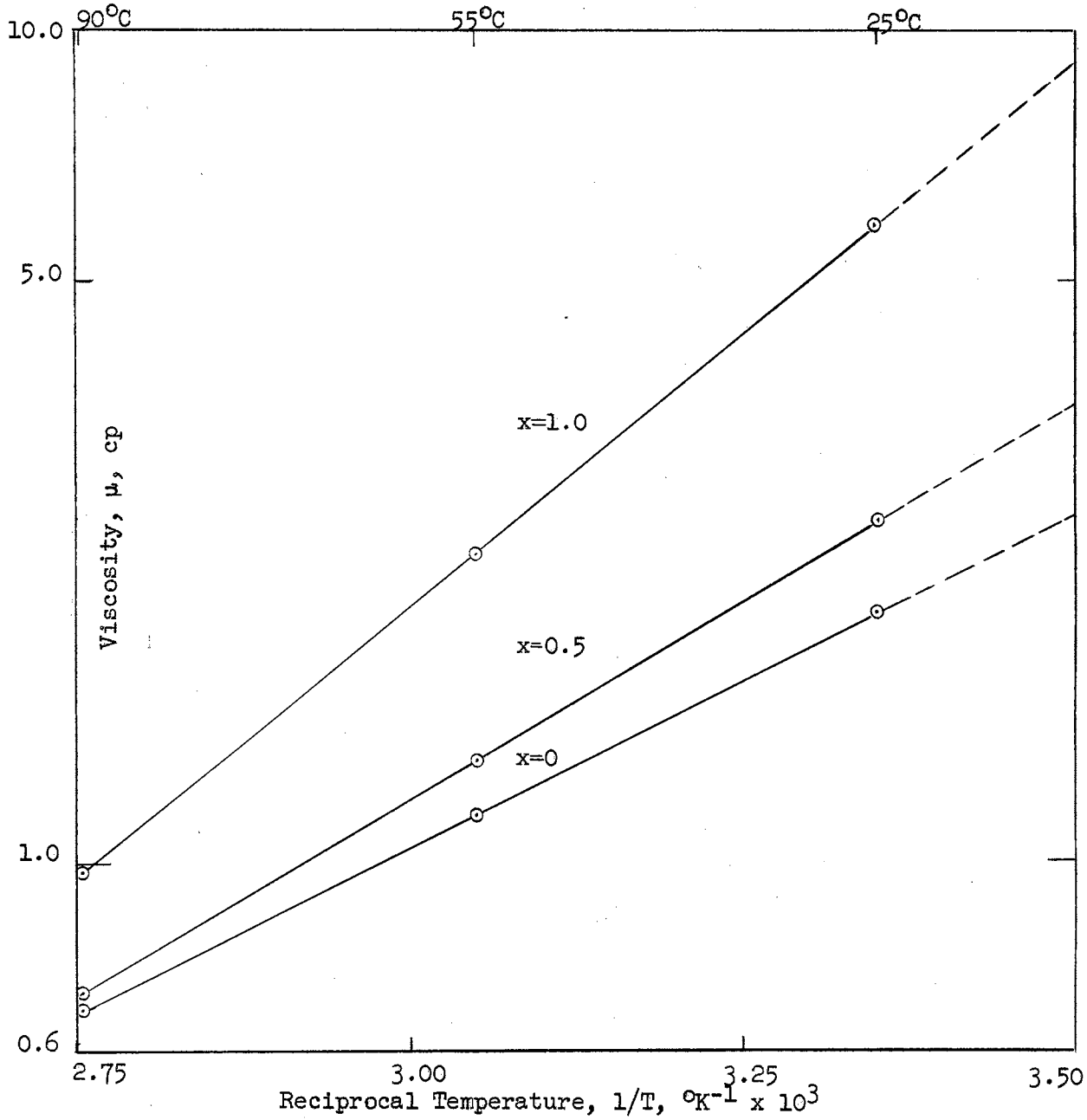

Figure 18

Viscosity-Temperature Relation for n-Heptanol-Cyclohexanone System

variation was found in $D\mu/T$:

Mole Fraction n-Heptanol	$D\mu/T$			
	10°C	25°C	55°C	90°C
0.0	6.82	6.62	5.33	4.45
1.0	3.88	3.89	3.68	3.54

where D is in cm^2/sec, μ in cp., T in °K. Unfortunately, these data show the $D\mu/T$ grouping is not in general constant with temperature changes. Such a parameter, if constant, would be quite valuable since data are required at only one temperature to predict the data at other conditions.

The other models need little discussion except to point out that Model 7 was not tested at intermediate concentrations due to inaccuracies in estimating heats of vaporization. The model, Equation III-18, suggested by Arnold is not included since results were so erroneous that percentage errors lose any meaning.

From the linear regression of lnD and lnμ as a function of 1/T, the activation energies for diffusion and viscous flow were determined, where these activation energies E_D and E_μ, respectively, are defined as

$$D = A\, e^{E_D/RT}$$
$$\mu = A'\, e^{-E_\mu/RT} \qquad \text{(VII-2)}$$

The activation energies so determined are illustrated in Figure 19.

Caldwell and Babb (15) found that $E_D - E_\mu$ was constant with composition for six ideal systems. However, Anderson, Hall, and Babb (3) studied several non-ideal non-electrolyte systems and found results similar to those of the present case. Garner and Marchant (33) found similar results in a study of diffusion of various solutes in water.

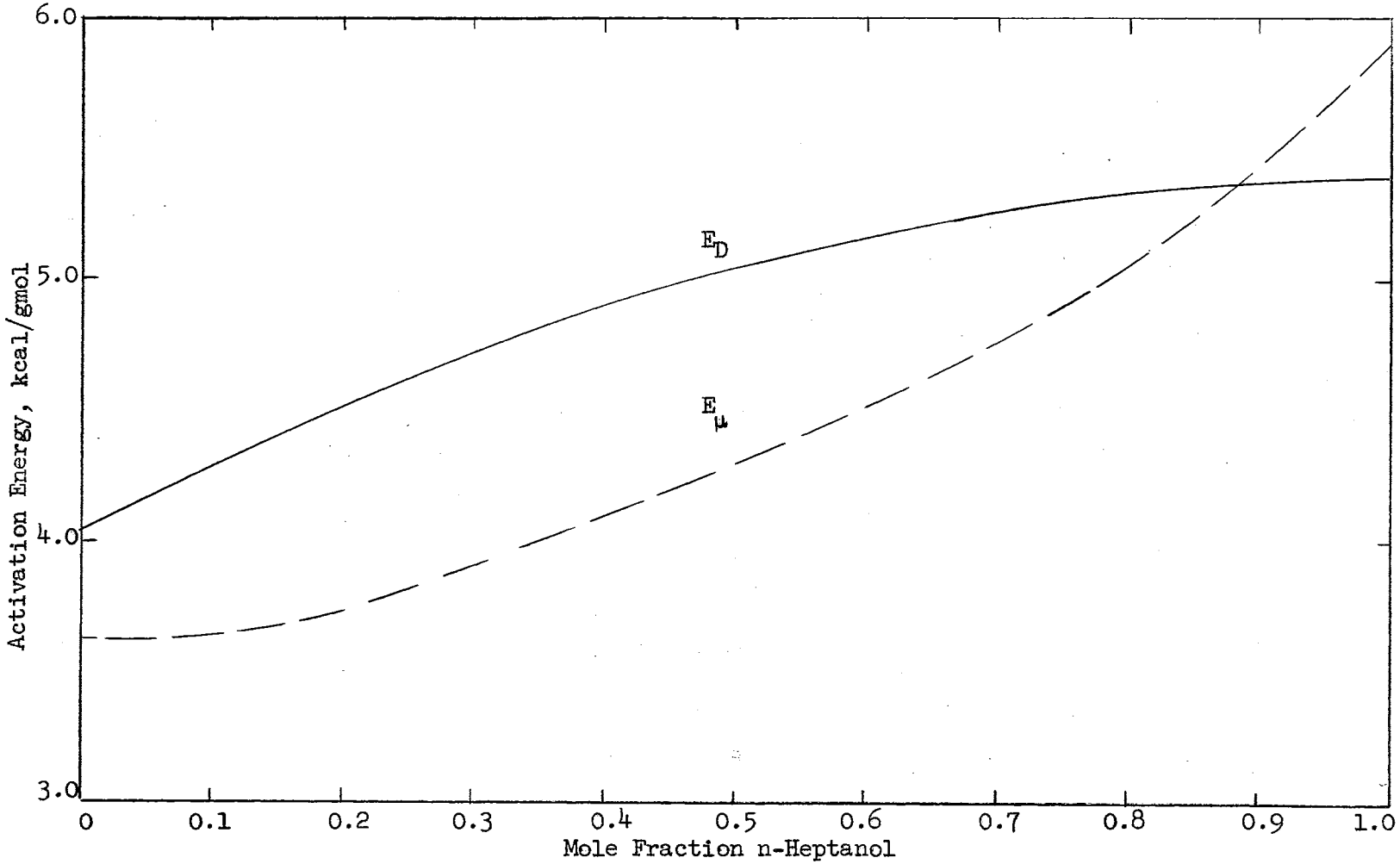

Figure 19

Activation Energies for the n-Heptanol-Cyclohexanone System

The activation energies for both viscosity and diffusion exhibit rather continuous, smooth variations with composition. This may be interpreted as indicative of a gradual variation in the interactions among the molecular entities in solution. Sharp variations in the activation energy curves have been interpreted as evidence of changes in the modes of association in solution (33).

The fact that the activation energies for diffusion and viscosity are apparently uncorrelated, even displaying different curvatures, points outs the difference in the mechanisms of the two processes. The numerous attempts to deduce general relations between D and μ seem to this author doomed to failure. The results of statistical mechanics have shown that only friction (or interaction) between the two diffusing species affects the mutual diffusion rates. Conversely, the flow process seems bound to be influenced both by friction between species and friction among the molecules of each individual species (46). However, in the special case of ideal solutions the $D\mu$ product has been shown to be linear in mole fraction (9). Figure 20 shows the $D\mu$ product for the n-heptanol-cyclohexanone system at the three temperatures where both properties were measured. The interesting feature of this figure is that, as expected, the $D\mu$ relation approaches the ideal solution behavior more closely (i.e., $D\mu$ linear in x) as the temperature rises.

Another interesting property of the frictional coefficients of statistical mechanical theory may be inferred from this data. If the postulate is accepted that

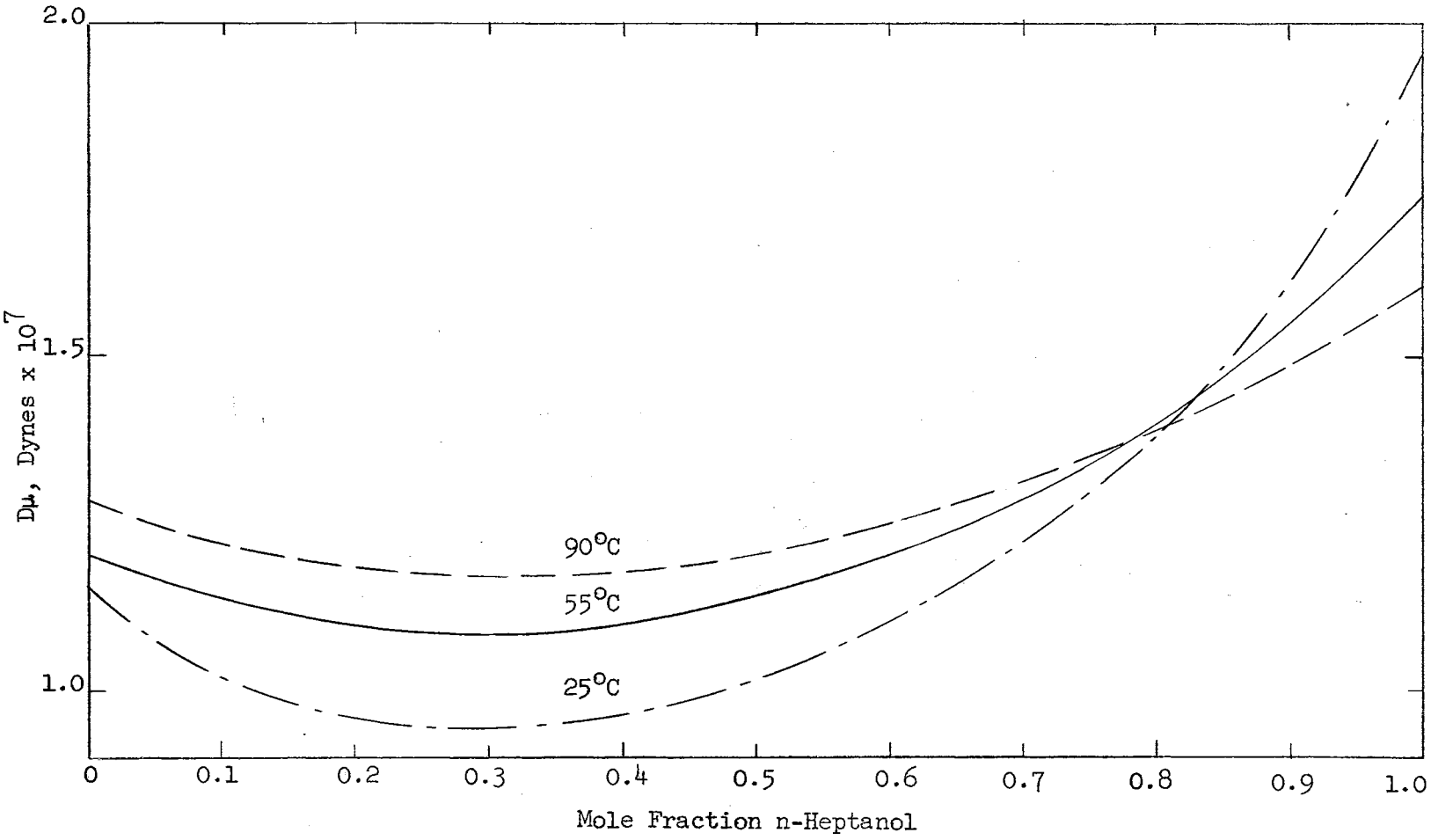

Figure 20

Diffusivity-Viscosity Product for the n-Heptanol-Cyclohexanone System

$$D = D(\zeta_{12})$$

$$\mu = \mu(\zeta_{11}, \zeta_{12}, \zeta_{22}) \qquad \text{(VII-3)}$$

then it appears from the linearity of the lnD versus lnμ relation that the friction coefficients ζ_{11}, ζ_{12}, ζ_{22} have the same functional dependance on temperature at fixed composition. The argument may be forwarded that perhaps ζ_{12} predominates in both D and μ, and thus no information on ζ_{11} and ζ_{22} may be inferred. However, the curves for D and μ as functions of composition are considerably different in the present system. The minimum in the viscosity curve is not reflected in the diffusivity curve, which strongly indicates that the ζ_{11} and/or ζ_{22} influence is present. Of course, these assertions must be tempered by the unknown effect of the thermodynamic factor on the diffusivity. Activity data on this system would aid in resolving this problem.

After the author had reached the above conclusions, Dunlop (28) presented evidence that for several systems where complete data are available, lnζ_{12} is linear in lnμ at infinite dilution. He offers no comments on the possible variations of ζ_{11} and ζ_{22}, but points out that if Stokes law represents the friction, the lnζ_{12} versus lnμ relation should have a slope of 1.0. For the system of this study slopes of 0.86 and 0.75 were obtained for mole fractions of 0 and 1.0 for n-heptanol.

From Figure 17 the diffusivity-temperature relation is extremely linear at the pure cyclohexanone axis. At other concentrations, small but preceptible variations from linearity are evident. These deviations indicate a slight decrease in activation energy with increasing temperature. Ewell and Eyring (30) attempted to explain similar decreases in E in hydrogen-bonded aqueous systems by considering the effect of temperature

on the hydrogen bond structure. As the temperature increases, they pictured a breakdown of the hydrogen bonds with attendant increase in the ease of formation of activated complexes. Similar arguments might be applied here to explain the deviations of the mixtures capable of hydrogen bond formation; the pure cyclohexanone, not hydrogen bonded, shows no such deviations.

Othmer and Thaker (58) found the D versus μ relation on logarithmic coordinates to be an excellent linear relation in a variety of cases at infinite dilution of solute. In certain systems showing "breaks" in the lnD or lnμ versus 1/T relation, the lnD versus lnμ relation showed no such breaks. This resulted from comparable effects of postulated structural rearrangements on D and μ. In the present case, however, note that for the n-heptanol rich end of the concentration range, 1/T furnishes a better correlation for lnD than does lnμ (see Table XXI); a 1.3% reduction in maximum deviation results when 1/T replaces lnμ. Nevertheless, in systems where structural rearrangements are known to occur, the use of lnD versus lnμ relation may be superior to lnD versus 1/T.

D. Comparison of Diffusion Coefficients for Four Homomorphic Systems of Varying Degrees of Non-Ideality

In the discussion of diffusional theories in Chapter III, the point was made that no theory is available to permit a quantitative prediction of diffusion rates in other than regular solutions. The complete statistical mechanical (and other equivalent) theories are applicable to the present non-regular systems, but these theories are phenomenological in outlook, making no effort to delineate the mechanism of the diffusion process.

In view of the above facts, the discussion of this section is not a quantitative one. The treatment of the data, albeit qualitative, is of value since it represents a first effort of its kind to separate the "physical" from the "chemical" (specific interaction) contribution to this transport process. Similar treatments are well known in the field of equilibrium thermodynamic properties (13, 4, 54).

The four systems studied at 25°C are listed below and numbered for reference purposes in the following discussions:

I. normal octane - methylcyclohexane

II. normal octane - cyclohexanone

III. normal heptanol - methylcyclohexane

IV. normal heptanol - cyclohexanone

The above systems were chosen, first, because they represent four structurally-similar (homomorphic) systems, each offering possibilities for different modes of molecular interactions. Second, since the plan was to eventually have each system studied over a wide range of temperatures, components with high boiling points were chosen. A boiling point of 100°C or higher was used as the criterion for selection.

Figure 21 presents the diffusion data on the four systems for ease of comparison. Of the four systems, notice that only system II (see list above) shows marked deviations from ideal behavior. Ideal behavior is characterized by a linear relation between D and x. The absence of pronounced deviations from ideality in these systems is no doubt due in part to the large hydrocarbon groups which mask the polar groups from one another. Shorter chain components, with probably larger deviations from ideality, were ruled out of this study by their higher volatilities.

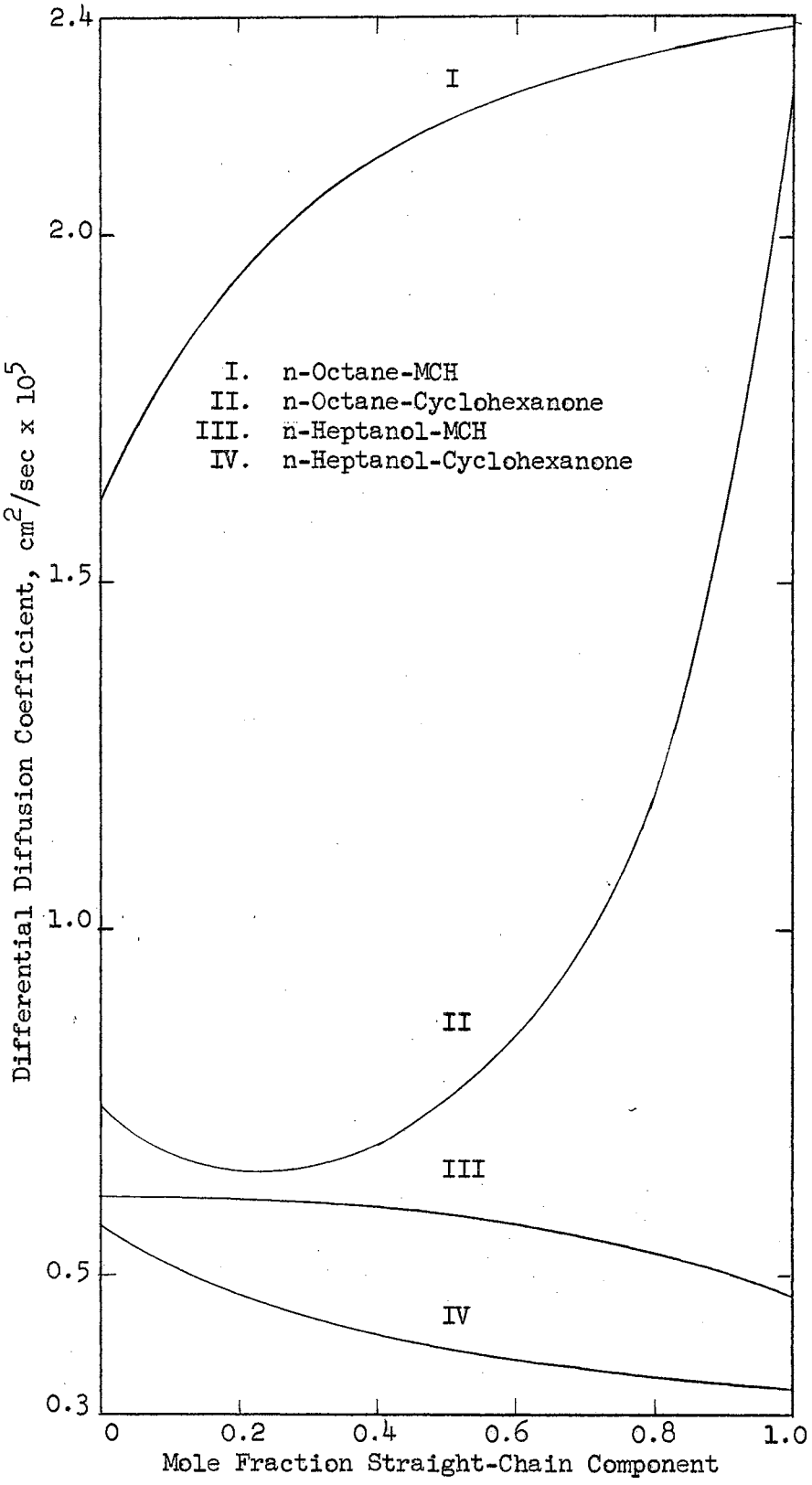

Figure 21

Diffusivity-Composition Relations at 25°C

If initial attention is directed to regions of infinitely dilute solute, where the activity correction (thermodynamic factor) need not be considered, some interesting comparisons are possible. Table XXII lists the diffusion coefficients for a) changing solutes in a given solvent, and b) changing solvents for a given solute. In all cases, the solute is infinitely dilute.

From Equation III-13, the statistical mechanical approach predicts that for two solutes, B and C, in a common solvent, A, the diffusion coefficients at infinite solute dilution are related by

$$\frac{D_{AB}}{D_{AC}} = \frac{\zeta_{AC}}{\zeta_{AB}} \qquad \text{(VII-4)}$$

Carrying the comparison a step further, suppose A is an inert solvent, B some associating substance, and C is the non-polar homomorph of B. If the difference in the friction coefficients, ζ_{ij}, for the two systems is assumed to be caused solely by association of B, then at infinite dilution of B these B-B interactions should approach zero and $\zeta_{AB} \rightarrow \zeta_{AC}$, or $D_{AB} \rightarrow D_{AC}$.

The above simplified argument may be tested from the data of Table XXII. For n-octane as a solvent, the above hypothesis is obeyed very well. Agreement is especially close since the value of 2.2 for the n-octane-cyclohexanone system is the most unreliable number in the table due to the rapid increase of D near the pure n-octane axis. Thus, at infinite dilution, the friction between solute and solvent appears to be determined essentially by the structure of the solute and not the polar nature of the species.

The above argument is shattered by the data with MCH as solvent. The diffusion coefficient for n-heptanol is three-fold lower than that of the

TABLE XXII

COMPARISONS OF DIFFUSION RATES

AT INFINITE DILUTION

Solute	Solvent	Diffusion Coefficient, D, $cm^2/sec \times 10^5$
	Solute Effect	
MCH	n-Octane	2.3
Cyclohexanone		2.2
n-Octane	MCH	1.6
n-Heptanol		0.6
MCH	n-Heptanol	0.5
Cyclohexanone		0.3
n-Octane	Cyclohexanone	0.7
n-Heptanol		0.6
	Solvent Effect	
n-Octane	MCH	1.6
	Cyclohexanone	0.7
MCH	n-Octane	2.3
	n-Heptanol	0.4
n-Heptanol	MCH	0.6
	Cyclohexanone	0.6
Cyclohexanone	n-Octane	2.2
	n-Heptanol	0.3

homomorphic n-octane. This strongly suggests that factors other than association of the alcohol influence the intermolecular friction (and diffusion rates).

Next note that for the polar solvents, diffusion rates are quite similar for the two homomorphic solutes. This is in spite of the fact that one would expect the polar solute to be hydrogen-bonded to the solvent. In three of the four cases above, behavior of the solute at infinite dilution is relatively insensitive to the polar nature of the solvent. Nevertheless, the case where this behavior might best be expected to be found, marked differences occur.

Turning to changes of solvent for a given solute, the effect of the polar group is more pronounced. For three of the four solutes, changing from a non-polar to a polar solvent results in a several-fold reduction of the diffusion rate. This result seems reasonable since in these cases the changes are for constituents in concentrated states, where interactions should be apparent. No explanation is obvious for the close agreement of diffusion rates for n-heptanol as solute.

Note that in no case studied does replacement of a non-polar group by a polar group increase the diffusion coefficient, while the opposite effect is common.

Moving from regions of infinite dilution to intermediate concentrations, the problem of making meaningful comparisons is increased by influence of the thermodynamic factor (see Equation III-13). In these regions both the friction and thermodynamic factors affect diffusion behavior. Unfortunately, no activity data were available on the systems of this study.

A simple inspection of the data in Figure 21 reveals that there are factors other than the purely structural (geometrical) configurations of the molecules influencing the diffusion coefficient. The "reference" non-polar-non-polar system, system I, differs by varying degrees from those containing polar constituents.

As mentioned in the previous section, inspection of the shapes of the diffusion coefficient and viscosity curves offers evidence of differences in mechanisms for the two processes. As noted previously, the viscosity curve for system IV exhibits a minimum which is not reflected in the diffusion data. Similarly, the diffusion coefficient shows a minimum for system II, while the viscosity curve has no extremum. Tentative explanations may be advanced for this behavior if the influence of the thermodynamic factor is neglected.

In system IV, as n-heptanol is added to cyclohexanone, the alcohol may tend to be dissociated and hydrogen-bonded to cyclohexanone. This process tends to remove the alcohol and ketone from interactions with molecules of their own kind with increased interaction between molecules. Subsequently, ζ_{11} and ζ_{22} may decrease and ζ_{12} increase. If ζ_{22} is the predominant factor at low heptanol concentration, a viscosity decrease would result, as is the case. As more heptanol is added, the alcohol may begin to associate, with rapid increase in ζ_{11}, and resulting increase in μ. From the diffusion curve, the variation in ζ_{12} appears to be quite continuous with composition. The above argument gives a possible explanation for the minimum in viscosity and continuous behavior of the diffusivity curve.

For system II, one may postulate that as cyclohexanone is added to

n-octane the friction ζ_{12} increases until rather high cyclohexanone concentrations are reached. At these high concentrations the ketone may begin to form "clusters", shielding a fraction of the cyclohexanone molecules from n-octane. This could result in a decrease in ζ_{12} and explain the minimum in the diffusion curve. For these clusters not to cause an extremum in the viscosity curve would require the clustering to have a much more pronounced effect on ζ_{12} than on ζ_{22}. From the present data, the likelihood of this being the case cannot be tested.

Systems I and III exhibit smooth curves for both D and μ, giving no evidence of changes of the modes of interactions.

Bearman (9) has shown that for ideal solutions, the $D\mu$ product is linear in the mole fraction. Reference to Figures 11 through 15 shows that none of the present systems fulfill this requirement. System I might appear to be amenable to application of regular solution theory, since it consists of non-polar constituents of comparable carbon numbers. Indeed an investigation of vapor liquid equilibrium data (18) showed both the systems n-octane-n-heptane and MCH-n-heptane to be essentially ideal. However, application of the Hartley-Crank diffusion theory to system I yields results in error by as much as 10%.

Thermodynamicists are accustomed to discussing anomalous behavior of equilibrium systems in terms of deviations from ideality (e.g., excess volumes, heats of mixing, etc.). This approach may be utilized here. As stated above, ideal diffusion behavior implies a linear D versus x relation. Experimental data on ideal systems (15) support this relation. These data suggest that for ideal systems the forces (or friction) between molecules is simply a molar average of the forces characteristic

of each species, the forces for the individual species being unaffected by composition changes. Such a relation of course implies no changes in the states of aggregation in the system.

Using the above basis, an "excess" diffusivity, ΔD, may be defined, analogous to excess volume, where

$$\Delta D = D - D_{Ideal} = D - D_{x=o} + (D_{x=1} - D_{x=o})\, x \qquad \text{(VII-5)}$$

where x is the mole fraction. Figure 22 presents the "excess" diffusivities for the four systems.

Two of the systems show positive deviations from ideality and two show the opposite behavior. System I is typical of non-ideal, non-polar systems where the diffusivity curve is convex downward. This behavior has been attributed (3) to a predominance of dispersion type forces, usually an attendant volume increase, and a larger "free volume" through which increased diffusion may occur. Anderson (4) characterized systems with diffusion coefficient curves convex upward as indicative of complex formation, i.e., the diffusion being hindered by complexing. Indeed, system IV, where intermolecular complexes seem most likely to occur, shows such behavior. However, the octane-cyclohexanone system shows much greater deviations, and octane-cyclohexanone complexes seem less likely than those in system IV. (Some spectropic evidence has been quoted (54) for association in all three binary systems formed from cyclohexane, piperidine, and tetrahydropyran.) Anderson's argument does not always hold, however, since the diethyl-ether-chloroform system exhibits positive deviations from linear behavior, and this system is known to form a 1:1 complex of ether and alcohol (1).

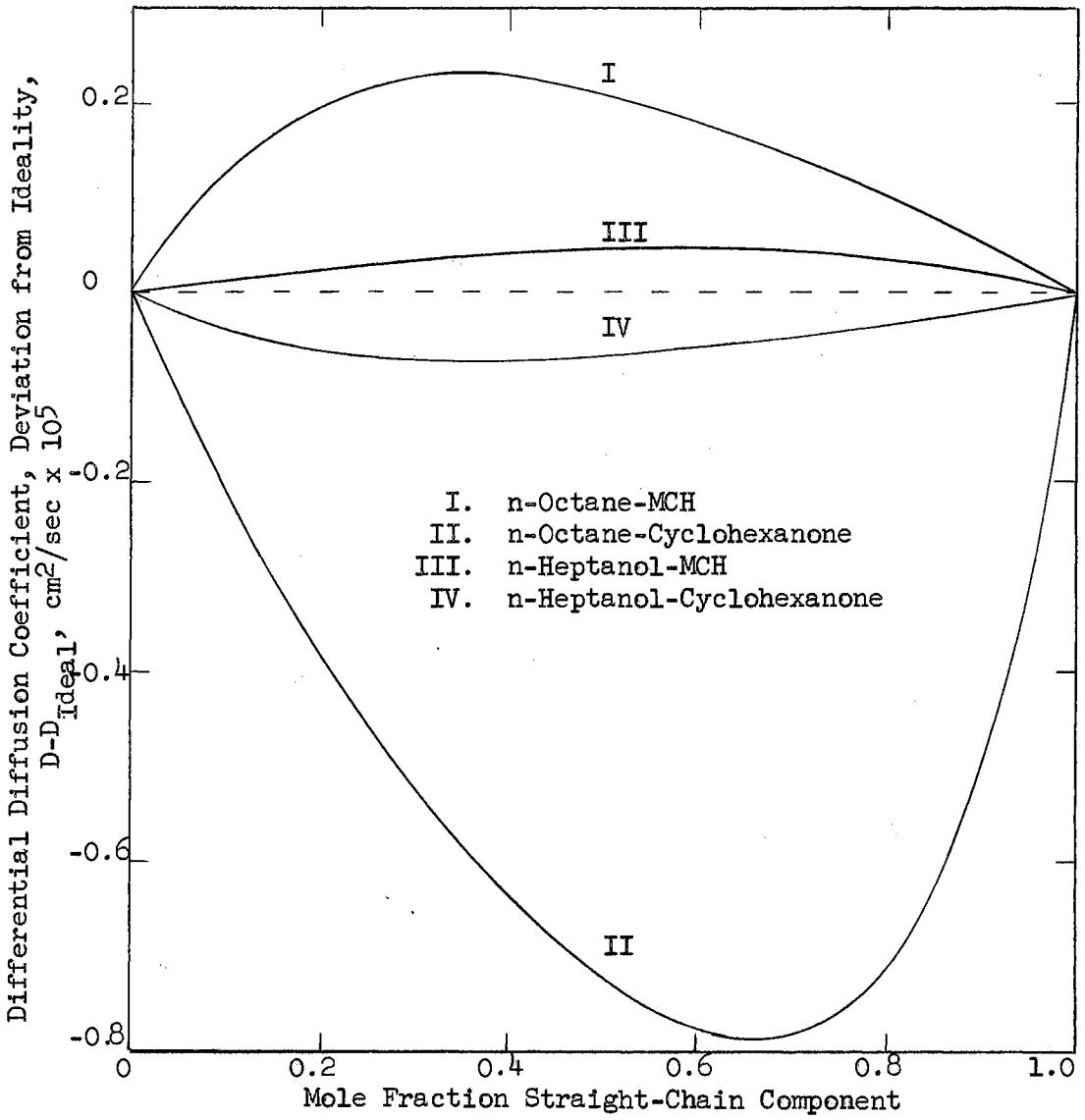

Figure 22

Deviation from Ideal Behavior of Diffusivity-Composition Relation

The analysis may be carried one step further by "backing out" the non-ideality due to physical interactions, as exemplified by system I, from the remaining systems. This difference may be construed as a measure of polar effects, if the non-polar and polar effects are assumed to be additive. Such separation has been attempted previously for equilibrium properties (4).

Figure 23 presents these deviations from ideality, relative to the reference non-polar system I. In both cases, the replacement of one of the non-polar by a polar homomorph results in a negative increase in the deviation from ideality. However, proceeding from the polar-non-polar system II to the polar-polar system IV actually decreases this deviation.

For all curves in Figures 22 and 23 the extrema occur near molecular ratios of 1:2 or 2:1. No explanation for this occurrence has been developed. (Spectroscopic or similar evidence of complex formation could serve as an aid in explaining this behavior.) Figure 23 does, however, clearly point to the fact that polar interactions exert an effect on not only the magnitude of the diffusion coefficient but also on the diffusivity-composition relation.

The above treatment ends in a position analagous to that encountered in thermodynamic studies (13, 4 , 54). The contributions of physical and chemical effects are separated, and in some cases the physical contribution may be evaluated, but the chemical effects remain beyond quantitative description.

A final insight into these systems may be obtained from the friction coefficient approach. Returning to Equation III-13 and considering again the case of a polar and non-polar homomorph in an inert solvent,

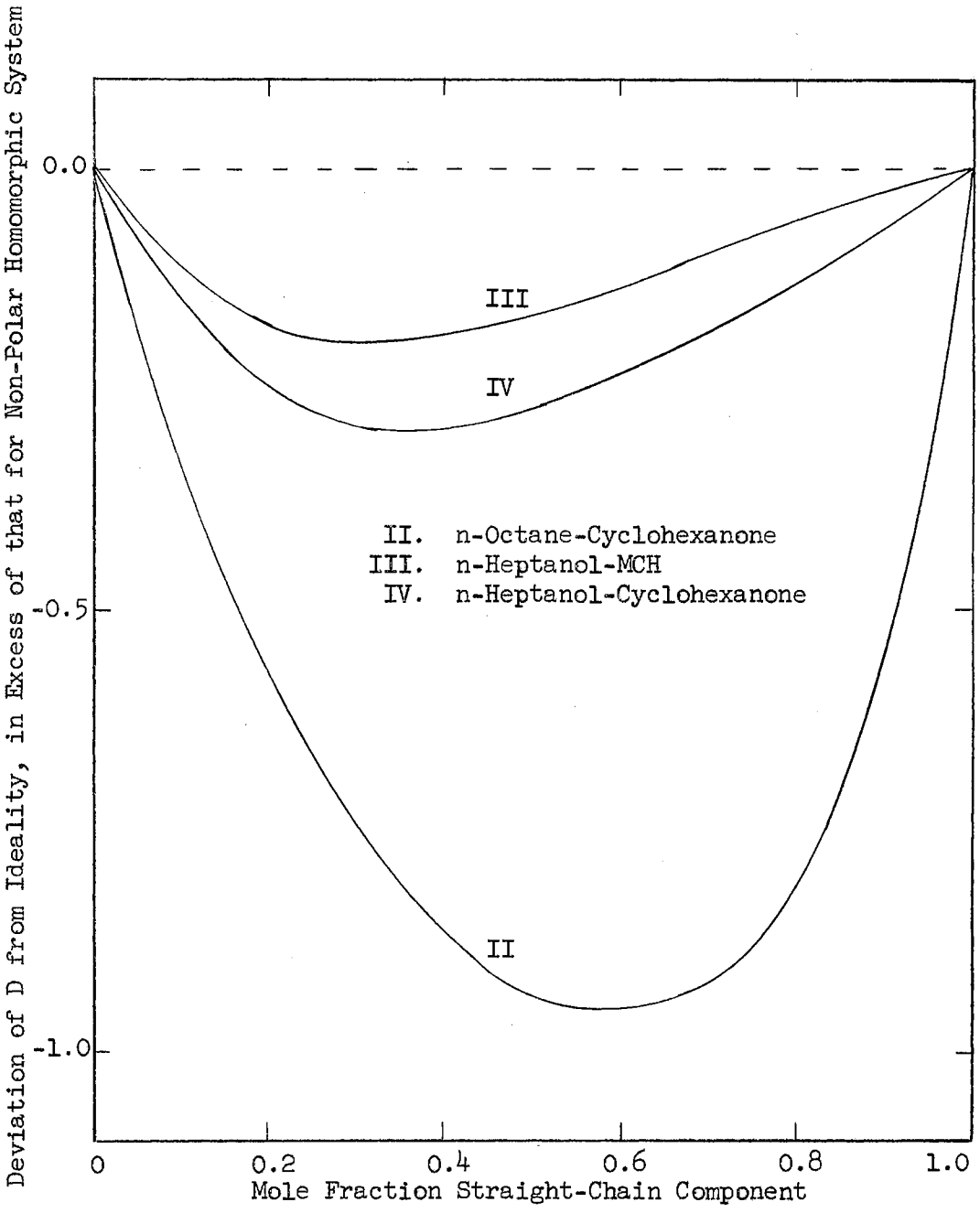

Figure 23

Deviation from Ideal Behavior of Diffusivity-Composition Relation
In Excess of that for Non-Polar Homomorphic System

$$\frac{D_{AB}}{D_{AC}} = \frac{(V_A)_B}{(V_A)_C} \frac{\zeta_{AC}}{\zeta_{AB}} \frac{(d\ln a_A/d\ln c_A)_B}{(d\ln a_A/d\ln c_A)_C} \qquad \text{(VII-6)}$$

For the present systems, V_A is very-nearly identical to the molal volume of A so the ratio of partial volumes vanishes. If, from lack of information, any changes in the ratio of thermodynamic factors are neglected, the ratio of the two friction coefficients, relative to their ratio at infinite solute dilution may be calculated as

$$\left(\frac{\zeta_{AC}}{\zeta_{AB}}\right)_R = \left(\frac{D_{AB}}{D_{AC}}\right)_R = \frac{D_{AB}}{D_{AC}} \Big/ \left(\frac{D_{AB}}{D_{AC}}\right)_\infty \qquad \text{(VII-7)}$$

where the subscript R refers to the value relative to the value at infinite solute dilution (∞).

The results of applying Equation VII-7 to the cases of n-octane and MCH as solvents are shown in Figure 24.

The ratio of friction coefficients for octane and heptanol in MCH (Figure 24, a) may be tentatively explained as follows. The initial rapid decrease in the relative friction curve may be due to formation of alcohol complexes as the alcohol is added to the solvent. These complexes may hinder movement of the alcohol and increase ζ_{AB} relative to the case of the non-polar ζ_{AC}. Then at higher concentrations there becomes little percentage increase of alcohol complexes as more is added, and the ζ_{AC}/ζ_{AB} ratio becomes linear in x.

Figure 24, b shows a comparable relation for n-octane as solvent. As in the above discussion of the n-octane-cyclohexanone system, the theory of cyclohexanone clusters may be used. As solute is added to the

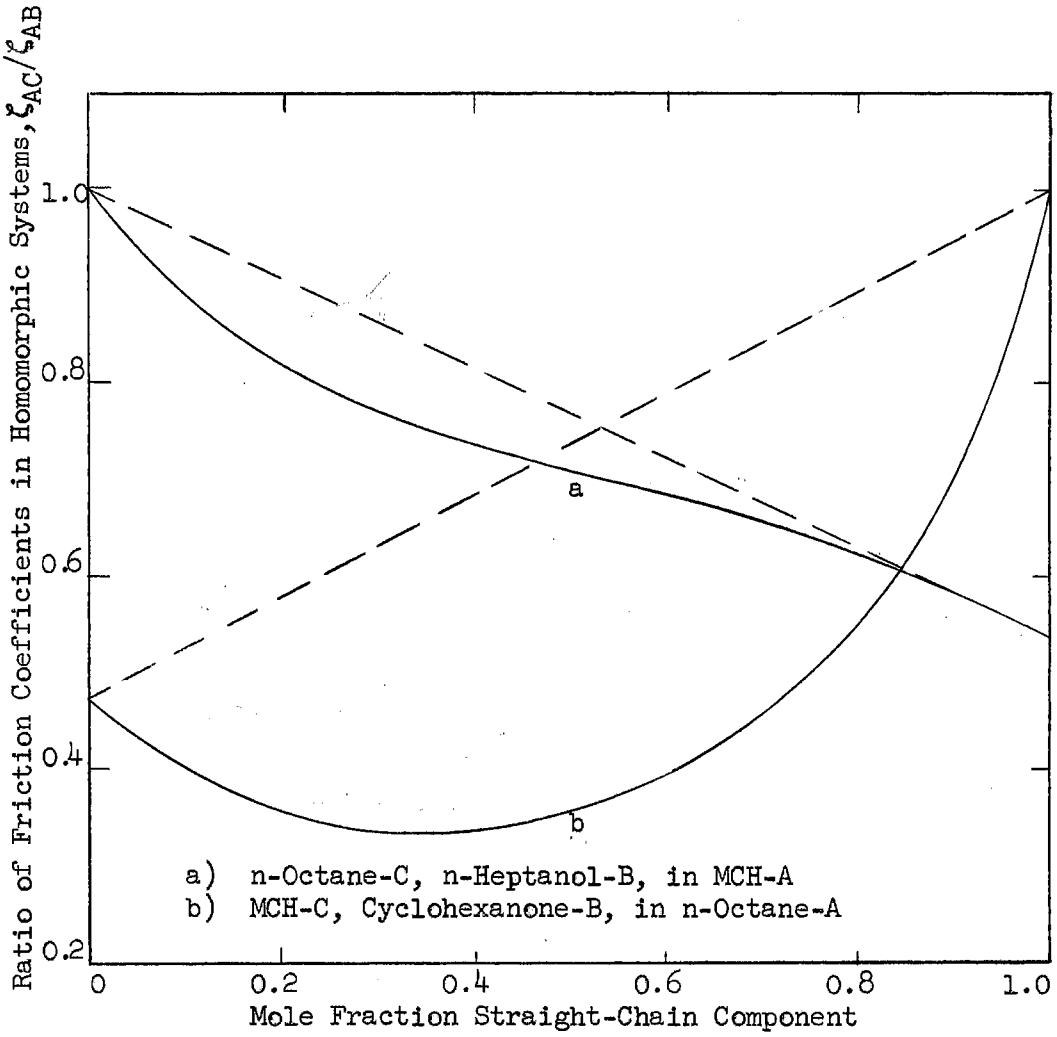

Figure 24

Friction Coefficient Comparisons for Homomorphic Solutes

octane the ratio of ζ_{AC}/ζ_{AB} ratio declines until clustering of cyclohexanone become prevalent. This causes ζ_{AB} to decrease with increased solute due to the aforementioned shielding of cyclohexanone molecules and the ζ_{AC}/ζ_{AB} ratio begins to increase.

In analyzing the data of this section, mention should be made of the excess volumes of the systems as an indicator of complex formation. Anderson (4) has contended that excess volume is a sensitive indicator of complex formation. He presented a semi-quantitative analysis in which he separated physical and chemical effects. He concluded that physical effects (differences in solubility parameters and compressibilities of the pure components) could yield positive or negative excess volumes while chemical effects (complex formation) caused negative deviations.

The excess volumes for the four systems of this study at 25°C are shown in Figure 25. The curves were obtained by fitting the density data to equations of the form

$$V = \frac{\bar{M}}{\rho} = \frac{M_2}{\rho_2} + \left(\frac{M_1}{\rho_1} - \frac{M_2}{\rho_1}\right) x_1 + (1 - x_1)(A + B\, x_1)\, x_1 \qquad \text{(VII-8)}$$

where M_i = molecular weight of component

$\bar{M}$ = average molecular weight

A,B = constants determined by least-squares curve fit

From Equation VII-8, the excess volume, V^E, is given by

$$V^E = x_1\,(1 - x_1)(A + B\, x_1) \qquad \text{(VII-9)}$$

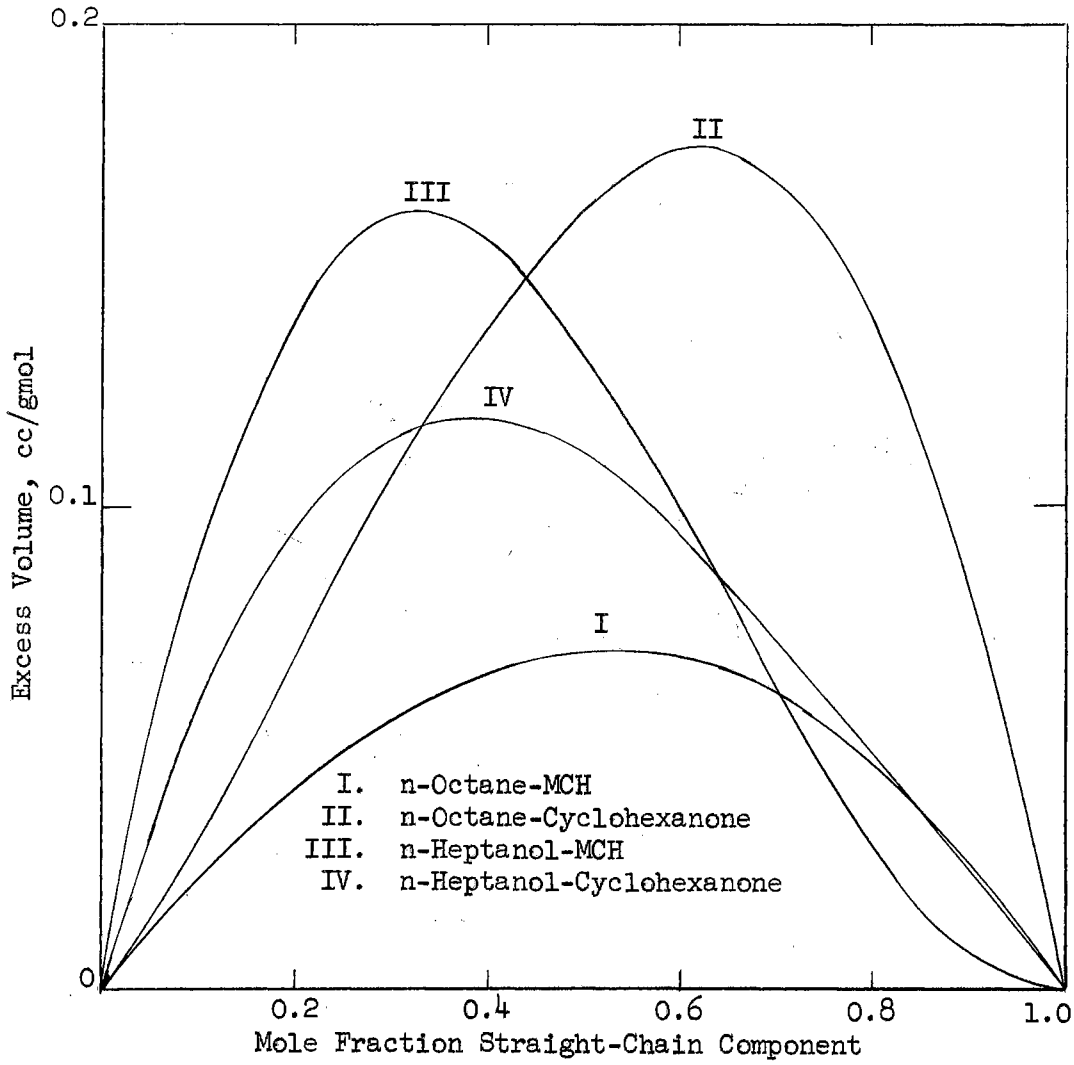

Figure 25

Excess Volumes for Systems at 25°C

This type relation has been recommended by Scatchard (55). The above equations yielded volumes agreeing with the experimental data within an average of 0.1%.

All excess volumes for the systems under study are positive. In view of Anderson's approach, complexes either are non-existant in these systems or are completely masked by physical interactions.

The sole indication of complex formation comes from the volume data on system IV at various temperatures. The maxima in the excess volume curves at 55° and 90°C (not shown in the figure) are 0.25 and 0.32 cc/gmole, respectively, compared to 0.175 cc/gmole at 25°C. For systems where only physical interactions occur, an increase in V^E should not be evidenced. This increase, in Anderson's scheme, would represent a decrease in an exothermic complex as temperature increases.

The descriptions given in this section are at best tentative. Nonetheless, the facts seem to be established that polar groups affect the diffusion process in a manner not equivalent to non-polar groups. Introduction of a polar group in place of a non-polar group appears to alter both the magnitude of the diffusivities and the diffusivity-composition relation. The effects are evident at infinite dilution, indicating that association is not the sole contributor to the polar effects.

E. Comparison of Diffusion Data with Empirical Correlations

In most engineering applications of diffusion coefficients, diffusion data are not available on the systems of interest. The general procedure is to use one of several available empirical correlations (6, 58, 63, 76) to estimate the required diffusivities. As part of this

study two commonly-used correlations were compared with the present diffusion data.

The correlations of Sitaraman, et al (63) and Othmer and Thacker (58) were chosen for comparison. The well-known correlations of Wilke (76) and Arnold (6) were excluded since they require the use of certain "association parameters" which must be estimated. These correlations are no better than the parameters assumed in their use. The correlation of Sitaraman, et al is a modification of Wilke's work in which they have expressed Wilke's association parameter in terms of physical properties.

The physical properties used in testing these correlations are listed in Table E-IV, where their sources of origin are noted. These empirical correlations are designed to apply in regions of infinite solute dilution, so the present data offer 14 data points to be tested. Results are summarized in Table XXIII.

The data in Table XXIII reveal that neither correlation is very satisfactory for the present data. Both methods predict diffusivities lower than the observed values in all cases except for n-heptanol in MCH. The Othmer correlation is consistently the poorer of the two; similar results have been observed by other investigators (6, 44, 48).

The poor results from these correlations may be in part due to the fact that much of the data fall in the extremities of the range of data on which the correlations are based.

F. Application of the General Equations for Calculation of Differential Diffusivities

A general set of equations was derived in Chapter II which permit calculation of differential diffusivities from diaphragm cell data

TABLE XXIII

COMPARISON OF DIFFUSION DATA

WITH EMPIRICAL CORRELATIONS

Solute/Solvent		Diffusion Coefficient, $cm^2/sec \times 10^5$		
		Observed	Sitaraman (63)	Othmer (58)
n-Heptanol/Cyclohexanone,	10°C	0.39	0.35	0.24
	25	0.58	0.50	0.37
	55	1.05	0.91	0.71
	90	1.92	1.65	1.20
Cyclohexanone/n-Heptanol,	10	0.19	0.14	0.08
	25	0.34	0.24	0.15
	55	0.74	0.62	0.37
	90	1.65	1.54	0.76
n-Octane/MCH,	25	1.61	1.34	0.99
MCH/n-Octane,	25	2.30	2.02	1.56
n-Octane/Cyclohexanone,	25	0.74	0.53	0.34
Cyclohexanone/n-Octane,	25	2.20	1.98	1.77
MCH/n-Heptanol,	25	0.47	0.24	0.09
n-Heptanol/MCH,	25	0.62	1.25	1.08

regardless of the magnitude of the volume changes during diffusion. At present, no data are available which afford a good opportunity to demonstrate the applicability of these equations. This situation exists because experimenters have always used very small concentration differences to minimize volume changes. Such procedures have circumvented the problem of volume changes but introduce increased analytical errors. The present study used large concentration differences, but the systems exhibited negligible volume changes.

Olander (57) has presented an approximate method for calculating D from diaphragm cell data when volume changes occur. He illustrated his equations by application to the ethanol-water data of Hammond and Stokes (36). This system exhibits volume decreases as large as 3%. Olander reported a 6% increase in D at pure ethanol when his equations were used in place of equations assuming no volume change. Thus, as part of this study, the new set of equations were also applied to the ethanol-water system. The data of Dullien (25) were used since Hammond and Stokes did not report complete data. (This forced Olander to make certain assumptions regarding initial concentrations, and use of Dullien's data avoided such assumptions.)

The calculations were carried out on an IBM 704 digital computer. The Fortran listing of the source program is given in Appendix G. Calculations were also performed using Gordon's complete equation (no volume changes considered) on an IBM 1410. The results of these calculations are compared with Dullien's graphical solution of Gordon's equation in Table XXIV.

The agreement of the three methods is excellent. The results indicate

TABLE XXIV

COMPARISON OF DIFFERENTIAL DIFFUSIVITIES

FOR ETHANOL-WATER SYSTEM

Concentration of Ethanol, gm/cc	Differential Diffusivity, $cm^2/sec \times 10^5$		
	Dullien (26)	Gordon's Equations	New General Equations
0.0	1.220	1.22	1.22
0.1	0.946	0.94	0.945
0.2	0.695	0.685	0.68
0.3	0.490	0.485	0.48
0.4	0.373	0.37	0.37
0.5	0.380	0.375	0.37
0.6	0.475	0.48	0.48
0.65	0.570	0.58	0.585
0.7	0.725	0.74	0.75
0.75	0.975	0.98	0.99
0.78507*	1.220	(1.245)	(1.235)

*Pure ethanol

negligible effect of volume changes in these experiments where very small concentration differences were employed. The values of D at pure ethanol are given in parenthesis since the extrapolation to pure ethanol is rather arbitrary due to the high curvature of the D verse ρ_A relation in this region.

These results certainly show no 6% error in the use of Gordon's equation. The conditions used by Dullien and Hammond and Stokes were sufficiently similar to render the influence of experimental differences negligible. The anomaly could be in Olander's method. He makes the following assumptions,

1. The denominator of Equation II-22 is of the form 1-x, and 1/1-x is approximated by 1 + x.
2. The solvent partial molal volume is taken at the average concentration in the diaphragm.
3. The partial volume ratio is taken as linear in concentration.

plus other simplifications. The results of such assumptions are difficult to assess, and their validity would vary from system to system.

In any event, Olander's method is not generally suitable if maximum concentration differences are to be used in future experiments. For example, if pure ethanol is allowed into pure water, assumption 1 above can be in error by over 80%. And the partial volume ratio is anything but linear in concentration (see Olander's article, Figure 1).

Permitting use of large concentration differences, with increase of experimental accuracy, seems to this author to be the single most important benefit of the equations which account for volume changes. Thus, the equations from this study appear much more useful than those of Olander.

In the course of this study, some factors arising through the use of large concentration differences merit discussion. First, in a system where an extremum in the diffusion curve occurs some caution is required. The method of calculation of differential diffusivities consists of shifting each point on the $\overline{D}$ versus ρ_A plot horizontally to a point $\overline{D}$ versus ρ_A^* where $\overline{D}$ becomes identical to D. However, note from Figure 5 that a considerable portion of the D versus ρ_A curve may exist below the lowest point in the $\overline{D}$ versus ρ_A curve. This portion of the D versus ρ_A curve will then contain no experimental points, making its shape somewhat uncertain. This difficulty is easily eliminated by performing a few runs in the area of the extremum using smaller concentration differences, causing the $\overline{D}$ and D values to be more nearly equal. Obviously, no such trouble arises for systems having no extrema in the D versus ρ_A curves.

Also, the relation

$$\overline{D} = \frac{1}{(\Delta \rho_A)_m} \int_{\rho'_{A_m}}^{\rho''_{A_m}} D \, d\rho_A \qquad \text{(VII-10)}$$

where $\rho_{A_m} = \frac{1}{2}(\rho_{Ao} + \rho_{Af})$ and $(\Delta \rho_A)_m = \rho''_{A_m} - \rho'_{A_m}$

has often been forwarded as being extremely accurate, although an approximation (35, 68). In some cases the fact that Equation VII-10 is an approximation is not even mentioned.

The applicability of Equation VII-10 is based on assumed constancy of the factor $F(\rho'_A, \rho''_A)$ in Equation II-36. For experiments using small concentration differences or short diffusion times, the equation should

apply well. However, when large concentration differences are employed, particularly in systems where the D versus ρ_A relation displays a high degree of curvature, Equation VII-10 may lead to errors, and the complete equations should be employed.

In summary, the new general equations are recommended for use in systems where volume changes occur, and the use of the maximum possible concentration differences is advocated (subject to the above comments).

CHAPTER VIII

CONCLUSIONS AND RECOMMENDATIONS

The present study consists of an investigation of diffusion in liquid binary systems of non-electrolytes. In particular, the effects of temperature and interactions of the components on the diffusion coefficient were studied.

The study involved measurement of diffusion rates using the diaphragm-cell technique. From this experimental work the conclusion was reached that the apparatus and procedures employed satisfactorily combine relative ease of operation and accuracy. The diffusion data from the study are nominally precise to $\pm$ 1%. Certain undetermined factors in addition to analytical errors have been found to contribute to the scatter of the data on the organic systems.

From the experimental work the following recommendations are made as guidelines for future work:

1. The cell support and stirring apparatus should be modified so that the gear table and diffusion cells rest on separate supports. This should lessen transmission of vibrations from the table to the cells.
2. The polyethylene screwclip valves proved to be difficult to operate and should be replaced.

Commercially-available teflon needle valves are possible replacements.

3. A filling and sampling technique should be developed which allows minimum contact of the solutions with the atmosphere, particularly at temperatures very far removed from that of the surroundings. The technique should allow filling to be done from bessels contained in the temperature bath; this would effectively eliminate introduction of temperature gradients into the cell.
4. Less tedious analytical methods should be considered. Selection of systems where refractometry is applicable would be a distinct advantage.
5. An experimental study should be instigated to determine the physical properties governing the "critical stirrer speed" for the diaphragm cells. A successful study of this nature would add considerably in removing diaphragm-cell technique from the stage of being an "art."

As a part of this study, the general diaphragm-cell technique was subjected to a certain amount of scrutiny. As a result, the following conclusions were reached:

1. A new set of general equations was derived relating the differential diffusion coefficient

to diaphragm cell results. These equations are applicable regardless of volume changes on mixing.

2. A criterion was established to estimate the optimum duration of a diaphragm-cell experiment. These equations indicate that deviations of 40% from the optimum duration cause increases of only 20% in the standard deviation of the measured diffusion coefficients. However, the standard deviation is inversely proportional to the initial concentration difference in the experiment. (In a work published too late for discussion herein, van Geet and Adamson (73) obtained results similar to the above.)

3. If large concentration differences are used in diaphragm cell experiments, the approximate relation

$$\bar{D} = \frac{1}{(\Delta \rho_A)_m} \int_{\rho'_{A_m}}^{\rho''_{A_m}} D \, d\rho_A$$

may lead to incorrect results, particularly in systems displaying a highly-curved D versus ρ_A relation.

From this portion of the study, the following recommendations are made:

1. To yield the most precise results, experiments should be carried out using the maximum possible

concentration differences. The general equations derived in this study should then be used to determine the differential diffusivities if volume changes occur during diffusion.

2. A study should be made of the new equations to see if any simplifications may be made to facilitate their application.
3. Further study of the "quasi-steady" state assumption is needed. Data are now becoming available with reputed accuracies to within a few tenths of one percent, and this may exceed the accuracy of the assumption used to determine the diffusivity.

From the study of the effect of temperature on the diffusion coefficient in the n-heptanol-cyclohexanone system in the range 10-90°C, the following conclusions were drawn:

1. The exponential rule, i.e., $D = Ae^{E_D/RT}$ was found to be obeyed to an excellent degree by the data. Such a variation agrees with the Eyring theory of diffusion as a rate process. This is the simplest type of relation possible, i.e., requiring no data other than D and T, which makes the results even more striking.
2. The exponential-type relation also applied for viscosities. Thus the D versus μ relation

was found to be linear on a logarithmic basis. Activation energies for diffusion and viscosity were found to differ and exhibited different composition dependencies.

3. For engineering applications, moderate extrapolations of diffusion coefficients as a function of temperature using the exponential rule should be very satisfactory. For systems where structural changes with temperature are suspected, reason exists to believe a logarithmic extrapolation of D against μ may be a better method. The well-known method of assuming $D\mu/T$ constant cannot be recommended as generally valid.
4. Tentative evidence exists that although the variation of the pair-wise intermolecular friction coefficients, ζ_{11}, ζ_{12}, and ζ_{22} vary in different manners with composition, their temperature dependences may be of the same functional form.

Four structurally-similar systems were studied in which each system offered different possibilities for inter-molecular interactions. From these data the following qualitative conclusions were made:

1. Polar groups in a diffusing species influence the diffusion process to an extent different from that attributable solely to the geometrical

configuration of the species, as exemplified by non-polar groups.

2. Polar interactions influence both the magnitude of the diffusivity and the diffusivity-composition relation. In all cases studied, replacement of a non-polar by a polar group reduced the diffusion rate in non-polar solvents.
3. Differences in diffusion rates between homomorphic polar and non-polar groups were evidenced at infinite dilution, so intermolecular association of the polar species cannot be assumed to be the sole cause of the polar influence.

From the above study, the following recommendations for future work are suggested:

1. Since only regular solutions are amenable to exact testing by present diffusion theories, attention should be directed to such systems. The various models available, although equally valid from a regular-solution standpoint, will not necessarily describe data with equal accuracy. Presently, data to allow evaluation of these models is practically non-existent.
2. Any studies made should be as comprehensive as possible, including data on the mutual and two tracer diffusion coefficients, viscosity, and activity of the solution. In addition, if complexing in solution is suspected, spectroscropic

or other means for detection of the complexes should be employed.

3. A study of temperature effects on the mutual and tracer diffusivities should be undertaken. From such data, the tentative hypothesis of identical temperature dependence of the three pair-wise intermolecular frictions, ζ_{11}, ζ_{12}, and ζ_{22} could be assessed.

A SELECTED BIBLIOGRAPHY

1. Anderson, D.K., and A.L. Babb, J. Phys. Chem. 65, 1281 (1961).

2. _____ , Ph.D. Thesis, Univ. of Washington (1960).

3. _____ , J.R. Hall, and A.L. Babb, J. Phys. Chem. 62, 404 (1958).

4. Anderson, R., Ph.D. Thesis, Univ. of California (1962).

5. API Research Project No. 44, "Selected Values of Physical and Thermodynamic Properties of Hydrocarbons and Related Compounds", A & M College of Texas, College Station, Texas (1953-date).

6. Arnold, J.H., J. Am. Chem. Soc. 52, 3937 (1930).

7. Barnes, C., Physics 5, 4 (1934).

8. Bauer, N., in "Physical Methods of Organic Chemistry", Pt. 1, Edited by A. Weissberger, Interscience, New York (1949).

9. Bearman, R.J., J. Phys. Chem. 65, 1961 (1961).

10. _____ , and J.G. Kirkwood, J. Chem. Phys. 28, 136 (1958).

11. Beers, Y., "Introduction to the Theory of Errors", Addison-Wesley Publishing Co., Reading, Mass. (1957).

12. Bird, R.B., W.E. Stewart, and E.N. Lightfoot, "Transport Phenomena", John Wiley and Sons, New York (1960).

13. Bondi, A., and D.L. Simkin, AIChE Journal 3, 473 (1957).

14. Burchard, J.K., and H.L. Toor, J. Phys. Chem. 66, 2016 (1962).

15. Caldwell, C.S., and A.L. Babb, J. Phys. Chem. 60, 51 (1956).

16. Carman, P.C., and L. Miller, Trans. Faraday Soc. 55, 1838 (1959).

17. _____ , and L. H. Stein, Trans. Faraday Soc. 51, 619 (1955).

18. Chu, J.C., et al., "Vapor-Liquid Equilibrium Data", J.W. Edwards, Ann Arbor, Mich. (1956).

19. Cohen, E., and H.R. Bruins, Z. physik. Chem. 103, 404 (1923).

20. Daniels, F., et al., "Experimental Physical Chemistry", McGraw-Hill Book Co., Inc., New York (1956).

21. _____ , and R.A. Alberty, "Physical Chemistry", John Wiley and Sons, New York (1955).

22. de Groot, S.R., "Thermodynamics of Irreversible Processes", Interscience, New York (1951).

23. Dullien, F.A.L., Trans. Faraday Soc. 59, 856 (1963).

24. _____ , and L.W. Shemilt, Trans. Faraday Soc. 58, 244 (1962).

25. _____ , and L.W. Shemilt, Can. J. Chem. Eng. 39, 242 (1961).

26. _____ , Ph.D. Thesis, Univ. of British Columbia, 1960.

27. Dunlop, P.J., J. Phys. Chem. 68, 26 (1964).

28. Ellerton, H.D., G. Reinfelds, D.E. Mulcahy, and P.J. Dunlop, J. Phys. Chem. 68, 403 (1964).

29. Ericksen, V.L. v., Brennstaff-chemie 33, 166 (1952).

30. Ewell, R.H., and H. Eyring, J. Phys. Chem. 5, 726 (1937).

31. Fick, A., Pogg. Ann. 94, 59 (1855), as quoted in reference 44.

32. Fishtine, S.H., Ind. Eng. Chem. 55, 47 (1963).

33. Garner, F.H., and P.J.M. Marchant, Trans. Inst. Chem. Engrs. 39, 397 (1961).

34. Gladstone, S., K.J. Laidler, and H. Eyring, "The Theory of Rate Processes", McGraw-Hill Book Co., Inc., New York (1941).

35. Gordon, A.R., Ann. N. Y. Acad. Sci. 46, 285 (1945).

36. Hammond, B.R., and R.H. Stokes, Trans. Faraday Soc. 49, 890 (1953).

37. Hapeman, R.C., Private Communications (Distillation Products Industries) 1963.

38. Hartley, G.S., and J. Crank, Trans. Faraday Soc. 45, 801 (1949).

39. Henrion, P.N., Trans. Faraday Soc. 60, 72 (1964).

40. Hildebrand, J.H., and R.L. Scott, "The Solubility of Nonelectrolytes", Reinhold Publishing Corp., New York (1950).

41. Hodgman, C.D., "Handbook of Chemistry and Physics", 36th Ed., Chemical Rubber Publishing Co., Cleveland, Ohio (1954).

42. Holmes, J.T., C.R. White, and D.R. Olander, J. Phys. Chem., 67, 1469 (1963).

43. Irani, R.R. and A.W. Adamson, J. Phys. Chem. 64, 199 (1960).

44. Johnson, P.A., and A.L. Babb, Chem. Rev. 56, 387 (1956).

45. Laity, R.W., J. Phys. Chem. 63, 80 (1959).

46. Lamm, O., Acta Chem. Scand. 8, 1120 (1954).

47. _____ , Arkiv Kemi, Min. Geol. A 18, No. 2, (1944).

48. Lewis, J.B., J. Appl. Chem. 5, 228 (1955).

49. McBain, J.W., and C.R. Dawson, Proc. Roy. Soc. A118, 32 (1935).

50. _____ , and T.H. Liu, J. Am. Chem. Soc. 53, 59 (1931).

51. McLaughlin, E., in "Progress in International Research on Thermodynamic and Transport Properties", ASME, Academic Press (1962).

52. Meyer, R.E., and N.H. Nachtrieb, J. Chem. Phys. 23, 1951 (1955).

53. Mills, R., J. Phys. Chem. 67, 600 (1963).

54. Moelwyn-Hughes, E.A., and P.L. Thorpe, Proc. Roy. Soc. A277, 423 (1964).

55. _____ , "Physical Chemistry", Pergamon Press, New York (1957).

56. Northrop, J.N., and M.L. Anson, J. Gen. Physiol. 12, 543 (1928).

57. Olander, D.R., J. Phys. Chem. 67, 1011 (1963).

58. Othmer, D.F., and M.S. Thakar, Ind. Eng. Chem. 45, 589 (1953).

59. Perry, J.H., "Chemical Engineers' Handbook", 3rd Ed., McGraw-Hill Book Co., Inc., New York (1950).

60. Prigogine, I., "Etude Thermodynamique des Phenomenes Irreversibles", Dunod, Paris (1947).

61. Reid, R.C., and T.K. Sherwood, "The Properties of Gases and Liquids", McGraw-Hill Book Co., Inc., New York (1960).

62. Scheffer, J.D.R., and F.E.C. Scheffer, Verslag Akad. Wetenschappen Amsterdam 25, 67 (1916).

63. Sitaraman, R., S.H. Ibrahim, and N.R. Kuloor, J. Chem. Eng. Data 8, 198 (1963).

64. Smith, I.E., and J.A. Storrow, J. Appl. Chem. (London) 2, 225 (1952).

65. Stokes, R.H., P.J. Dunlop, and J.R. Hall, Trans. Faraday Soc. 49, 886 (1953).

66. _____, J. Am. Chem. Soc. 73, 3527 (1951).

67. _____, J. Am. Chem. Soc. 72, 763 (1950).

68. _____, J. Am. Chem. Soc. 72, 2243 (1950).

69. Taylor, H.S., "Treatise on Physical Chemistry", 2nd Ed., D. van Nostrand Co., Inc., New York (1931).

70. Timmermans, J., "The Physio-chemical Constants of Binary Systems in Concentrated Solutions", Interscience, New York (1960).

71. _____, "The Physio-chemical Constants of Pure Organic Compounds", Elsevier Publishing Co., New York (1950).

72. Toor, H.L., J. Phys. Chem. 64, 1580 (1960).

73. van Geet, A.L., and A.W. Adamson, J. Phys. Chem. 68, 238 (1964).

74. Vogel, A.I., J. Chem. Soc., 1814 (1948).

75. White, J.R., J. Chem. Phys. 24, 470 (1956).

76. Wilke, C.R., and P. Chang, AIChE Journal 1, 264 (1955).

APPENDIX A

DERIVATION OF EQUATION II-3 FROM EQUATION II-2

The derivation of Equation II-3 from the definition of the diffusion coefficient, Equation II-2, is presented in this section. The derivation is given in detail since the author has not seen the equation, in mass terms, in the literature. (The counterpart of Equation II-3 in molar terms appears in an article by Olander (57).) Note also that Equation II-2 cannot be derived, but is the definition of the diffusion coefficient. The following is simply a change of coordinates from the mass-average velocity to the laboratory frame of reference.

The following may be defined

v_A = average velocity of species A, cm/sec

v = mass-average velocity, cm/sec

The mass-average velocity is given by

$$v = v_A \omega_A + v_B \omega_B = (v_A \rho_A + v_B \rho_B)/ \rho \qquad \text{(A-1)}$$

The mass flux of A with respect to v is

$$(v_A - v) \rho_A = J_A = \text{Mass flux A, gm A/cm}^2 \text{ sec} \qquad \text{(A-2)}$$

The mass-average velocity in Equation A-2 may be replaced by the volume-average velocity through the following transformations. From Equations A-1 and A-2,

$$(v_A - v)\ \rho_A = \rho \left[v_A - \{(v_A\ \rho_A + v_B\ \rho_B)/\ \rho\} \right] \quad \text{(A-3)}$$

Recalling $\rho = \rho_A + \rho_B$, Equation A-3 may be written

$$(v_A - v)\ \rho_A = \rho_A\ \rho_B\ (v_A - v_B)/\ \rho \quad \text{(A-4)}$$

or

$$v_A - v = (\rho_B/\ \rho)\ (v_A - v_B) \quad \text{(A-5)}$$

Now define the volume-average velocity, v^*, as

$$v^* = v_A\ \rho_A\ V_A + v_B\ \rho_B\ V_B \quad \text{(A-6)}$$

so

$$v_A - v^* = v_A\ (1 - \rho_A\ V_A) - v_B\ \rho_B\ V_B \quad \text{(A-7)}$$

Combining Equation II-17 with Equation A-7 yields

$$v_A - v^* = \rho_B\ V_B\ (v_A - v_B) \quad \text{(A-8)}$$

From the definition of the diffusion coefficient, Equation II-2, and Equation A-2,

$$\rho_A\ (v_A - v) = -\ \rho\ D\ \nabla\omega_A \quad \text{(A-9)}$$

But from Equations A-5 and A-8,

$$\rho_A\ (v_A - v) = (\rho_A\ \rho_B/\ \rho\ )\ (v_A - v_B) = (\rho_A/\ \rho V_B)\ (v_A - v^*) \quad \text{(A-10)}$$

and Equation A-9 becomes

$$(\rho_A/\ \rho\ V_B)\ (v_A - v^*) = -\ \rho\ D\ \nabla\omega_A \quad \text{(A-11)}$$

The "driving force", $\nabla\omega_A$, may be replaced by $\nabla\rho_A$ by the following means.

Since $\rho_A = \rho\,\omega_A$,

$$\nabla\rho_A = \rho\nabla\omega_A + \omega_A\nabla\rho \tag{A-12}$$

From Equation II-17,

$$\rho_A V_A + (\rho - \rho_A) V_B = 1$$

so

$$\rho = (1 - \rho_A V_A + \rho_B V_B)/ V_B \tag{A-13}$$

Forming the gradient of each side of Equation A-13 results in the relation

$$\nabla\rho = \left[1 - \frac{V_A}{V_B}\right]\nabla\rho_A - \frac{1}{V_B}(\rho_A\nabla V_A + \rho_B\nabla V_B) \tag{A-14}$$

From Equation II-20,

$$\rho_A\, dV_A + \rho_B\, dV_B = 0 \tag{II-20}$$

The differential of V_A may be written at any given instant as

$$dV_A = \nabla V_A\cdot d\vec{r} \tag{A-15}$$

where $\vec{r}$ refers to the direction vector parallel to which the change in V_A is being measured. Equation II-20 becomes, using Equation A-15,

$$(\rho_A\nabla V_A + \rho_B\nabla V_B)\cdot d\vec{r} \tag{A-16}$$

which implies

$$\rho_A\nabla V_A + \rho_B\nabla V_B = 0 \tag{A-17}$$

and Equation A-14 becomes

$$\nabla\rho = \left[1 - \frac{V_A}{V_B}\right]\nabla\rho_A \tag{A-18}$$

Thus Equation A-12 becomes

$$\nabla\rho_A\left[1 - \omega_A + \frac{\omega_A V_A}{V_B}\right] = \rho\nabla\omega_A \tag{A-19}$$

Using Equation II-15, Equation A-19 becomes

$$\nabla \omega_A = \frac{1}{\rho^2 V_B} \nabla \rho_A \tag{A-20}$$

so Equation A-11 may be written

$$\frac{\rho_A}{\rho V_B} (v_A - v^*) = - \frac{D}{\rho V_B} \nabla \rho_A$$

or

$$\rho_A (v_A - v^*) = - D \nabla \rho_A \tag{A-21}$$

Now, the mass flux of A with respect to a stationary observer (laboratory reference system) is

$$N_A = \rho_A v_A \tag{A-22}$$

so Equation A-21 becomes

$$N_A = - D \nabla \rho_A + \rho_A v^* \tag{A-23}$$

and from Equations A-6 and A-22, A-23 may be written

$$N_A = - D \nabla \rho_A + \rho_A (N_A V_A + N_B V_B) \tag{II-3}$$

which is Equation II-3, the equation desired.

APPENDIX B

CONSIDERATION OF ANALYTICAL ERRORS

An evaluation of the major factors influencing the scatter of the experimental diffusion data may be made using statistical methods. Application of the statistics to these data requies certain simplifications, but the results provide a suitable insight into the major sources of error.

A. The KCl-Water Data

The precision of the cell constant, β, values may be estimated as follows. Neglecting errors in the time and D values for KCl-water, the following equation (analagous to Equation II-47) may be written for the fractional standard deviation in β as follows;

$$\frac{s_\beta}{\beta} = \frac{\sqrt{2}\, s}{(\rho''_A - \rho'_A)_o \ln R} \sqrt{R + 3} \qquad \text{(B-1)}$$

where s is defined by Equation II-41. Now,

$$\rho_A = \frac{W_r}{V} \qquad \text{(B-2)}$$

where V refers to the pipet volume, and ρ_A refers to the KCl concentration. Applying Equation II-37 to B-2,

$$s_\rho^2 = \left(\frac{1}{V}\right)^2 s_{W_r}^2 + \left(\frac{W_r}{V^2}\right)^2 s_V^2 \qquad \text{(B-3)}$$

From Equation V-1, the following relation results

$$s^2_{W_r} = 4\, s^2_W \tag{B-4}$$

where s_W = standard deviation of the weight of a sample bottle. The value of s_W was estimated as follows. A set of four sample bottles was weighed a total of six times over a period of a few days. the results are given in Table B-I. From any combination of weighings (i.e., 1-2, 3-6, etc.) from Table B-I, four estimates of the change in weight of Bottle 43, ΔW^{43}_{ij}, are possible. From Equation C-10, derived in Appendix C,

$$\Delta W^{43}_{ij} = \frac{W^{43}_j}{W^k_j} \Delta W^k_{ij} , \quad k = 43,45,53,59 \tag{B-5}$$

Forming all ij combinations ($i > j$), 15 sets of four estimates each for ΔW^{43}_{ij} were calculated. Pooling the sums of squares for these 15 sets, each with $4 - 1 = 3$ degrees of freedom, gave the following result,

$$s_{\Delta W} = 4 \times 10^{-5} \text{ gm} \tag{B-6}$$

From Equation B-5, the result follows that

$$s_{\Delta W} \approx \sqrt{2}\, s_W \tag{B-7}$$

so

$$s_W \approx 3 \times 10^{-5} \text{ gm}$$

and

$$s_{W_r} \approx 6 \times 10^{-5} \text{ gm} \tag{B-8}$$

From the data in Table E-I, the average absolute deviation of

134 residue weights from their 46 respective means is 8×10^{-5} gms. Due to the small sample sizes, only three repetitions per sample, no estimate of the standard deviation seems warranted.

The volume of the pipet used to deliver the KCl-water samples was determined four times. The average volume was 9.974 cc with residuals of -1, 1, -2, and 2×10^{-3} cc. From these data the estimate was made that

$$s_V \approx 2 \times 10^{-3} \text{ cc} \tag{B-9}$$

Applying Equation B-3, using a high value of 0.08 gms for W_r,

$$s_\rho^2 \approx \left(\frac{1}{10}\right)^2 (6 \times 10^{-5})^2 + \left(\frac{0.08}{10^2}\right)^2 (2 \times 10^{-3})^2$$

$$\approx 36 \times 10^{-12} + 3 \times 10^{-12}$$

or

$$s_\rho \approx 6 \times 10^{-6} \text{ gm/cc} \tag{B-10}$$

Notice that the major source of error in ρ comes from W_r, not from V.

Typical conditions for the calibration runs were

$$(\rho''_A - \rho'_A)_o = 8 \times 10^{-3} \text{ gm/cc}$$
$$R = 2 \tag{B-11}$$

From Equation B-1,

$$\frac{s_\beta}{\beta} = \frac{1.414 \times 6 \times 10^{-6}}{8 \times 10^{-3} \times 0.7} \sqrt{7} = 4 \times 10^{-3} \tag{B-12}$$

Thus s_β should be approximately 0.4% of β. However, the data on β from

Table II indicate a lower scatter in β, nearer 0.1%.

The statistical analysis indicates that the very close agreement of the experimental β values may be fortuitous. On the other hand, the approximate nature of this statistical treatment should be remembered. A likely prospect is that the actual value of s_β is somewhat between 0.1 and 0.4% of β. At least, the inference may be made that no large unaccounted-for sources of error were present in the calibration runs.

B. The Organic Data

The standard deviation of the diffusion coefficients for the organic runs is given by Equation II-47. For the pycnometric analyses

$$\rho = \frac{W^o_{B+S} - W^o_B}{V} \qquad \text{(B-13)}$$

where W^o_{B+S} = in-vacuo weight of pycnometer and sample, gms

W^o_B = in-vacuo weight of empty pycnometer, gms

V = pycnometer volume, cc

ρ = density of sample, gms/cc

Values of W^o_B were determined four times for each of the six pycnometers over a period of a few days. The results are given in Table B-II. Equations C-3 and C-16 were used to calculate W^o_B. From these data four estimates of the weight (in vacuo) of each of the six pycnometers were obtained. Assuming that $s_{W^o_B}$ is independent of the magnitude of W^o_B, the sums of squares for the six pycnometers were pooled (yielding 6 x (4-1) = 18 degrees of freedom) and the following result followed;

$$s_{W^o_B} = 5.5 \times 10^{-5} \text{ gm} \qquad \text{(B-14)}$$

The value of s_V was determined from the pycnometer calibrations. From the data in Table E-III, a reasonable estimate of s_V seems to be

$$s_V \approx 4 \times 10^{-4} \text{ cc} \tag{B-15}$$

Then from Equation B-13,

$$s_\rho^2 = 2\left(\frac{1}{V}\right)^2 s_{W^o}^2 + \left(\frac{W^o_{B+S} - W^o_B}{V^2}\right)^2 s_V^2 \tag{B-16}$$

Since $V \approx 20$ cc, and $W^o_{B+S} - W^o_B \approx 16$ gms,

$$s_\rho^2 \approx 2\left(\frac{1}{20}\right)^2 (5.5 \times 10^{-5})^2 + \left(\frac{16}{20^2}\right)^2 (4 \times 10^{-4})^2$$

$$\approx 15 \times 10^{-12} + 256 \times 10^{-12}$$

or

$$s_\rho \approx 1.6 \times 10^{-5} \text{ gm/cc} \tag{B-17}$$

Note that the major source of variation in ρ arises through variation in V, not in the weighings.

The 127 pairs of density determinations in Table E-II exhibit an average absolute deviation from their respective means of 1.5×10^{-5} gm/cc. For large samples s is 1.25 times the average absolute deviation (11). If this relationship is applied here as an approximation, the result is

$$s_\rho \approx 1.9 \times 10^{-5} \text{ gm/cc} \tag{B-18}$$

which agrees very well with the predicted result, Equation B-17.

The systems of this study show essentially linear relations between ρ and ρ_A, i.e.,

$$\rho = \rho^o_B + \left[(\rho^o_A - \rho^o_B)/\rho^o_A\right] \rho_A \tag{B-19}$$

so

$$s_{\rho_A} = \left[\rho^o_A/(\rho^o_A - \rho^o_B)\right] s_\rho \tag{B-20}$$

where the superscript o refers to pure component densities.

The percentage standard deviation of the D values may now be estimated from Equation II-47. Since certain variables in Equation II-47 differ for each data point, the following typical values will be used:

$$\rho_A^o - \rho_B^o = 0.12 \quad gm/cc$$

$$\rho_A^o = 0.8 \quad gm/cc$$

$$(\rho_A'' - \rho_A')_o = 0.3 \quad gm/cc$$

$$R = 2.2$$

The above values yield,

$$\frac{s_D}{D} \approx \frac{1.414 \times 1.6 \times 10^{-5} \times 0.8}{0.12 \times 0.3 \times 0.8} \sqrt{7.8} \approx 2 \times 10^{-3}$$

Thus, from errors in the measured quantities, the average percentage standard deviation in D should be 0.2%. From the results in Figures 4 through 10, the actual variation in D is larger. The seven systems show an average percentage absolute deviation of about 0.8% from the smooth curves through the data.

The above results are similar to those found by Dullien (26), who reported an expected error of 0.4% compared to an actual error of 2%. He suggested evaporation, temperature fluctuations, and unlevel diaphragms as possible sources of the enhanced errors. No definite conclusion as to the cause of these increased errors is forwarded here. However, the presence of some undetermined error-causing factors is acknowledged.

TABLE B-I

REPLICATE TARE WEIGHTS

OF SAMPLE BOTTLES

Weighing	Bottle Weight, gms			
	Bottle 43	Bottle 45	Bottle 53	Bottle 59
1	76.78105	78.15994	77.26308	76.56384
2	76.78102	78.15986	77.26299	76.56369
3	76.78125	78.16014	77.26322	76.56399
4	76.78115	78.16010	77.26315	76.56390
5	76.78110	78.15998	77.26307	76.56377
6	76.78105	78.15998	77.26310	76.56380

TABLE B-II

REPLICATE IN-VACUO

PYCNOMETER WEIGHTS

Pycnometer Identification	In-vacuo Weight, gms			
	Weighing			
	1	2	3	4
1S	34.54851	34.54856	34.54845	34.54859
2S	34.96201	34.96203	34.96196	34.96205
3S	35.01727	35.01733	35.01724	35.01737
1L	37.60424	37.60423	37.60429	37.60427
2L	37.14312	37.14304	37.14321	37.14305
3L	38.18616	38.18608	38.18617	38.18609

APPENDIX C

BOUYANCY CORRECTIONS IN GRAVIMETRIC ANALYSES

In order to obtain maximum precision in the analyses of the KCl and organic samples, bouyancy corrections were required for each weighing. These bouyancy corrections were based on the following equilibrium force balance:

Actual weight of object - weight of air displaced by object = actual weight of weights - weight of air displaced by weights.

In equation form this relation becomes

$$W_B^o - W_B^o\left[\frac{\rho_a}{\rho_B}\right] = W_w^o - W_w^o\left[\frac{\rho_a}{\rho_w}\right] \qquad \text{(C-1)}$$

where W^o = in-vacuo weight of object, gm

a refers to air

B refers to the object being weighed

w refers to the weights used on the balance

The apparent weight in air, W_B, of the object is equal to the actual weight of the weights, W_w^o, on the balance. Thus Equation C-1 may be written

$$W_B^o\left[1 - \frac{\rho_a}{\rho_B}\right] = W_B\left[1 - \frac{\rho_a}{\rho_w}\right] \qquad \text{(C-2)}$$

Equation C-2 may be expressed as

$$W_B^o = W_B \left[1 + \rho_a \left(\frac{1}{\rho_B} - \frac{1}{\rho_w} \right) \right] \qquad (C\text{-}3)$$

where terms in ρ_a^2 and higher powers have been neglected. For a bottle containing a sample, S,

$$W_{B+S}^o = W_{B+S} \left[1 + \rho_a \left(\frac{1}{\rho_{B+S}} - \frac{1}{\rho_w} \right) \right] \qquad (C\text{-}4)$$

A. The KCl-Water Analyses

In the KCl-water runs, a standard bottle, identical to the other bottles, was weighed with each set of sample bottles. The standard bottle differed from the others in that it received no sample. For this bottle, denoted by the subscript s,

$$W_s^o = W_s \left[1 + \rho_a \left(\frac{1}{\rho_s} - \frac{1}{\rho_w} \right) \right] \qquad (C\text{-}5)$$

However, $\rho_s = \rho_B$ = density of glass, so from Equations C-3 and C-5, for the tare weights of the sample bottles,

$$\frac{W_B^o}{W_s^o} = \frac{W_B}{W_s} \qquad (C\text{-}6)$$

since the bracketed terms in the two equations are identical.

If a single prime is used to denote the weight of the standard bottle at the time of the gross weighings, from Equation C-5,

$$W_s' - W_s \equiv \Delta W_s = W_s^o \, \Delta \left\{ \left[1 + \rho_a \left(\frac{1}{\rho_s} - \frac{1}{\rho_w} \right) \right]^{-1} \right\} \qquad (C\text{-}7)$$

Since the standard bottle receives no sample, $\rho_s' = \rho_s = \rho_B$, and any change in the bracketed term is due to a change in ρ_a.

Consider the hypothetical case of a sample bottle which receives no sample. The change in weight of this bottle would be given by an expression analogous to Equation C-7,

$$\Delta W_B^* = W_B^* - W_B = W_B^o \Delta \left\{ \left[1 + \rho_a \left(\frac{1}{\rho_B} - \frac{1}{\rho_w} \right) \right]^{-1} \right\} \qquad (C\text{-}8)$$

where the * refers to the hypothetical gross weight of the sample bottle <u>if</u> it had received no sample.

From Equations C-7 and C-8, since the bracketed terms are identical,

$$\frac{\Delta W_B^*}{\Delta W_s} = \frac{W_B^o}{W_s^o} \qquad (C\text{-}9)$$

and W_B^* may be found by combining Equations C-6 and C-9,

$$W_B^* = W_B + \frac{W_B}{W_s} \Delta W_s \qquad (C\text{-}10)$$

If the bouyancy on the KCl residue in the sample bottle is neglected (this is a satisfactory approximation since the residue weight, W_r, was < 0.07 gm), the residue weight is given by

$$W_r = W_{B+S} - W_B^* \qquad (C\text{-}11)$$

or from Equation C-10,

$$W_r = (W_{B+S} - W_B) - \frac{W_B}{W_s} \Delta W_s \qquad (C\text{-}12)$$

Equation C-12 was used to determine the KCl residue weight from known values of the apparent weights of the sample bottle and standard bottle. Equation C-12 is identical to Equation V-1.

Residue weights were converted to concentrations by dividing them

by the volume of the aqueous sample from which the residue came.

B. The Organic Analyses

For the pycnometric analyses of the organic systems, the in-vacuo weights of the samples, W_S^o, were calculated by the relation

$$W_S^o = W_{B+S}^o - W_B^o \qquad (C\text{-}13)$$

using Equations C-3 and C-4. The values of the air density were found by use of a standard bottle, as described below.

The standard bottle used in the pycnometric analyses was a 125 cc erlenmeyer flask which had been sealed at the neck. Over a period of several days, the weight of the flask was periodically determined. At the time of each weighing, the air density was also determined from measurements of temperature, pressure, and humidity in the room. Air density was calculated from the relation (8)

$$\rho_a = \frac{1.7013 \times 10^{-6} (p - k)}{1 + 0.00367\ t} \qquad (C\text{-}14)$$

where p = pressure, mm Hg

$k = 0.0048\ H\ p'$

H = relative humidity, %

p' = vapor pressure of water, mm Hg

t = temperature, °C

From the series of ρ_a versus W_s observations, an analytical relation was established for the air density as a function of bottle weight. From Equation C-3, the form of the analytical equation was

$$\rho_a = A + B/W_s \qquad \text{(C-15)}$$

where $A = -\left(\frac{1}{\rho_s} - \frac{1}{\rho_w}\right)^{-1}$

$B = -A\,W_s^o$

Linear regression yielded the values

$$A = -1 / 3.10808, \text{ gm/cc}$$

$$W_s^o = 53.15155 \text{ gm}$$

or

$$\rho_a = \frac{53.15155 - W_s}{3.10808\,W_s} \qquad \text{(C-16)}$$

Figure C-1 illustrates the ρ_a versus W_s^{-1} relation.

The calculation of the actual weight of the empty pycnometer, W_B^o, was straightforward from Equation C-3 where $\rho_B = 2.23$ gm/cc, the density of glass, and $\rho_w = 8.4$ gm/cc was used for the weights. Calculation of the actual weight of the filled pycnometers required a trial-and-error calculation since both W_{B+S}^o and ρ_{B+S} were unknown. Solution required assuming ρ_{B+S}, calculating W_{B+S}^o, then checking the assumption from the relation

$$\rho_{B+S} = W_{B+S}^o / (V + W_B/\rho_B) \qquad \text{(C-17)}$$

where V is the pycnometer volume. This trial-and-error process was repeated until the assumed and calculated densities agreed to within 0.00001 gm/cc. The sample density was then found by the relation

$$\rho_S = (W_{B+S}^o - W_B^o) / V \qquad \text{(C-18)}$$

All sample residue and density calculations were performed on an IBM 1620 digital computer.

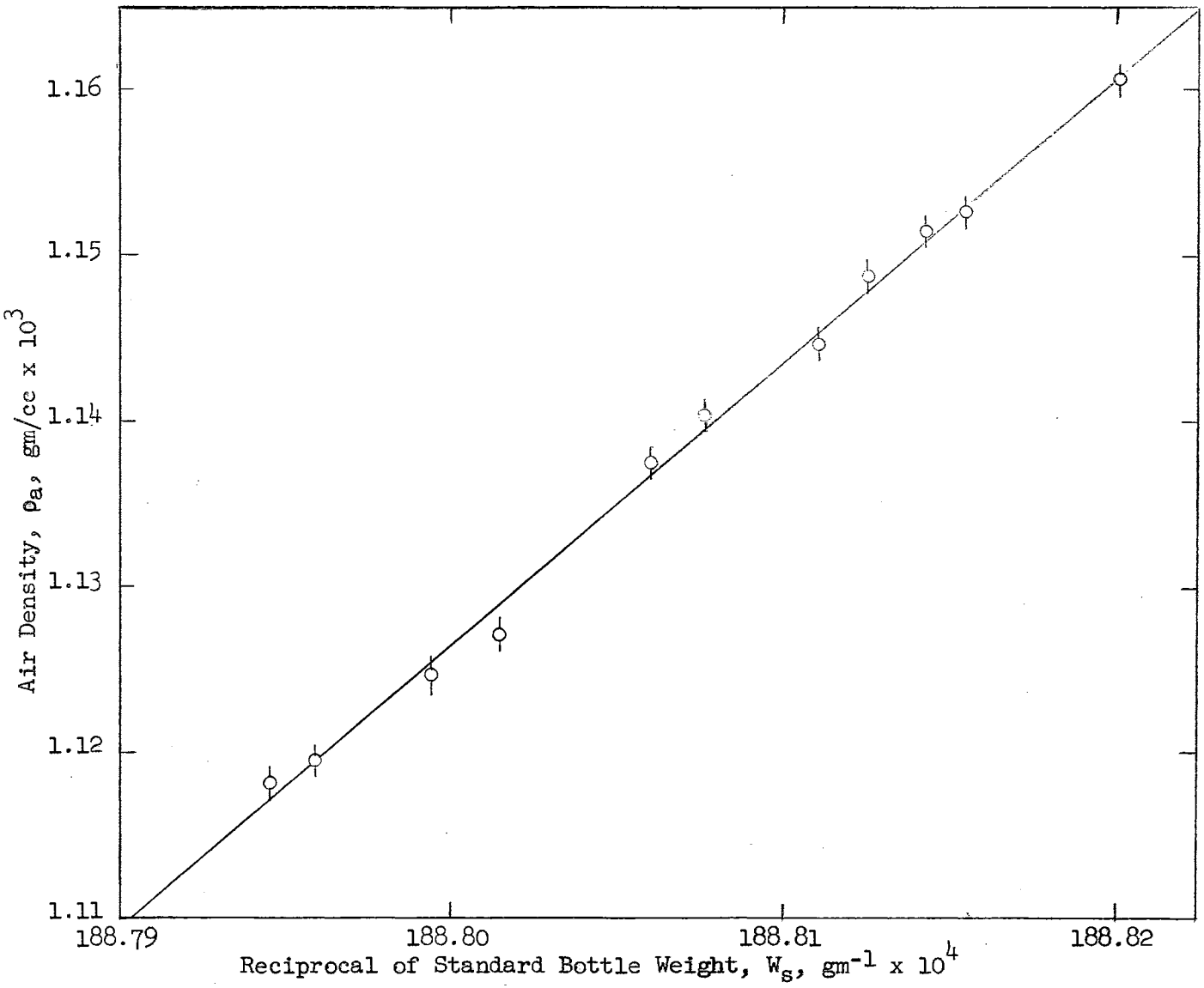

Figure C-1

Relation of Standard Bottle Weight to Air Density

APPENDIX D

RELATION OF THE "INTRINSIC" DIFFUSION COEFFICIENTS TO THE MUTUAL DIFFUSION COEFFICIENT

The so-called "intrinsic" diffusion coefficients defined by Hartley and Crank (38) have gained wide acceptance. Carman and Stein (17) have referred to the "five diffusion coefficients characterizing a binary mixture": D, the mutual diffusion coefficient; D_A^* and D_B^*, the self-diffusion coefficients; and $\mathscr{D}_A$ and $\mathscr{D}_B$, the intrinsic diffusion coefficients. They quote experimental evidence of differences in $\mathscr{D}_A$ and $\mathscr{D}_B$.

Bearman (9) first cast doubt on the independence of $\mathscr{D}_A$ and $\mathscr{D}_B$, deriving the relations

$$\mathscr{D}_A = D\, V/V_A \tag{D-1}$$

$$\mathscr{D}_B = D\, V/V_B \tag{D-2}$$

Mills (53), contridicted Bearman's relations, and used intuitive arguments to show

$$\mathscr{D}_A = \mathscr{D}_B = D \tag{D-3}$$

A closer examination, in terms of diffusion equations is presented here to resolve this problem.

Hartley and Crank define a diffusion coefficient, D^V, in a manner identical to that in Equation II-2 of this work, i.e., with respect to

a frame across which there is no net volume transport. However, they find this reference frame inconvenient when volume changes (and resultant bulk flow) occur. They then decide

> It is desirable to define new diffusion coefficients $\mathscr{D}_A$ and $\mathscr{D}_B$ in terms of the rate of transfer of A and B, respectively, across a section fixed so that no mass-flow occurs through it.

They term these new coefficients "intrinsic diffusion coefficients."

Hartley and Crank's nomenclature in the above definition is misleading since from the later developments in their work it becomes obvious that "no mass flow" refers to no mass transfer by the <u>bulk</u> flow mechanism. This is the point in which Bearman erred, interpreting Hartley and Crank's definition to mean no total (net) mass flow. As a result, Bearman's results are, as Mills observed, incorrect.

Now, utilizing the definitions of $\mathscr{D}_A$, equations for the mass flux, N_A, past a laboratory-fixed reference plane may be derived. The flux of A across the plane of no bulk mass transfer is given by

$$-\mathscr{D}_A \frac{d\rho_A}{dx} \qquad \text{(D-4)}$$

according to the definition of $\mathscr{D}_A$. Now the flux of A across a stationary (laboratory) reference plane will simply be the sum of the above flux and the flux of A due to bulk transport. However, the flux of A via bulk transport is simply the total volume flux times ρ_A

$$(N_A V_A + N_B V_B)\ \rho_A \qquad \text{(D-5)}$$

Thus, the flux of A relative to the fixed axis becomes the sum of the above fluxes,

$$N_A = (N_A V_A + N_B V_B)\ \rho_A - \mathscr{D}_A \frac{d\rho_A}{dx} \qquad (D\text{-}6)$$

However, this equation is entirely analagous to Equation II-3. So, it is apparent

$$D = \mathscr{D}_A \qquad (D\text{-}7)$$

and by similar reasoning

$$D = \mathscr{D}_B \qquad (D\text{-}8)$$

as Mills concluded.

Hartley and Crank presented the following relation between D (or D^V) and $\mathscr{D}_A$ and $\mathscr{D}_B$,

$$D = \rho_A V_A (\mathscr{D}_B - \mathscr{D}_A) + \mathscr{D}_A \qquad (D\text{-}9)$$

which the above derivation finds to be a correct, although trivial, relation.

This discussion indicates that the intrinsic diffusivities are not fundamentally significant independent quantities, and they need not be considered separately from D in discussions of diffusion.

The above results agree with those of Mills, but the author feels that the demonstration of the equalities of Equations D-7 and 8 are developed here in a more logical manner, without recourse to the intuitive arguments employed by Mills. Note that the above development is completely general with no restrictions concerning volume changes during diffusion.

APPENDIX E

TABULATION OF DATA

TABLE E-I

DATA FROM KCL-WATER CALIBRATION MEASUREMENTS

In this table, the residue weight, W_R, refers to the KCl residue from a 9.974cc sample of the KCl-water solution. These residue weights divided by 9.974 equal the final concentrations of KCl in the respective compartments. The initial concentration in the upper compartment was zero in all cases. The following data are in the same chronology as those of Table II. As is evident from the table, most samples were measured in triplicate. Weights are corrected for bouyancy.

Cell	Residue Weight, gms.		Diffusion Time,
	W''_r	W'_r	sec x 10^{-5}
1	0.02314	0.05615	
	0.02329	0.05663	3.5400
	0.02310	0.05640	
1	0.02235	0.05504	
	0.02235	0.05515	3.5148
	0.02265	0.05483	
	0.02240	0.05465	
1	0.02265	0.05252	
(Recalibration)	0.02239	0.05249	3.7458
	0.02264	0.05257	
2	0.01746	0.05953	
	0.01762	0.05955	3.5550
	0.01724	0.05915	
2	0.01902	0.06506	
	0.01920	0.06529	3.5874
	0.01928	0.06518	
2	0.01757	0.05994	
	0.01755	0.06008	3.5472
	-	0.05994	

TABLE E-I (Continued)

Cell	Residue Weight, gms.		Diffusion Time,
	W_r''	W_r'	sec x 10^{-5}
2	0.01709	0.05611	
(Recalibration)	0.01712	0.05620	3.7464
	0.01724	0.05629	
3	0.02053	0.05633	
	0.02051	0.05657	3.5526
	0.02052	0.05629	
3	0.02269	0.06195	
	0.02268	0.06209	3.5892
	-	0.06188	
3	0.02059	0.05668	
	0.02053	0.05671	3.5490
	0.02053	0.05650	
3	0.02030	0.05315	
(Recalibration)	0.02011	0.05342	3.7476
	0.02021	0.05357	
4	0.01808	0.06281	
	0.01806	0.06291	3.5484
	0.01806	0.06336	
4	0.01697	0.06038	
	0.01684	0.06008	3.4542
	0.01678	0.06027	
4	0.01736	0.05613	
(Recalibration)	0.01735	0.05606	3.7494
	0.01728	-	
5	0.02308	0.05833	
	0.02313	0.05822	3.5514
	0.02337	0.05847	
5	0.02224	0.05704	
	0.02231	0.05745	3.4554
	0.02219	0.05734	
5	0.02204	0.05576	
	0.02219	0.05577	3.5322
	0.02211	0.05572	

TABLE E-I (Continued)

Cell	Residue Weight, gms.		Diffusion Time,
	W_r''	W_r'	sec x 10^{-5}
5	0.02225	0.05338	
(Recalibration)	0.02216	0.05301	3.7500
	0.02219	-	
6	0.02256	0.07551	
	0.02246	0.07560	3.5172
	0.02243	0.07573	
6	0.01846	0.06137	
	0.01858	0.06129	3.5316
	0.01860	0.06130	
6	0.01743	0.05982	
	0.01768	0.05983	3.4548
	0.01772	0.05964	
6	0.01907	0.06205	
	0.01886	0.06176	3.6102
	0.01891	0.06172	
6	0.01764	0.05532	3.7662
(Recalibration)	0.01759	0.05525	
	-	-	

TABLE E-II

DATA FROM ORGANIC DIFFUSION MEASUREMENTS

In this table, ρ refers to solution density. The numbers in parentheses are the concentrations of the first-named component calculated from the densities. The initial upper density, ρ_o'', was calculated from the known mixture composition and thus does not represent a pycnometric measurement. The average concentrations are also given.

Run	ρ_o'', gm/cc	ρ_f'', gm/cc	ρ_f', gm/cc	$(\rho_A)_{Avg}$, gm/cc	Diffusion Time, sec x 10^{-5}
		n-Octane-Methylcyclohexane, 25°C			
2.1/2	0.72876	0.73905	0.75367		
		0.73907	0.75365		
	(0.39099)	(0.27977)	(0.12329)	(0.20064)	4.9260
2.1/3	0.70050	0.70984	0.71711		
		0.70981	0.71704		
	(0.70050	(0.59764)	(0.51807)	(0.55670)	4.9254
2.1/4	0.70050	0.71712	0.74635		
		0.71721	0.74632		
		0.71726			
	(0.70050)	(0.51720)	(0.20159)	(0.35898)	4.0572
2.2/1	0.75453	0.75800	0.76165		
		0.75801	0.76165		
	(0.11400)	(0.07700)	(0.03815)	(0.05879)	4.5036
2.2/2	0.70050	0.71367	0.73203		
		0.71367	0.73204		
	(0.70050)	(0.55550)	(0.35549)	(0.45433)	4.5036
2.2/3	0.74428	0.75042	0.75809		
		0.75044	0.75816		
	(0.22368)	(0.15780)	(0.07572)	(0.11602)	4.5024
2.2/4	0.70050	0.70560	0.71231		
		0.70562	0.71234		
	(0.70050)	(0.64400)	(0.57019)	(0.60697)	4.5030
2.2/5	0.71538	0.73222	0.74768		
		0.73226	0.74769		
	(0.53666)	(0.35333)	(0.18723)	(0.27278)	4.5018

TABLE E-II (Continued)

Run	ρ_o'', gm/cc	ρ_f'', gm/cc	ρ_f', gm/cc	$(\rho_A)_{Avg}$, gm/cc	Diffusion Time, sec x 10^{-5}
2.4/4	0.70050	0.70590	0.71170		
		0.70591	0.71171		
	(0.70050)	(0.64080)	(0.57699)	(0.60876)	5.1630
2.4/5	0.70050	0.70366	0.70552		
		0.70368	0.70551		
	(0.70050)	(0.66542)	(0.64499)	(0.65568)	5.1648
2.4/6	0.70050	0.70990	0.71958		
		0.70991	0.71961		
	(0.70050)	(0.59676)	(0.49056)	(0.54280)	5.1558
		n-Octane-Cyclohexanone, 25°			
3.1/1	0.70050	0.75196	0.88862		
		0.75189	0.88874		
	(0.70050)	(0.54842)	(0.15480)	(0.35280)	5.7084
3.1/3	0.90508	0.91419	0.93222		
		0.91420	0.93219		
	(0.10769)	(0.08144)	(0.02951)	(0.05518)	8.6328
3.1/4	0.70050	0.70929	0.71583		
		0.70931	0.71582		
	(0.70050)	(0.67419)	(0.65478)	(0.66443)	8.6346
3.1/5	0.70050	0.76698	0.87585		
		0.76692	0.87592		
	(0.70050)	(0.50463)	(0.19152)	(0.35075)	8.6352
3.2/1	0.90469	0.91511	0.93190		
		0.91512	0.93191		
	(0.10881)	(0.07879)	(0.03038)	(0.05482)	8.6460
3.2/2	0.75766	0.79502	0.90261		
		0.79507	0.90257		
	(0.53167)	(0.42338)	(0.11485)	(0.26825)	8.6436
3.2/3	0.70050	0.70891	0.71212		
		0.70890	-		
	(0.70050)	(0.67538)	(0.66579)	(0.67030)	8.6442
3.2/4	0.82676	0.85034	0.91822		
		0.85032	0.91819		
	(0.33224)	(0.26471)	(0.06992)	(0.16716)	8.6442
3.2/5	0.70050	0.72843	0.75163		
		0.72849	0.75162		
	(0.70050)	(0.61733)	(0.54930)	(0.58445)	8.6436
3.3/1	0.70050	0.72606	0.75451		
		0.72605	0.75454		
	(0.70050)	(0.62442)	(0.54083)	(0.58322)	6.9186

TABLE E-II (Continued)

Run	ρ_o'', gm/cc	ρ_f'', gm/cc	ρ_f', gm/cc	$(\rho_A)_{Avg}$, gm/cc	Diffusion Time, sec x 10^{-5}
3.3/2	0.70050	0.71448	0.73510		
		-	0.73513		
	(0.70050)	(0.65876)	(0.59769)	(0.62789)	6.9174
3.3/3	0.79091	0.82200	0.90893		
		0.82200	0.90900		
	(0.43529)	(0.34589)	(0.09653)	(0.22021)	7.1700
3.3/4	0.70050	0.71564	0.70635		
		0.71566	0.70635		
	(0.70050)	(0.68300)	(0.65528)	(0.66910)	5.2782
3.3/5	0.70050	0.74980	0.83467		
		0.74984	0.83467		
	(0.70050)	(0.55456)	(0.30957)	(0.43405)	7.7556
3.3/6	0.70050	0.73222	0.79567		
		0.73221	0.79566		
	(0.70050)	(0.60623)	(0.42160)	(0.51314)	8.0586
		Methylcyclohexane-n-Heptanol, 25°C			
4.1/1	0.80830	0.81123	0.81637		
		0.81125	0.81636		
	(0.14635)	(0.10552)	(0.03373)	(0.06994)	11.4204
4.1/2	0.76524	0.77179	0.81108		
		0.77181	0.81108		
	(0.76524)	(0.66126)	(0.10774)	(0.38367)	6.0810
4.2/1	0.76524	0.76935	0.77478		
		0.76937	0.77480		
	(0.76524)	(0.69902)	(0.61614)	(0.65810)	11.9274
4.2/2	0.78227	0.79034	0.81034		
		0.79040	0.81031		
	(0.50733)	(0.39360)	(0.11832)	(0.25504)	11.9418
4.2/3	0.76524	0.77130	0.78139		
		0.77129	0.78144		
	(0.76524)	(0.66892)	(0.51947)	(0.59311)	11.9580
4.2/4	0.76524	0.77387	0.79250		
		0.77386	0.79250		
	(0.76524)	(0.63005)	(0.36410)	(0.49677)	12.8046
4.2/5	0.79865	0.80462	0.81339		
		0.80468	0.81339		
	(0.27935)	(0.19679)	(0.07549)	(0.13726)	12.8172
4.2/6	0.76524	0.76690	0.77003		
		0.76692	0.77008		
	(0.76524)	(0.73798)	(0.68809)	(0.71281)	12.7722

TABLE E-II (Continued)

Run	ρ_o'', gm/cc	ρ_f'', gm/cc	ρ_f', gm/cc	$(\rho_A)_{Avg}$, gm/cc	Diffusion Time, sec x 10^{-5}
		n-Heptanol-Cyclohexanone, 25°C			
1.1/1	0.81874	0.83603	0.90793		
		0.83603	0.90790		
	(0.81874)	(0.70227)	(0.22291)	(0.46350)	7.3518
1.1/2	0.81874	0.82367	0.86407		
		0.82361	0.86407		
	(0.81874)	(0.78579)	(0.51350)	(0.64938)	6.4812
1.1/3	0.81874	0.82190	0.84399		
		0.82192	0.84404		
	(0.81874)	(0.79743)	(0.64838)	(0.72266)	6.3324
1.1/5	0.81874	0.83310	0.92806		
		-	0.92802		
	(0.81874)	(0.72203)	(0.09222)	(0.40845)	5.0370
1.1/6	0.81874	0.82621	0.88417		
		0.82617	0.88424		
	(0.81874)	(0.76861)	(0.37919)	(0.57349)	6.4632
1.3/1	0.92501	0.92989	9.93740		
		0.92988	0.93741		
	(0.11179)	(0.08036)	(0.03201)	(0.05643)	11.6484
1.3/2	0.81874	0.83441	0.92418		
		-	-		
	(0.81874)	(0.71320)	(0.11716)	(0.41433)	8.2506
1.3/3	0.90996	0.91749	0.93405		
		0.91751	0.93408		
	(0.20958)	(0.16047)	(0.05345)	(0.10641)	11.0322
1.3/4	0.88229	0.89339	0.93021		
		0.89336	0.93026		
	(0.39187)	(0.31843)	(0.07804)	(0.19807)	10.8270
1.3/5	0.85841	0.87780	0.92265		
		0.87779	0.92265		
	(0.55149)	(0.42174)	(0.12706)	(0.27617)	10.8180
1.3/6	0.83754	0.85455	0.92285		
		0.85455	0.92285		
	(0.69208)	(0.57744)	(0.12577)	(0.35066)	10.1034
1.4/1	0.82776	0.85159	0.91824		
		0.85151	0.91826		
	(0.75804)	(0.59763)	(0.15560)	(0.37787)	9.7494
1.4/5	0.81874	0.82382	0.84233		
		0.82379	0.84231		
	(0.81874)	(0.78471)	(0.65984)	(0.72274)	9.7362
1.4/6	0.90927	0.91546	0.93561		
		0.91548	0.93563		
	(0.21409)	(0.17367)	(0.04343)	(0.10822)	9.7524

TABLE E-II (Continued)

Run	ρ_o'', gm/cc	ρ_f'', gm/cc	ρ_f', gm/cc	$(\rho_A)_{Avg}$, gm/cc	Diffusion Time, sec x 10^{-5}
		n-Heptanol-Cyclohexanone, 10°C			
7.1/1	0.81874	0.82419	0.83955		
		0.82417	0.83956		
	(0.81874)*	(0.78215)	(0.67846)	(0.73059)	20.1102
7.1/2	0.88749	0.89924	0.92958		
		0.89927	0.92961		
	(0.35737)	0.27970	(0.08216)	(0.18030)	20.1114
7.1/3	0.91105	0.91953	0.93324		
		0.91947	0.93325		
	(0.20247)	(0.14748)	(0.05873)	(0.10249)	20.1120
7.1/4	0.81874	0.84149	0.91904		
		-	0.91901		
	(0.81874)	(0.66544)	(0.15060)	(0.40768)	20.1072
7.1/5	0.81874	0.82438	0.84180		
		0.82438	0.84181		
	(0.81874)	(0.78080)	(0.66335)	(0.72259)	20.1018
7.1/6	0.81874	0.83325	0.88608		
		0.83322	0.88609		
	(0.81874)	(0.72109)	(0.36672)	(0.54310)	20.1120
		n-Heptanol-Cyclohexanone, 55°C			
5.1/1	0.87517	0.89372	0.92322		
		0.89371	0.92319		
	(0.42708)**	(0.30722)	(0.11980)	(0.21445)	6.5304
5.1/3	0.84610	0.86904	0.91644		
		0.86903	0.91647		
	(0.61664)	(0.46646)	(0.16267)	(0.31288)	6.5310
5.1/4	0.81874	0.82937	0.86372		
		0.82936	0.86371		
	(0.79752)	(0.72731)	(0.50129)	(0.61414)	6.5304
5.1/5	0.91957	0.92624	0.93525		
		0.92626	0.93522		
	(0.14195)	(0.10069)	(0.03866)	(0.07024)	6.5298
5.1/6	0.81874	0.83601	0.88801		
		0.83603	0.88803		
	(0.79752)	(0.68372)	(0.34414)	(0.51299)	6.5298

*Concentrations refer to 25°C

**Concentrations refer to 55°C

TABLE E-II (Continued)

Run	ρ_o'', gm/cc	ρ_f'', gm/cc	ρ_f', gm/cc	$(\rho_A)_{Avg}$, gm/cc	Diffusion Time, sec x 10^{-5}
		n-Heptanol-Cyclohexanone, 90°C			
6.1/1	0.81874	0.82950	0.84034		
		0.82952	-		
	(0.77044)*	(0.70142)	(0.63254)	(0.66752)	5.0394
6.1/2	0.87437	0.89305	0.92242		
		0.89304	0.92240		
	(0.41745)	(0.30084)	(0.12072)	(0.20984)	5.0502
6.1/3	0.81874	0.84519	0.87449		
		0.84516	-		
	(0.77044)	(0.60172)	(0.39792)	(0.49793)	5.0592
6.1/4	0.81874	0.83349	0.85895		
		0.83350	0.85896		
	(0.77044)	(0.67599)	(0.51457)	(0.59507)	5.0688
6.1/5	0.91994	0.92868	0.93601		
		-	0.93601		
	(0.13560)	(0.08248)	(0.03835)	(0.06114)	5.0790
6.2/1	0.91446	0.92473	0.93302		
		0.92477	0.93301		
	(0.16889)	(0.10634)	(0.05608)	(0.08170)	5.1810
6.2/2	0.81874	0.83692	0.86737		
		0.83694	0.86737		
	(0.77044)	(0.65387)	(0.46113)	(0.55656)	5.1822
6.2/3	0.81874	0.82852	0.84053		
		0.82858	0.84053		
	(0.77044)	(0.70762)	(0.63125)	(0.66873)	5.1822
6.2/6	0.84041	0.86817	0.91070		
		0.86817	0.91072		
	(0.63203)	(0.45621)	(0.19182)	(0.32256)	5.1798

*Concentrations refer to 90°C

TABLE E-III

VOLUMETRIC DATA FOR ANALYTICAL APPARATUS

Pipet for KCl-Water Samples

Volume, cc

9.9723
9.9745
9.9745
9.9755

Avg. 9.9742

Pycnometers for Organic Analyses

Pycnometer Identification	Volume, cc, 25°C			
	1	2	3	Average
1S	19.6478	19.6484	19.6478	19.6480
2S	19.6971	19.6985	19.6972	19.6976
3S	19.3007	19.3011	19.3017	19.3012
1L	19.1937	19.1940	19.1937	19.1938
2L	19.4902	19.4906	19.4904	19.4904
3L	20.1426	20.1433	20.1423	20.1427

TABLE E-IV

DATA FOR CORRELATION TESTS

The sources of data used to test the correlation schemes are listed below. Literature sources are given in parentheses. Properties of water were taken from reference 41.

Property	Substance			
	n-Octane	MCH	n-Heptanol	Cyclohexanone
Mol. Wt.(41)	114.23	98.18	116.20	98.14
L, cal/gm, 25°C	86.8(5)	86.1(5)	131.0	114.6
10**			133.2	116.6
55			126.6	111.1
90			122.2	106.5
NBP	72.6	76.1	104.9(59)	96.5****
NBP, °C (41)	125.8	100.3	176.	156.
μ, cp*, 25	0.517	0.680	5.868	2.000
10***			10.0	2.79
20***	0.55	0.73	6.75	2.21
55			2.350	1.149
90			0.982	0.670
V, cc/gmol*, 25	163.07	128.30	141.93	104.14
10***			140.3	102.8
55			145.70	107.15
90			150.83	111.03
NBP***			165.	120.
T_c, °C	296.(5)	299.(5)	365.(41)	383.*****

*Taken from data of present work
**Effects of temperature on L were estimated via Watson's method (32).
***Interpolated or extrapolated values
****Estimated via Fishtine's correlation (32)
*****Estimated via Lynderson's correlation (61)

APPENDIX F

SAMPLE CALCULATIONS

The techniques and relations used in calculating the system properties from experimental data are demonstrated here.

A. KCl Concentration Calculation

The concentrations of KCl in the aqueous samples were calculated from the following type of data:

Tare weights:

Sample bottle,	76.01846 gms
Standard bottle,	78.02400

Gross weights:

Sample bottle + residue,	76.04114
Standard bottle,	78.02352

Pipet volume, 9.974 cc

The residue weight, W_r, was found via Equation C-12,

$$W_r = (76.04114 - 76.01846) - (76.01846/78.02400)(78.02352 - 78.02400)$$

$$= 0.02268 - (0.97430)\ (-0.00048) = 0.02314 \text{ gm}$$

The above residue weight corresponds to an entry in Table E-I for the first calibration of Cell 1.

The KCl concentration was found by dividing the residue weight by the sample volume (pipet volume):

$$\text{KCl concentration, } \rho_{KCl} = 0.02314 \text{ gm}/9.974 \text{ cc} = 0.002320 \text{ gm/cc}$$

B. Organic Density Calculation

Typical data for density measurements are:

Tare weights:

Pycnometer + wire on caps + hook,	34.64022 gms
Standard bottle,	52.96285

Gross weights:

Pycnometer + sample + wire + hooks,	51.04658
Standard bottle,	52.96338
Weight of wire + hook,	1.65535
Volume of pycnometer,	19.6480 cc

Weight of empty pycnometer, $W_B = 34.64022 - 1.65535 = 32.98487$ gms

From Equation C-16,

$$\text{Air density, } \rho_a = (53.15155 - 52.96285)/(3.10808)\ (52.96285)$$
$$= 1.1463 \times 10^{-3} \text{ gm/cc}$$

From equation C-4, the empty pycnometer weight, corrected to vacuo, W_B^o, is

$$W_B^o = 32.98487 \left[1.0 + (1.14683 \times 10^{-3})\ (1.0/2.23 - 1.0/8.4) \right]$$
$$= 32.99734 \text{ gms}$$

A similar calculation for air density at the time of the gross weighings yields $\rho_a = 1.1431 \times 10^{-3}$ gm/cc.

Assume $\rho_{B+S} = 1.43485$ gm/cc. This is the assumed density of the filled pycnometer, glass and sample.

Weight of filled pycnometer, $W_{B+S} = 51.04658 - 1.65535$

$$= 49.39123 \text{ gms}$$

From Equation C-4,

$$W_{B+S}^o = 49.39123 \left[1.0 + (1.1431 \times 10^{-3})\ (1.0/1.43485 - 1.0/8.4) \right]$$
$$= 49.42388 \text{ gms}$$

Thus, from Equation C-17,

$$\rho_{B+S} = 49.42388 \,/\, \left[(32.99734/2.23) + 19.6480\right] = 1.43486 \text{ gm/cc}$$

The assumed and calculated values of ρ_{B+S} agree to within 0.00001 gm/cc. No additional iterations are needed.

Finally, from Equation C-18, the sample density is found to be

$$\rho_S = (49.42388 - 32.99734)/19.6480$$
$$= 0.83604 \text{ gm/cc}$$

The density value applies to Run 1.1/1 in Table E-2, and agrees well with the computer solution.

C. Cell Constant Calculation

Typical data from calibration runs are:

KCl concentrations:

Final,

$\rho''_{rf} = 0.001751$ gm/cc

$\rho'_{rf} = 0.005963$

Initial,

$\rho''_{ro} = 0.0$

Diffusion time = 3.555×10^5 sec

Cell compartment volumes:

Upper, V" =	48.62 cc
Lower, V' =	47.10
Diaphragm, V"' =	0.31

The initial KCl concentration in the lower compartment was found by material balance assuming no volume changes occurred:

$$V'\rho'_{ro} + V''\rho''_{ro} + V'''\tfrac{1}{2}(\rho'_{ro}+\rho''_{ro}) = V'\rho'_{rf} + V''\rho''_{rf} + V'''\tfrac{1}{2}(\rho'_{rf}+\rho''_{rf})$$

or

$$\rho'_{ro} = \left[\rho'_{rf}(V'+\tfrac{1}{2}V''') + \rho''_{rf}(V''+\tfrac{1}{2}V''') - \rho''_{ro}(V''+\tfrac{1}{2}V''')\right] / (V'+\tfrac{1}{2}V''')$$

$$V'' + \tfrac{1}{2}V''' = 48.755 \text{ cc}$$
$$V' + \tfrac{1}{2}V''' = 47.255$$

so

$$\rho'_{ro} = \left[(0.005963)(48.775)+(0.001751)(48.775)-0.0\right] / 47.255$$
$$= 0.007770 \text{ gm/cc}$$

Thus the average concentration is

$$(\rho_r)_{Avg} = \tfrac{1}{4}\,(0.0 + 0.007770 + 0.005963 + 0.001751)$$
$$= 0.003871 \text{ gm/cc}$$

From Stoke's data (66), at the above average concentration,

$$D = 1.8674 \times 10^{-5} \text{ cm}^2/\text{sec}$$

The cell constant is then calculated from Equation II-19,

$$\beta = \ln(\Delta \rho_{ro}/\Delta \rho_{rf}) / \bar{D}\,\theta$$

$$\Delta \rho_{ro} = 0.0 - 0.007770 = -0.007770$$
$$\Delta \rho_{rf} = 0.001751 - 0.005963 = -0.004212$$
$$\ln(\Delta \rho_{ro}/\Delta \rho_{rf}) = \ln(1.8447) = 0.61232$$

Thus,

$$\beta = 0.61232 / (1.8674 \times 10^{-5})(3.555 \times 10^{5})$$
$$= 0.09223 \text{ cm}^{-2}$$

This value of β corresponds to the entry in Table II for the first calibration of Cell 2.

D. Organic Diffusivity Calculation

The calculation of $\bar{D}$, the integral diffusion coefficient, from the simple logarithmic formula, Equation II-19, is exactly analogous to the calculation of β, except the places of β and $\bar{D}$ are reversed. These

calculations are too similar to require repetition.

E. Viscosity Calculation

Viscosities were calculated from the relation (20),

$$\frac{\mu}{\mu_W} = \frac{\rho\,\theta}{\rho_W\,\theta_W}$$

where θ is the flow time, and W refers to water, the calibration fluid. Typical data are:

Temperature = 25°C

ρ = 0.70050 gm/cc

θ = 80.6 sec

ρ_W = 0.99704 gm/cc (41)

θ_W = 97.8 sec

μ_W = 0.8937 cp (41)

Then,

$$\mu = (0.70050)(80.6)(0.8937) / (0.99704)(97.8)$$

$$= 0.517_4 \text{ cp}$$

This value of viscosity corresponds to the viscosity of pure n-octane listed in Table XVI.

APPENDIX G

FORTRAN LISTING OF PROGRAM FOR CALCULATING
DIFFERENTIAL DIFFUSIVITIES

```
C     DIFFERENTIAL DIFFUSIVITIES FROM EXPTL DATA - R. ROBINSON
      DIMENSIONCN4(10,4),CN1(10,4),VU(30),CONL(21),VB(30)
      DIMENSIONTIM(30),T(3,4)
      DIMENSIONR(30,4),TH(30),V1(30),V2(30),V3(30),BO(30)
      DIMENSIONCN2(10,4),CN3(10,4),B1(10,4),B2(10,4),C(30,4)
      DIMENSIONDB(30)
      DIMENSION DSIM(30),NWP(10),NWF(10),XA(30),YA(30),CAV(30)
      DIMENSIONTAK(30),AOL(30),CONU(21),RHOU(21),RHOL(21)
      DIMENSIONVOLU(21),DELC(30),BETA(30),CNCN(21),FOR(30)
      DIMENSIONVOV(21),FUNC(21),GOR(30),NC(3),A(3,4),X(3)
      COMMON R1,RO,CX,CY,AA,BB,CC,VAR,B1,B2,CN1,CN2,CN3,AB,BA,
     9CT,V1,V2,V3,R,C,DD,CN4,KOOL,KOOP,KOOT,UEE,V,RS,RT
    2 FORMAT(6F10.5)
   22 FORMAT(1H ,6F10.5)
   39 READ INPUT TAPE 7,2,UAA
C     UAA DETERMINES IF CERTAIN INTERMEDIATE RESULTS ARE
C     PRINTED  1-YES,  0-NO
      READ INPUT TAPE 7,2,BUMPY,RUMP
C     BUMPY = MAX. NUMBER OF ITERATIONS ALLOWED TO OBTAIN
C             D FROM DBAR
C     RUMP = FRACTIONAL CHANGE IN ASSUMED VALUE OF CONCN.
C     FOR WHICH DBAR EQUALS D, FRACTION OF DIFFERENCE BETWEEN
C     THE PREVIOUSLY ASSUMED AND CALCULATED CONCNS.
      KOOT=UFF
      KAAT=UBB
      READ INPUT TAPE7,2,P,RO,R1
C     P = NO. OF DATA POINTS IN INPUT
C     RO,R1 = DENSITY OF PURE COMPONENTS B AND A, RESPECTIVELY
      WRITE OUTPUT TAPE6,22,P,RO,R1
      N=P
      DO41=1,N
      READ INPUT TAPE 7,2,C(I,1),C(I,2),C(I,3),TH(I)
C     C(I,J) = CONCENTRATION OF COMPONENT A FOR CELL I
C              J = 1, UPPER INITIAL.  2, UPPER FINAL
C              3, LOWER FINAL.  4, LOWER INITIAL
C     TH = DIFFUSION TIME, SEC
    4 READ INPUT TAPE7,2,V1(I),V2(I),V3(I),BO(I)
C     V1,V2,V3 = VOLUMES OF UPPER, LOWER COMPARTMENTS
C                AND DIAPHRAGM
C     BO = CELL CONSTANT
```

```
      DO6J=1,4
      DO6I=1,KOOT
      READ INPUT TAPE 7,2,CN1(I,J),CN2(I,J),CN3(I,J),CN4(I,J)
C     CN1(I,J) =1ST CONSTANT FOR 3RD ORDER CURVE FIT. I REFERS
C              TO THE SECTION OF THE CURVE BEING FITTED.
C              (MAX. I = 4).  J REFERS TO THE PROPERTY
C              FITTED.  1, D.  2, DENSITY.  3, PARTIAL
C              VOLUME.  4, PARTIAL VOLUME RATIO
      READ INPUT TAPE 7,2,B1(I,J),B2(I,J)
C     B1(I,J) = LOWER LIMIT ON CONCN. FOR WHICH ABOVE CURVE
C              FIT APPLIES
C     B2(I,J) = UPPER LIMIT CORRESPONDING TO B1(I,J)
      WRITE OUTPUT TAPE 6,22,CN1(I,J),CN2(I,J),CN3(I,J),
     9CN4(I,J)
  6   WRITE OUTPUT TAPE 6,22,B1(I,J),B2(I,J)
      DO8I=1,N
      DO8J=1,3
      VAR=C(I,J)
      CALL VARCO(2)
  8   R(I,J)=RO+((R1-RO)/R1)*VAR+AA+BB*VAR+CC*VAR**2+
     9DD*VAR**3
      DO10I=1,N
      RS=R(I,3)+R(I,2)-R(I,1)
      RT=R(I,1)
      CT=C(I,1)
      CALL DLFDU (I,0)
      R(I,4)=RS
      C(I,4)=CX
      VU(I)=V
      CAV(I)=(C(I,1)+C(I,2)+C(I,3)+C(I,4))/4.0
      DB(I)=LOGF((C(I,1)-C(I,4))/(C(I,2)-C(I,3)))/(BO(I)*TH(I))
      SIM=(C(I,3)*BA+(C(I,2)-C(I,1))*AB)/BA
      DSIM(I)=LOGF((C(I,1)-SIM)/(C(I,2)-C(I,3)))/(BO(I)*TH(I))
      IF(UAA)10,10,81
  81  WRITE OUTPUT TAPE6,22,R(I,1),R(I,2),R(I,3),R(I,4),TH(I)
      TIM(I)=(4.0*CAV(I)-C(I,4)+SIM)/4.0
C     R(I,J) = DENSITY CORRESPONDING TO C(I,J)
      TAK(I)=TIM(I)
      WRITE OUTPUT TAPE6,22,C(I,1),C(I,2),C(I,3),C(I,4),SIM
      WRITE OUTPUT TAPE 6,22,DSIM(I)
C     SIM = INITIAL LOWER CONCN., ASSUMING NO VOLUME CHANGES
C      DSIM = INTEGRAL DIFFUSIVITY CALCULATED ASSUMING NO
C             VOLUME CHANGES
  10  CONTINUE
  371 DO11I=1,KAAT
      READ INPUT TAPE7,2,XNP,XNF
C     XNP = NO. OF DBAR POINTS TO BE FITTED IN A GIVEN
C           SECTION OF THE CONCENTRATION RANGE
C     XNF = NUMBER OF THE FIRST DBAR VALUE IN THE SECTION TO
C           BE FITTED
      WRITE OUTPUT TAPE6,22,XNP,XNF
      NWP(I)=XNP
```

```
  11 NWF(I)=XNF
 35  CONNN=0.0
     DO13NZ=1,KAAT
     NPTS=NWP(NZ)
     XNP = NPTS
     IF(XNP)13,13,102
102  DO15J=1,NPTS
     NOP=NWF(NZ)+J-1
     XA(J)=TAK(NOP)
 15  YA(J)=DSIM(NOP)
     DO171=1,3
 17  NC(I)=I-1
     NVAR=3
     DO 130 I = 1,NVAR
     DO 130 J = I,NVAR
     A(J,I) = 0.0
     DO 150 K = 1, NPTS
150  A(J,I) = A(J,I) + XA(K)**(NC(I) + NC(J))
130  A(I,J) = A(J,I)
     NP = NVAR + 1
     DO 170 I = 1,NVAR
     A(I,NP) = 0.0
     DO 170 J= 1,NPTS
170  A(I,NP) = A(I,NP) +YA(J)*XA(J)**NC(I)
     DO230 I = 1,NVAR
230  T(I,1) = A(I,1)
     DO 40 I = 2,NP
40   T(1,I) = A(1,I)/A(1,1)
     I = 1
61   I = I + 1
     DO 70 J = I,NVAR
     T(J,I) = A(J,I)
     M = I - 1
     DO 70 L = 1,M
70   T(J,I) = T(J,I) - T(J,L)*(T(L,I))
     IM = I + 1
     DO 80 J = IM,NP
     T(I,J) = A(I,J)/T(I,I)
     N1 = I - 1
     DO 80 L = 1,N1
80   T(I,J) = T(I,J) - T(I,L)*(T(L,J))/T(I,I)
     IF(NVAR - I)85,85,61
85   X(NVAR) = T(NVAR,NP)
     IZZ = NVAR - 1
147  DO 90 I = 1,IZZ
     K = NVAR - I
     X(K) = T(K,NP)
     L = K + 1
     DO 90 J = L,NVAR
90   X(K) = X(K) - X(J)*T(K,J)
 988 CN1(NZ,1)=X(1)
     CN2(NZ,1)=X(2)
```

```
      CN3(NZ,1)=X(3)
   13 CONTINUE
      HYGO=CN1(1,1)
      IF(UAA)83,83,82
   82 WRITE OUTPUT TAPE 6,22,HYGO
C     HYGO = D(ZERO) OF EQUATION 22-24
   83 DO31=1,KAAT
      CN4(I,1)=CN4(I,1)/HYGO
      CN2(I,1)=CN2(I,1)/HYGO
      CN3(I,1)=CN3(I,1)/HYGO
    3 CN1(I,1)=CN1(I,1)/HYGO - 1.0
      DO771=1,KAAT
      WRITE OUTPUT TAPE 6,22,CN1(I,1),CN2(I,1),CN3(I,1),
     9CN4(I,1)
C     THE ABOVE CONSTANTS ARE FOR THE CURVE FOR F OF CONCN.
C     OF EQUATION 11-24
   77 WRITE OUTPUT TAPE 6,22,B1(I,1),B2(I,1)
      DO 121=1,N
      AOL(I)=BO(I)/(1.0/V1(I)+1.0/V2(I))
      BEL=0.10*(C(I,2)-C(I,1))
      DO 19J=1,11
      FAC=J-1
      CONU(J)=C(I,1)+BEL*FAC
      CT=CONU(J)
      VAR=CT
      CALL VARCO (2)
      RT=RO+((R1-RO)/R1)*CT+AA+BB*CT+CC*CT**2+DD*CT**3
      RS=R(I,1)+R(I,4)-RT
      CALL DLFDU (I,1)
      RHOU(J)=RT
      RHOL(J)=RS
      CONL(J)=CX
      VOLU(J)=V
      DELC(J)=CONU(J)-CONL(J)
      BETA(J)=AOL(I)*(1.0/V2(I)+1.0/VOLU(J))
   79 DO14K=1,11
      DAC=K-1
      CNCN(K)=CONL(J)+0.10*(CONU(J)-CONL(J))*DAC
      VAR=CNCN(K)
      CALL VARCO (1)
      FOR(K)=AA+BB*VAR+CC*VAR**2+DD*VAR**3
      CALL VARCO (3)
      VB(K)=AA+BB*VAR+CC*VAR**2+DD*VAR**3
      VAR=CONL(J)
      CALL VARCO(4)
      VOV(K)=AA+BB*VAR+CC*VAR**2+DD*VAR**3
      VAR=CNCN(K)
      CALL VARCO (4)
      VOV(K)=AA+BB*VAR+CC*VAR**2+DD*VAR**3-VOV(K)
   87 VB(K)=VB(K)*VOV(K)*VAR
   14 VB(K)=(1.0+FOR(K))/(1.0-VB(K))
      SUM=0.0
```

```
      DO16KK=1,10
16    SUM=SUM+(VB(KK)+VB(KK+1))/2.0
      SUM=SUM/10.0
19    FUNC(J)=(1.0/SUM)-1.0
      DO18JJ=1,10
      FUNC(JJ)=(FUNC(JJ)+FUNC(JJ+1))/2.0
      BETA(JJ)=(BETA(JJ)+BETA(JJ+1))/2.0
      GOR(JJ)=(DELC(JJ)+DELC(JJ+1))/2.0
      CONU(JJ)=(CONU(JJ)+CONU(JJ+1))/2.0
      FOR(JJ)=(VOLU(JJ)+VOLU(JJ+1))/2.0
      FOR(JJ)=(1.0+FUNC(JJ))*CONU(JJ)/(BETA(JJ)*GOR(JJ)*
     9FOR(JJ))
      FUNC(JJ)=FUNC(JJ)/(BETA(JJ)*GOR(JJ))
      VOV(JJ)=1.0/(BETA(JJ)*GOR(JJ))
      VOV(JJ)=VOV(JJ)*(DELC(JJ+1)-DELC(JJ))
      FOR(JJ)=FOR(JJ)*(VOLU(JJ+1)-VOLU(JJ))
18    FUNC(JJ)=FUNC(JJ)*(DELC(JJ+1)-DELC(JJ))
      BETA(I)=0.0
      DELC(I)=0.0
      VB(I)=0.0
      DO20IL=1,10
      BETA(I)=BETA(I)+FOR(IL)
      DELC(I)=DELC(I)+FUNC(IL)
20    VB(I) =VB(I)+VOV(IL)
      GOR(I)=-1.0*(LOGF((C(I,1)-C(I,4))/(C(I,2)-C(I,3))))/
     9VB(I)
      BETA(I)=BETA(I)/(HYGO*TH(I))
      DELC(I)=DELC(I)/(HYGO*TH(I))
      FOR(I)=(GOR(I)/BO(I))*(1.0+BETA(I)+DELC(I))-(DB(I)-
     9DSIM(I))/HYGO
89    VAR=TAK(I)
      CALL VARCO (1)
      SUM=AA+BB*VAR+CC*VAR**2+DD*VAR**3+1.0
      DEL=SUM-FOR(I)
      U=TAK(I)
29    U=U+0.0003
      VAR=U
      CALL VARCO (1)
      SUM=AA+BB*VAR+CC*VAR**2+DD*VAR**3+1.0
      BEL=SUM-FOR(I)
      IF(ABSF(BEL)-ABSF(DEL))26,26,28
26    DEL=BEL
      GO TO 29
28    U=U-0.0006
      VAR=U
      CALL VARCO (1)
      SUM=AA+BB*VAR+CC*VAR**2+DD*VAR**3+1.0
      DEL = SUM-FOR(I)
      IF(ABSF(DEL)-ABSF(BEL))31,31,30
31    BEL=DEL
      GO TO 28
30    IF(ABSF(VAR-TAK(I))-0.0030)32,32,33
```

```
   33  CONNN=1.0
       XSON=VAR-TAK(I)
       PP=I
       WRITE OUTPUT TAPE6,22,PP,XSON
C      PP = THE NUMBER OF THE DATA POINT UNDER CONSIDERATION
C      XSON = THE DIFFERENCE BETWEEN THE ASSUMED  AND
C             CALCULATED CONCN. FOR WHICH DBAR = D
   32  TAK(I)=TAK(I)+RUMP*(VAR-TAK(I))
   12  CONTINUE
       BUMPY=BUMPY-1.0
       IF(BUMPY)376,377,377
  376  DO378I=1,N
  378  WRITE OUTPUT TAPE6,22,TAK(I)
C      TAK = ASSUMED VALUE OF CONCENTRATION AT WHICH DBAR = D
       GO TO 39
  377  IF(CONNN)34,34,35
   34  DO361=1,N
       VAR=TAK(I)
       CALL VARCO (2)
       V1(I)=RO+((R1-RO)/R1)*TAK(I)
       V1(I)=V1(I)+AA+BB*TAK(I)+CC*TAK(I)**2+DD*TAK(I)**3
       V1(I)=TAK(I)/V1(I)
   36  WRITE OUTPUTTAPE6,22,DSIM(I),TIM(I),TAK(I),V1(I)
C      DSIM = D FROM SIMPLE LOGARITHMIC FORMULA
C      TIM = AVERAGE CONCENTRATION FOR THE RUN
C      TAK = CONCENTRATION AT WHICH DSIM EQUALS THE TRUE D
C      V1 = MASS FRACTION CORRESPONDING TO TAK
       GO TO 39
       SUBROUTINE VARCO (ME)
C      THIS SUBROUTINE SELECTS THE APPROPRIATE CONSTANTS FOR
C      THE SECTION OF THE CURVE INVOLVED IN A GIVEN CALCULATION
C      THE DIMENSION AND COMMON STATEMENTS FROM THE MAIN
C      PROGRAM MUST BE LISTED HERE ALSO, BUT ARE DELETED FOR
C      THE SAKE OF BREVITY
       DO51LIK=1,KOOT
       IF(VAR-B1(LIK,ME))51,51,52
   52  IF(VAR-B2(LIK,ME))53,53,51
   53  AA=CN1(LIK,ME)
       BB=CN2(LIK,ME)
       CC=CN3(LIK,ME)
       DD=CN4(LIK,ME)
   51  CONTINUE
       RETURN
       SUBROUTINE DENSC (Q)
C      THIS SUBROUTINE DETERMINES THE CONCN. FROM THE DENSITY
C      THE DIMENSION AND COMMON STATEMENTS FROM THE MAIN
C      PROGRAM MUST BE LISTED HERE ALSO, BUT ARE DELETED FOR
C      THE SAKE OF BREVITY
   22  FORMAT(1H ,6F10.5)
       KOOP=0
       DR=0.0
       CX=(R1/(R1-RO))*(Q-RO-DR)
```

```
      CY=CX
   57 KOOP=KOOP+1
      IF(KOOP- 30)297,297,299
C     KOOP LIMITS THE NO. OF ITERATIONS TO CONVERGE ON CONCN.
C     FROM KNOWN DENSITY
  299 WRITE OUTPUT TAPE 6,22,CY,CX
      GO TO 56
  297 CONTINUE
      CX=(CX+CY)/2.0
      VAR=CX
      CALL VARCO (2)
      DR=AA+BB*CX+CC*CX**2+DD*CX**3
      CY=(R1/(R1-RO))*(Q-DR-RO)
      IF(ABSF(CX-CY)-UEE)56,56,57
   56 RETURN
      SUBROUTINE DLFDU (I,NUT)
C     THIS SUBROUTINE WRITES OVERALL AND COMPONENT MATERIAL
C     BALANCES OVER THE CELL TO GIVE CONDITIONS IN ONE
C     COMPARTMENT FROM KNOWN CONDITIONS IN THE OTHER
C     COMPARTMENT
C     THE DIMENSION AND COMMON STATEMENTS FROM THE MAIN
C     PROGRAM MUST BE LISTED HERE ALSO, BUT ARE DELETED FOR
C     THE SAKE OF BREVITY
   22 FORMAT(1H ,6F10.5)
      KOOL=0
      AB=V1(I)+0.5*V3(I)
      BA=V2(I)+0.5*V3(I)
      IF(NUT)62,62,92
   62 V=((RS-R(I,3))*BA+RT*AB)/R(I,2)-0.5*V3(I)
      CMTL=(C(I,3)*BA+C(I,2)*(V+0.5*V3(I))-CT*AB)/BA
      GO TO 93
   92 V=(R(I,1)*AB+(R(I,4)-RS)*BA)/RT - 0.5*V3(I)
      CMTL=(C(I,1)*AB+C(I,4)*BA-CT*(V+0.5*V3(I)))/BA
   93 Q=RS
      KOOL=KOOL+1
      IF(KOOL- 30)352,352,298
C     KOOL LIMITS THE NO. OF ITERATIONS FOR CONVERGENCE OF
C     THE MATERIAL BALANCE
  298 WRITE OUTPUT TAPE6,22,CX,CMTL,I
      GO TO 60
  352 CALL DENSC (Q)
      IF(ABSF(CX-CMTL)-UEE)60,61,61
   61 CX=0.5*(CX+CMTL)
      VAR = CX
      CALL VARCO (2)
      RS=RO+((R1-RO)/R1)*CX+AA+BB*CX+CC*CX**2+DD*CX**3
      IF(NUT)62,62,92
   60 CX=CMTL
      RETURN
```

NOMENCLATURE

A	=	mass transfer area in diaphragm
A, A'	=	constants in Equations VII-2
a	=	constant in Equation III-17
a_i	=	activity of component i
A, B	=	constants in Equations VI-1, VI-9, C-15
c	=	molar concentration
D	=	diffusion coefficient defined by Equation II-2
D_{Fick}	=	diffusion coefficient defined by Equation II-1
D	=	diffusion coefficient defined by Equation II-6
$\overline{D}$	=	diffusion coefficient defined by Equation II-9
D_*	=	diffusion coefficient defined by Equation II-23
D^o	=	diffusion coefficient defined by Equation III-18
D_o	=	D at zero concentration of component A, Equation II-24
D_i^*	=	tracer (self)-diffusion coefficient of component i
$\mathcal{D}_i$	=	intrinsic diffusion coefficient of Hartley-Crank theory
E	=	internal energy
E_D, E_μ	=	activation energies for diffusion and viscous flow, respectively, defined by Equations VII-2
e	=	constant, base of natural logarithms
F, F^*	=	partition functions for normal and activated molecules, respectively
F_r	=	frictional force on a particle, defined by Equation III-1
$F(\rho_A', \rho_A'')$	=	function defined by Equation II-29

f_i = friction coefficient defined by Equation III-1

$f(D)$ = function of D, dependent variable in Equation VII-1

$f(\rho_A)$ = function defined by Equation II-24

$G(\rho_A, \rho_A')$ = function defined by Equation II-24

$g(T)$ = function of T, independent variable in Equation VII-1

H = relative humidity

h = Planck's constant

J_i = mass flux of component i relative to the mass-average velocity

K = equilibrium constant for dimerization, defined by Equation III-19

= parameter in Equation C-14

k = rate constant of Eyring's theory of rate processes

$\tilde{k}$ = Boltzmann's constant

L = diffusion path length, i.e., the diaphragm thickness

L_i = latent heat of vaporization of component i

M = molecular weight

m = reduced mass

N_i = mass flux of component i relative to the laboratory reference frame

$\tilde{N}$ = Avagadro's number

NBP = normal boiling point

n = parameter in Eyring's theory, $\Delta E_{vap}/\epsilon_o$

p = pressure

p' = vapor pressure

R = ratio of the initial to the final concentration difference in a diaphragm-cell experiment

r_i = radius of particle i

$\vec{r}$ = the direction vector

s = standard deviation

T = absolute temperature

t = temperature, ^{o}C

= time

T_c = critical temperature

V = volume of cell compartment

V_T = specific volume of solution

V_i = partial volume of component i

v = velocity

v_f = "free" volume of Eyring's theory

W = weight, in air

W^o = weight, in vacuo

ΔW^k_{ij} = change in weight of object k between weighings i and j

x = mole fraction

x, y = variables in Equation II-37

x, y, z = designations of the rectangular coordinate axes

y = length or distance

Greek Symbols

β = cell constant for diaphragm cell, defined in Equation II-8

$\bar{\beta}$ = average value of the cell constant, defined in Equation II-32

β_o = cell constant for case where no volume changes occur

Δ = change in a variable

δ = deviation from the mean

ϵ_o = activation energy per molecule at $0^{o}K$

ζ_{ij} = pair-wise intermolecular friction coefficient for the i-j pair, defined in Equation III-14

θ = time

$\theta_{opt.}$ = optimum diffusion time

λ = jump length in Eyring's theory

μ = viscosity

= chemical potential

π = constant

ρ = density

ρ_i = concentration of component i

$(\rho_A)_{Avg}$ = mean concentration in diaphragm cell, the average of the two initial and two final concentrations

ρ_A^* = concentration of A at which $\bar{D}$ is numerically equal to D

$\tilde{\rho}_{ij}$ = correlation coefficient for the i-j interaction, defined by Equation II-39

$\sum$ = summation sign

σ = parameter, analogous to the molecular radius, with dimensions of length

ω = mass fraction

Subscripts

A,B,C = components A, B, and C, respectively

a = air

B = pycnometer (bottle)

i,j = components or dummy variables

m = mean value

o,f = initial and final conditions, respectively

r = KCl residue

S = sample in pycnometer

s = standard bottle

= solvent

w = weights used in balance

Superscripts

E	=	value in excess of that for an ideal system
o	=	in vacuo
	=	pure component
', "	=	lower and upper compartments, respectively

Miscellaneous

d	=	differential operator
ln	=	natural logarithm
∂	=	partial operator
∇	=	gradient, the del operator
$\propto$	=	proportionality sign
∞	=	infinitely-dilute state
$\equiv$	=	identity sign, denotes a definition
$\int$	=	integral sign

VITA

Robert Louis Robinson, Jr.

Candidate for the Degree of

Doctor of Philosophy

Thesis: A STUDY OF CERTAIN VARIABLES INFLUENCING LIQUID DIFFUSION RATES

Major Field: Chemical Engineering

Biographical:

Personal Data: Born in Muskogee, Oklahoma, June 14, 1937, the son of Robert L. and Bess W. Robinson. Married to G. Gayle Nixon, Muskogee, Oklahoma, in May, 1958.

Education: Attended elementary school in Muskogee, Oklahoma; graduated from Muskogee Central High School in 1955; received the Bachelor of Science degree in Chemical Engineering from Oklahoma State University in 1959; received the Master of Science degree with a major in Chemical Engineering, May, 1962; completed requirements for the Doctor of Philosophy degree in May, 1964.

Professional Experience: Employed as an engineering trainee with Brockway Glass Company in the summer of 1957. Employed as an engineering trainee with Humble Oil and Refining Company in the summer of 1958. Employed in the summer of 1960 as an engineer (temporary) with Jersey Production Research Company. Currently employed as a Senior Research Engineer at Pan American Petroleum Corporation.